

“GREEN SYNTHESIS, CHARACTERIZATION, AND EVALUATION OF *IN VITRO* ANTIMICROBIAL, ANTIOXIDANT, AND *IN VIVO* WOUND HEALING ACTIVITY OF SILVER NANOPARTICLES LOADED IN TOPICAL GEL USING HYDROALCOHOLIC ROOT EXTRACT OF *POTENTILLA FULGENS*.”

THESIS SUBMITTED TO THE



ASSAM SCIENCE AND TECHNOLOGY UNIVERSITY

**IN PARTIAL FULFILLMENT OF THE REQUIREMENT FOR THE DEGREE
OF**

**MASTER OF PHARMACY
IN
PHARMACEUTICS**

SUBMITTED BY:

**ALAKESH BHARALI
REG. NO.: 387005219 of 2019-2020
ROLL NO.: 190520011001**

UNDER THE SUPERVISION OF:

**Dr. BHANU PRATAP SAHU (ASSOCIATE PROFESSOR)
HOD, DEPARTMENT OF PHARMACEUTICS, GIPS, GHY-17**

CO-GUIDED BY:

**Dr. DAMIKI LALOO (ASSOCIATE PROFESSOR)
DEPARTMENT OF PHARMACOGNOSY, GIPS, GHY-17**



**GIRIJANANDA CHOWDHURY INSTITUTE OF PHARMACEUTICAL
SCIENCE (GIPS), HATHKHOWAPARA, AZARA, GUWAHATI-781017,
KAMRUP, ASSAM (INDIA).**



**COPYRIGHT@ GIRIJANANDA CHOWDHURY INSTITUTE OF
PHARMACEUTICAL SCIENCE,**

HATKHOWAPARA, AZARA, GUWAHATI-781017

ALL RIGHTS RESERVED

2021

Dedication



**Dedicated to
my family, my
guide and co-guide**



GIRIJANANDA CHOWDHURY INSTITUTE OF PHARMACEUTICAL SCIENCE (GIPS)

(A unit of Shrimanta Shankar Academy)

Approved by AICTE & PCI, New Delhi, Affiliated to Assam Science and
Technology University

N.H. 37, Hathkhowapara, Azara, Guwahati-781017

Telephone: (0361) 2843405

Email: gips_guwahati@rediffmail.com

CERTIFICATE FROM THE PRINCIPAL

This is to certify that the thesis entitled **“GREEN SYNTHESIS, CHARACTERIZATION, AND EVALUATION OF *IN VITRO* ANTIMICROBIAL, ANTIOXIDANT, AND *IN VIVO* WOUND HEALING ACTIVITY OF SILVER NANOPARTICLES LOADED IN TOPICAL GEL USING HYDROALCOHOLIC ROOT EXTRACT OF *POTENTILLA FULGENS*”** being submitted by **ALAKESH BHARALI**, bearing **Roll no.: 190520011001 & Registration. no.: 387005219** of **2019-2020** in partial fulfillment of the requirement for the award degree of **Master of Pharmacy (M.Pharm) in Pharmaceutics** of the **Department of Pharmaceutics, Girijananda Chowdhury Institute of Pharmaceutical Science (GIPS)**, affiliated to **Assam Science and Technology University, Guwahati, Assam** is a bonafide assignment which is being carried out under my direct supervision and guidance.

Prof (Dr.) Gouranga Das
Principal,
Girijananda Chowdhury Institute of
Pharmaceutical Science.
Azara, Guwahati-17



GIRIJANANDA CHOWDHURY INSTITUTE OF PHARMACEUTICAL SCIENCE (GIPS)

(A unit of Shrimanta Shankar Academy)

Approved by AICTE & PCI, New Delhi, Affiliated to Assam Science and
Technology University

N.H. 37, Hathkhowapara, Azara, Guwahati-781017

Telephone: (0361) 2843405

Email: gips_guwahati@rediffmail.com

CERTIFICATE FROM THE HOD

This is to certify that the thesis entitled **“GREEN SYNTHESIS, CHARACTERIZATION, AND EVALUATION OF *IN VITRO* ANTIMICROBIAL, ANTIOXIDANT, AND *IN VIVO* WOUND HEALING ACTIVITY OF SILVER NANOPARTICLES LOADED IN TOPICAL GEL USING HYDROALCOHOLIC ROOT EXTRACT OF *POTENTILLA FULGENS*”** being submitted by **ALAKESH BHARALI**, bearing **Roll no.: 190520011001 & Registration. no.: 387005219 of 2019-2020** in partial fulfillment of the requirement for the award degree of **Master of Pharmacy (M. Pharm) in Pharmaceutics** of the **Department of Pharmaceutics, Girijananda Chowdhury Institute of Pharmaceutical Science (GIPS)**, affiliated to **Assam Science and Technology University, Guwahati, Assam** is a bonafide assignment which is being carried out under my direct supervision and guidance.

Dr. Bhanu Pratap Sahu
Associate Professor & HoD Pharmaceutics,
Girijananda Chowdhury Institute of
Pharmaceutical Science.
Azara, Guwahati-17



GIRIJANANDA CHOWDHURY INSTITUTE OF PHARMACEUTICAL SCIENCE (GIPS)

(A unit of Shrimanta Shankar Academy)

Approved by AICTE & PCI, New Delhi, Affiliated to Assam Science and
Technology University

N.H. 37, Hathkhowapara, Azara, Guwahati-781017

Telephone: (0361) 2843405

Email: gips_guwahati@rediffmail.com

CERTIFICATE FROM THE GUIDE

This is to certify that the thesis entitled **“GREEN SYNTHESIS, CHARACTERIZATION, AND EVALUATION OF *IN VITRO* ANTIMICROBIAL, ANTIOXIDANT, AND *IN VIVO* WOUND HEALING ACTIVITY OF SILVER NANOPARTICLES LOADED IN TOPICAL GEL USING HYDROALCOHOLIC ROOT EXTRACT OF *POTENTILLA FULGENS*”** being submitted by **ALAKESH BHARALI**, bearing **Roll no.: 190520011001 & Registration. no.: 387005219** of 2019-2020 in partial fulfillment of the requirement for the award degree of **Master of Pharmacy (M. Pharm) in Pharmaceutics** of the **Department of Pharmaceutics, Girijananda Chowdhury Institute of Pharmaceutical Science (GIPS)**, affiliated to **Assam Science and Technology University, Guwahati, Assam** is a bonafide assignment which is being carried out under my direct supervision and guidance during the academic session **2020-2021**.

Dr. Bhanu Pratap Sahu
Associate Professor & HoD Pharmaceutics,
Girijananda Chowdhury Institute of
Pharmaceutical Science.
Azara, Guwahati-17



GIRIJANANDA CHOWDHURY INSTITUTE OF PHARMACEUTICAL SCIENCE (GIPS)

(A unit of Shrimanta Shankar Academy)

Approved by AICTE & PCI, New Delhi, Affiliated to Assam Science and
Technology University

N.H. 37, Hathkhowapara, Azara, Guwahati-781017

Telephone: (0361) 2843405

Email: gips_guwahati@rediffmail.com

CERTIFICATE FROM THE CO-GUIDE

This is to certify that the thesis entitled **“GREEN SYNTHESIS, CHARACTERIZATION, AND EVALUATION OF *IN VITRO* ANTIMICROBIAL, ANTIOXIDANT, AND *IN VIVO* WOUND HEALING ACTIVITY OF SILVER NANOPARTICLES LOADED IN TOPICAL GEL USING HYDROALCOHOLIC ROOT EXTRACT OF *POTENTILLA FULGENS*”** being submitted by **ALAKESH BHARALI**, bearing **Roll no.: 190520011001 & Registration. no.: 387005219 of 2019-2020** in partial fulfillment of the requirement for the award degree of **Master of Pharmacy (M. Pharm) in Pharmaceutics** of the **Department of Pharmaceutics, Girijananda Chowdhury Institute of Pharmaceutical Science (GIPS)**, affiliated to **Assam Science and Technology University, Guwahati, Assam** is a bonafide assignment which is being carried out under my direct supervision and guidance during the academic session **2020-2021**.

Dr. Damiki Laloo
Associate Professor, Dept. of Pharmacognosy
Girijananda Chowdhury Institute of
Pharmaceutical Science.
Azara, Guwahati-17



GIRIJANANDA CHOWDHURY INSTITUTE OF PHARMACEUTICAL SCIENCE (GIPS)

(A unit of Shrimanta Shankar Academy)

Approved by AICTE & PCI, New Delhi, Affiliated to Assam Science and
Technology University

N.H. 37, Hathkhowapara, Azara, Guwahati-781017

Telephone: (0361) 2843405

Email: gips_guwahati@rediffmail.com

DECLARATION

I hereby declare that the thesis entitled **“GREEN SYNTHESIS, CHARACTERIZATION, AND EVALUATION OF *IN VITRO* ANTIMICROBIAL, ANTIOXIDANT, AND *IN VIVO* WOUND HEALING ACTIVITY OF SILVER NANOPARTICLES LOADED IN TOPICAL GEL USING HYDROALCOHOLIC ROOT EXTRACT OF *POTENTILLA FULGENS*”** is a bonafide and genuine research work carried out by me under the supervision of **Dr. Bhanu Pratap Sahu, Associate Professor, Department of Pharmaceutics** and **Dr. Damiki Laloo, Associate Professor, Department of Pharmacognosy, Girijananda Chowdhury Institute of Pharmaceutical Science, Azara, Guwahati-17**. The work embodied in this thesis is original and has not been submitted in part or full for the award of degree, diploma, associateship or fellowship of any other University or Institution.

ALAKESH BHARALI

Roll no.: 190520011001

Reg. no.: 387005219 of 2019-2020

Dept. of Pharmaceutics

Girijananda Chowdhury Institute of
Pharmaceutical Science.

Azara, Guwahati-17



भारत सरकार / GOVERNMENT OF INDIA
पर्यावरण एवं वन मंत्रालय / MINISTRY OF ENVIRONMENT AND FORESTS
संयुक्त निदेशक कार्यालय / OFFICE OF THE JOINT DIRECTOR
भारतीय वनस्पति सर्वेक्षण / BOTANICAL SURVEY OF INDIA
पूर्वी क्षेत्रीय केन्द्र / EASTERN REGIONAL CENTRE
शिलांग-793003 / SHILLONG-793003



दूरभाष / Telephone: 0364- 2223971, 2223618 ई-मेल / e-mail-bsibshill@yahoo.co.in Telefax: 0364 -2224119

संख्या / No.: BSI/ERC/2010/Plant identification/ 281

दिनांक /Dated: 15. 07. 2010

To,

Mr. Damiki Laloo
Research Scholar,
Dept. of Pharmaceutics
Institute of Technology
Banaras Hindu University
Varanasi-01.

Sub: - Identification of plant species- Reg.

Sir,

This is with reference to your letter no. NIL dated 15th July'10 requesting for identification of plant species, it is hereby informed that the plant species are identified as (1). *Potentilla fulgens* Wall., (2). *Potentilla polyphylla* Wall. and (3). *Agrimonia pilosa* Ledeb. var. *nepalensis* (D. Don.) Nakai. belonging to the family Rosaceae.

समन्वयवाद / Thanking you.

भवदीय /Yours faithfully

(Dr. N. Odyuo)
Scientist C- in charge

Certificate
This is to certify that the project proposal no. GIPS/IAEC/MPH/PRG/01/2021 entitled
"Green Synthesis, Characterization and Evaluation of Antimicrobial and Wound Healing Activity of
silver nanoparticles loaded in nanogel using Hydroalcoholic extract of *Potentilla fulgens*" submitted by
Mr. Alakesh Bhattacharya has been approved/recommended by the IAEC of Gurjananda Chowdhury
Institute of Pharmaceutical Science, Azara, Guwahati-781017 in its meeting held on 25/02/2021 and
..... (Number and Species of animals) have been sanctioned under this.
06 Rats

Authorized by

Name

Signature

Date

Chairman:

Gouranga Das



02.03.2021

Member Secretary:

Gouranga Das



02.03.2021

Main Nominee of
CPCSEA:

Dr. Smriti Lakshmi Das



02.03.21

(Kindly make sure that minutes of the meeting duly signed by all the participants are
maintained by Office)

Background and Rationale: Nanoparticle systems are being explored widely because of their advantages of increased solubility, bioavailability, and efficacy. However, conventional synthesis methods require the use of hazardous chemicals and also produce particles of non-uniform size. The present study focuses on the green synthesis of silver nanoparticles (AgNPs) by using hydro-alcoholic root extract of the *Potentilla fulgens* and thereby evaluating its antioxidant and wound healing activity.

Methodology: After collection, drying, and grinding, extraction of the plant was carried out. For the optimum synthesis of AgNPs, different concentrations of silver nitrate were allowed to react with different concentrations of plant extract. The optimum formulation was characterized by using a UV-visible spectrophotometer, transmission electron microscopy (TEM), Fourier transform infrared spectrometer (FTIR), and X-ray diffraction (XRD). The antioxidant potential of the AgNPs-PF was evaluated using 2,2-diphenyl-1-picrylhydrazyl (DPPH) free radical scavenging assay. Further, the AgNPs-PF were loaded into a topical gel and evaluated for *in vivo* wound healing potential in experimental rats. For the *in vivo* experiment, after creating the cutaneous wound, the rats were randomly divided into five groups and treated for 21 days. For histopathological analysis, a 3x3 cm section was prepared from the wound area on day 21. All data of antioxidant and cutaneous wound-healing examinations were analyzed using student t-test and 2 way ANOVA respectively.

Results and Discussion: Results showed that the ratio of different concentrations of silver nitrate to plant extract significantly affected the particle size, shape, yield as well as stability of the AgNPs-PF. The appearance of the reddish-brown color indicated the completion of the reaction. A UV-visible absorption band of around 410-440 nm indicated the synthesis of AgNPs. Direct imaging by TEM showed that the AgNPs-PF were in the size range of 10-20 nm and spherical in shape. FTIR analysis revealed the presence of phenols, terpenoids, and

ABSTRACT

flavonoids responsible for the reduction and stabilization of the AgNPs. XRD pattern confirmed the crystallinity of the synthesized AgNPs-PF. The studies of phytochemical analysis of nanoparticles indicated that the adsorbed components on the surface of nanoparticles were mainly polyphenolics in nature. Homogenous AgNP-PF loaded gel was obtained with desired physicochemical properties. The use of AgNPs-PF gel in the treatment groups substantially reduced the wound area and remarkably raised the wound contracture, fibrocytes and fibroblast compared with other groups excepting the standard control.

Conclusion: Results suggested that green synthesis is an efficient and effective method for the synthesis of AgNPs. Seemingly, AgNPs can be used as a medical supplement owing to their antioxidant and cutaneous wound-healing properties. Further, *in vitro* antibacterial potential and biochemical estimations are under process.

Keywords: Green synthesis, silver nanoparticles, antioxidant, wound healing.

ACKNOWLEDGEMENT

“Never stop fighting until you arrive at your destined place-that is, the unique you. Have an aim in life, continuously acquire knowledge, work hard, and have perseverance to realize the great life.”

-A.P.J Abdul Kalam

I humbly submit my dissertation work, to the hands of Almighty, who is the source of all wisdom and knowledge for the successful completion of my thesis. It is a great time for me to acknowledge those without whom this work would not be fruitful.

First and foremost I want to express a deep sense of gratitude to my esteemed co-guide, **Dr. Damiki Laloo** (M.Pharm., Ph.D., PGDS; Associate Professor, Dept. of Pharmacognosy), and my guide, **Dr. Bhanu Pratap Sahu** (M.Pharm., Ph.D., Post-Doc. Associate Professor, Dept. of Pharmaceutics), for their erudite guidance, support, and perpetual encouragement.

I want to pay all my homage and emotions to my mother **Mrs. Mridula Bharali** and sister **Miss. Swity Bharali** for their precious love, affection, and moral support which guided me on the right path and also the backbone for all successful endeavors in my life.

I consider it is a great privilege & honor to had the opportunity to undergo the project work in **Girijananda Chowdhury Institute of Pharmaceutical Science**, Guwahati, Assam. Hence, I owe a deep debt of gratitude to principal of GIPS, **Prof. (Dr.) Gouranga Das**, M. Pharm, and Ph. D who has allowed me to go through a practical project.

ACKNOWLEDGEMENT

It is my pleasure to express my sedulous gratitude to **Dr. Biswajit Das** (M.Pharm., Ph.D., Ex- Assistant Professor, Dept. of Pharmaceutics) for his invaluable advice and guidance.

I consider it a great honor to express my deep sense of gratitude and indebtedness to **Mr. Suman Kumar** and **Mr. Susankar Kushari**, M.Pharm; Ph.D. (pursuing); Assistant Professor; Department of Pharmaceutical Chemistry for their continued encouragement, helping hand in every aspect, patient guidance and invaluable advice.

I extend my profound gratitude and respectful regards to all the teaching and non-teaching staff for providing adequate facilities in the institution to carry out this work.

I owe my gratitude and thanks to **Prof. (Dr.) Pritam Mohan**; College of Veterinary Science, Assam Agricultural University; for helping me in pursuing the animals.

Words can't express my sincere gratitude and obligation to **Mr. Himangsho Sharma**, Junior Research Fellowship (JRF), Institute of Advanced Study in Science and Technology (IASST) for his support, co-operation, and constant inspiration.

I would like to thank, **Mr. Biren Kalita**, Animal Caretaker, Animal House, GIPS for his constant support and helping hand during the *in vivo* study.

I wish to extend my special thanks to my friends **Mr. Sivam Nayak**, **Miss. Santa Sarma**, **Mr. Damanbhalang Rynjah**, **Mr. Bhargab Deka** for their kind support and cooperation.

ACKNOWLEDGEMENT

I would like to thank my batch mates, seniors, and juniors who directly or indirectly helped during my work.

My sincere thanks to all those who have directly or indirectly helped me to complete this project work.

Once again, Special and heartfelt thanks to my co-guide **Dr. Damiki Laloo** (M.Pharm., Ph.D., PGDS; Associate Professor, Dept. of Pharmacognosy) for his constant holding hands during the entire project work.

Alakesh Bharali

It is with great pleasure and privilege to submit this project work in its current form. The progress of scientific research has been increasing substantially in the last two decades particularly in the field of Pharmacy. And the most growing field is the use of nanotechnology for various pharmaceutical and biological applications. However, conventional synthesis methods require the use of hazardous chemicals and also produce particles of non-uniform size. The present study focuses on the green synthesis of silver nanoparticles (AgNPs) by using hydro-alcoholic root extract of the *Potentilla fulgens* and thereby evaluating its antioxidant and wound healing activity.

The current investigation consists of different chapters which include:

- **Chapter 1:** Dealing with the introduction of nanoparticles, different methods of synthesis of nanoparticles, introduction to green synthesis, necessity and benefits of green synthesis, green synthesis of silver nanoparticles from different plants, and its characterization using analytical techniques.
- **Chapter 2:** Deals with the literature survey of the plant *Potentilla fulgens* Wall. ex Hook and recent studies on green synthesis and pharmacological applications of silver nanoparticles.
- **Chapter 3:** Deals with the aim and objective of the research work and the comprehensive plan of work of the current research.
- **Chapter 4:** Deals with the detailed procedures of the materials and methods incorporated while performing the extraction, biosynthesis, characterization, quantitative estimation of polyphenolics, formulation and characterization of a topical gel, and evaluation of *in vitro* antioxidant and *in vivo* wound healing activity of silver nanoparticles.

- **Chapter 5:** Deals with the compilation of all the results obtained after performing the research work.
- **Chapter 6:** It is the drafted summary and conclusion of the whole work performed and the future perspective of the study.

CONTENTS

CHAPTER	CONTENTS	PAGE NO.
1	INTRODUCTION	1-21
2	LITERATURE REVIEW	22-62
3	AIM AND OBJECTIVES	63-64
4	MATERIALS AND METHODS	65-88
5	RESULTS AND DISCUSSION	89-117
6	SUMMARY AND CONCLUSION	118-122
	BIBLIOGRAPHY	123-142
	PUBLICATIONS	143-145

LIST OF TABLES

SL. NO.	TABLE NO.	PARTICULARS	PAGE NO.
1	1.1	Different plants used for the synthesis of silver nanoparticles	7
2	2.1	Ethnomedicinal and traditional uses of <i>P. fulgens</i> in the higher and lower Himalayan regions	27
3	4.1	List of chemicals used	65
4	4.2	List of major instruments and equipment used	67
5	5.1	Comparative data of UV, PDI, Z-average after till 1 month	91
6	5.2	Quantification of total major phenolic, simple phenolic, tannin, and flavonoid content in AgNPs-PF	106
7	5.3	IC ₅₀ values of standard quercetin and AgNPs-PF	108
8	5.4	Pharmaceutical evaluation of the plain gel formulation	109
9	5.5	Evaluation of the topical gel loaded with AgNPs-PF	111
10	5.6	Effect of topical treatment of 0.2% w/w AgNP-PF and standard 0.2% w/w AgNO ₃ gel on wound contraction in 21 days excision wounded rats.	114

LIST OF FIGURES

SL. NO.	FIGURE NO.	PARTICULARS	PAGE NO.
1	1.1	Different types of nanoparticles synthesis from plant resources	4
2	1.2	Green synthesis and applications of metallic nanoparticles in different fields	12
3	1.3	Synthesis of Silver nanoparticles using plant extract	14
4	2.1	<i>Potentilla fulgens</i> Wall. ex Hook. Plant	25
5	2.2	Distribution of <i>Potentilla fulgens</i> in India and the state of Meghalaya	25
6	5.1	Biosynthesis of AgNPs using <i>P. fulgens</i> extract	90
7	5.2 (a)	UV spectrum of 1 mg of plant extract reacting with different concentrations of silver nitrate	93
8	5.2 (b)	UV spectrum of 2.5 mg of plant extract reacting with different concentrations of silver nitrate	94
9	5.2 (c)	UV spectrum of 5 mg of plant extract reacting with different concentrations of silver nitrate	95

LIST OF FIGURES

10	5.2 (d)	UV spectrum of 10 mg of plant extract reacting with different concentrations of silver nitrate	96
11	5.3 (a)	Size distribution by the intensity of the synthesized AgNPs-PF	97
12	5.3 (b)	Statistics graph of the synthesized AgNPs-PF	97
13	5.4	Zeta potential distribution of the synthesized AgNPs-PF	98
14	5.5	FTIR spectra of the synthesized Ag-NPs-PF	99
15	5.6	TEM micrograph of the AgNPs-PF	100
16	5.7	Energy-dispersive X-ray spectroscopy (EDX) micrograph of the AgNPs-PF	101
17	5.8	Percentage of elements present in the synthesized AgNPs	102
18	5.9	X-ray diffraction (XRD) spectra of AgNPs-PF	103
19	5.10	Standard calibration curve for the estimation of total phenolic, total simple phenolic, and total tannin content	105
20	5.11	Standard calibration curve for the estimation of	106

LIST OF FIGURES

		total flavonoid content	
21	5.12	DPPH radical scavenging activity of standard quercetin and AgNP-PF synthesized from <i>P. fulgens</i>	107
22	5.13	Topical gel formulation before and after loading the silver nanoparticles	112
23	5.14	Wound structural changes and healing effects from day 0 to day 21 after treating with tested samples	113
24	5.15	Histological section of the skin tissue obtained from the 21 st day excision wound model.	116

LIST OF ABBREVIATIONS

NPs: Nanoparticles

MNPs: Metallic nanoparticles

AgNPs: Silver nanoparticles

AgNPs-PF: Silver nanoparticles biosynthesized from *Potentilla fulgens*

PDI: Polydispersity index

DLS: Dynamic Light Scattering

XRD: X-Ray Diffraction

FTIR: Fourier Transform Infrared Spectroscopy

EDX: Energy-dispersive X-ray spectroscopy

TEM: Transmission Electron Microscopy

FC: Folin-Ciocalteu

CF: collagen fibers

DE: Damaged epidermis

FC: Fibroblast cells

HF: Hair follicle

IFC: Inflammatory cells

RE: Re-epithelialization

CHAPTER-1

INTRODUCTION

1.0 Introduction

Humanity has gone through a number of technological revolutions that have had a significant impact on the course of history. The first is the Industrial Revolution that introduced steel and steam engines whereas the second introduced electricity on a large scale. The most recent, we've had the Information Revolution, which was marked by the widespread adoption of computing devices and the internet. Nanotechnology is regarded as the foundation for the next technological revolution (Buchanan *et al*; 2020).

Richard P Feynman, a Nobel Laureate in physics, first introduced the concept of nanotechnology in his famous lecture "There's Plenty of Room at the Bottom" at the American Physical Society meeting in December 1959. Since then, numerous breakthroughs in physics, chemistry, and biology have demonstrated Feynman's concepts of exploiting matter at the atomic level. In 1974, the term nanotechnology was coined by Professor Norio Taniguchi. Modern nanotechnology was born with the development of a scanning tunneling microscope that could visualize matter at the individual atomic level (Benelmekki *et al*; 2005).

Nanotechnology is a broad-based branch of science and technology that deals with the design and development of material at the nanoscale level, i.e., 1-100 nm (Panda *et al*; 2020). It has sparked a lot of interest because of its broad array of applications in medicine, agriculture, surface science, marine science, space science, geology, geography, biology, physics, and chemistry (Lin *et al*; 2007).

The global nanotechnology market expanded rapidly during the past decade. It was valued at \$1,055.1 million in 2018 and is expected to reach \$2,231.4 million by the year 2025, growing at a CAGR of 10.5% from 2019 to 2025. (<https://www.alliedmarketresearch.com/nanotechnology-market>). The European Union (EU) designated nanotechnology as a priority in research in the year 2002. The majority of the developed and developing countries today have national nanotechnology programs. As per the United States National Nanotechnology Initiative (NNI) budget, the total investment for nanotechnology research and development was \$ 1,853.3 million in 2019. This will lead to discoveries that will advance a wide range of areas including medicine and industries of the future (<https://www.nano.gov/about-nni/what/funding>).

1.1 Nanoparticles

Nanoparticles are defined as particles in the size range of 1–100 nm with one or more dimensions. They can be made up of one or more atomic or molecular species and have a variety of size-dependent properties. Within this size range, the particles exhibit novel physical, chemical, and biological characteristics as compared to the individual atoms/molecules or the mass material (Johnston *et al*; 2012). This is due to the higher surface area to volume ratio, increased reactivity or stability in a chemical reaction, increased mechanical strength, and so on (Hasan *et al*; 2015). These unique properties of NPs made it a material of the 21st century.

NPs exist in different sizes, shapes, and structures such as spheres, cones, cylinders, flat, tubes, or irregular. Some nanoparticles are crystalline or amorphous, with single or multi-crystal solids that can be loose or clumped together. The surface modifications on

nanoparticles are usually tailored to meet the needs of the specific applications for which they will be used (Ealia *et al*; 2017). The immense diversity of NPs arising from morphology, shape, nature, dispersion state of the particles, and most importantly numerous possible surface modifications to which NPs can be subjected makes this an influential field of science and research today.

1.2 Metallic nanoparticles

Noble metal nanoparticles, such as Ag (Silver), Ti (Titanium), Pt (Platinum), Au (Gold), and Pd (Palladium) are the most successfully studied nanoparticles today. These metallic nanoparticles are widely applied in products that directly come in contact with the human body, such as shampoos, soaps, detergents, shoes, cosmetic products, and toothpaste, besides medical and pharmaceutical applications (Antony *et al*; 2017). There is a growing interest in noble metal nanoparticles as they provide superior material properties with functional versatility. Due to their size, features, and advantages over available chemical imaging drug agents and drugs, inorganic particles have been examined as potential tools for medical imaging as well as for treating diseases. Inorganic nanomaterials have been widely used for cellular delivery due to their versatile features like wide availability, rich functionality, good compatibility, and capability of targeted drug delivery and controlled release of drugs (Xu *et al*; 2009). Fig. 1.1 shows different types of metallic nanoparticles synthesized from plant resources.

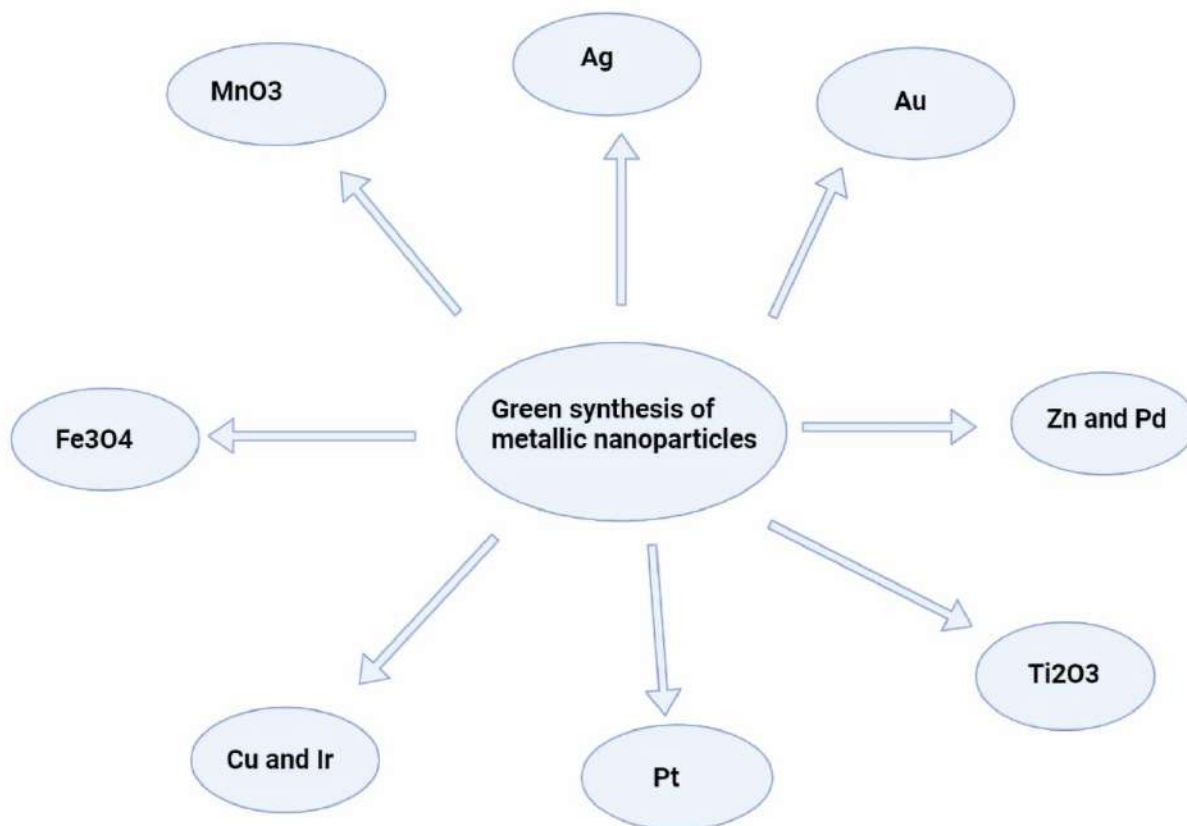


Figure 1.1 Different types of nanoparticles synthesis from plant resources

1.3 Different methods for nanoparticle synthesis

Currently, a large number of physical, chemical, biological, and hybrid methods are available to synthesize different types of nanoparticles (Zhang *et al*; 2016).

1.3.1 Physical methods

Nanoparticles are prepared by evaporation-condensation using a tube furnace at atmospheric pressure. Conventional physical methods including spark discharging and

pyrolysis were used for the synthesis of AgNPs. The advantages of physical methods are speed, radiation used as reducing agents, and no hazardous chemicals involved, but the downsides are low yield and high energy consumption, solvent contamination, and lack of uniform distribution (Zhang *et al*; 2016).

1.3.2 Chemical methods

This method uses water or organic solvents to prepare the silver nanoparticles. This process usually employs three main components, such as metal precursors, reducing agents, and stabilizing/capping agents. Basically, the reduction of silver salts involves two stages:

(1) Nucleation

(2) Subsequent growth

In general, “top-down” and “bottom-up” are the two methods by which nanoparticles can be prepared.

In the “top-down” method mechanical grinding of bulk metals with subsequent stabilization using colloidal protecting agents occurs. “Bottom-up” methods include chemical reduction, electrochemical methods, and sono decomposition. High yield is the major advantage of the chemical method compare to the physical method. These methods are extremely expensive and the chemical reagents used are Thio-glycerol, 2-mercaptoethanol, citrate, borohydride are toxic and hazardous. And also the manufactured particles are not of expected purity, as their surfaces were found to be settled with chemicals. Preparation AgNPs with definite size along with the prevention of agglomeration is very difficult as well as in chemical methods toxic and hazardous chemicals are excised out as byproducts (Ahmed *et al*, 2016).

1.3.2 Biological methods

Biological methods have emerged to overcome all the problems related to physical and chemical methods. Silver nanoparticles are synthesized with definite size using different biological systems including bacteria, fungi, plant extracts, and small biomolecules like vitamins and amino acids as an alternative method to chemical methods not only for AgNPs but also for the synthesis of several other nanoparticles.

In recent years, the development of efficient green chemistry methods employing natural reducing, capping, and stabilizing agents to prepare silver nanoparticles with desired morphology and size has become a major focus of researchers. Biological methods can be used to synthesize silver nanoparticles without the use of any harsh, toxic and expensive chemical substances. The bioreduction of metal ions by combinations of biomolecules found in the extracts of certain organisms (eg enzymes/proteins, amino acids, alkaloids, alcohol, polysaccharides, and vitamins) is eco-friendly (Iravani *et al*; 2013).

Biologically-mediated synthesis of nanoparticles is simple, cost-effective, dependable, and environmentally friendly approaches and much attention has been given to the high yield production of AgNPs.

1.4 Green synthesis of metallic NPs

Green chemistry introduces a new approach to the synthesis of nanoparticles for reducing threats to the environment and health (Bhosale *et al*, 2014). These new approaches are known as

- Environmentally Benign Chemistry

- Clean Chemistry
- Atom Economy
- Benign-by-design Chemistry

The basic idea of green synthesis is to protect the environment from pollution. Thus, the goal of green synthesis is to create better, safer chemicals while choosing the safest and most efficient ways to synthesize them and reduce wastes (Ahmed *et al*; 2011).

A large number of plants are reported to facilitate silver nanoparticles synthesis which are reported as:

Table 1.1: Different plants used for the synthesis of silver nanoparticles

Plants	Plant part used	Size (nm)	Shape	References
<i>Aloe vera</i>	Leaves	50.350	Spherical and triangular	Chandran <i>et al</i> ; 2006
<i>Allium sativum</i>	Leaves	4–22	Spherical	Ahmed <i>et al</i> ; 2011
<i>Acorus calamus</i>	Rhizome	31-32	Spherical	Nakkala <i>et al</i> ; 2014

<i>Abutilon indicum</i>	Leaves	7-17	Spherical	Sadeghi <i>et al</i> , 2015
<i>Acalypha indica</i>	Leaves	0.5	Spherical	Kumarasamyraja <i>et al</i> ; 2013
<i>Argyreia nervosa</i>	Seeds	20-50	-	Thombre <i>et al</i> ; 2014
<i>Alternanthera dentate</i>	Leaves	50-100	Spherical	Nakkala <i>et al</i> ; 2014
<i>Brassica rapa</i>	Leaves	16-17	-	Narayanan <i>et al</i> ; 2014
<i>Boerhaavia diffusa</i>	Whole plant	25	Spherical	Suna <i>et al</i> ; 2014
<i>Carum copticum</i>	Seeds	21	Spherical and triangular	Qais <i>et al</i> ; 2020
<i>Cocous nucifera</i>	Inflorescence	22	Spherical	Mariselvam <i>et al</i> ; 2014

<i>Cymbopogon citratus</i>	Leaves	32	-	Masurkar <i>et al</i> ; 2011
<i>Carica papaya</i>	Leaves	25-50	-	Jain <i>et al</i> ; 2009
<i>Citrus sinensis</i>	Peel	10-35	Spherical	Kaviya <i>et al</i> ; 2011
<i>Coccinia indica</i>	Leaves	10-20	-	Kumar <i>et al</i> ; 2013
<i>Centella asiatica</i>	Leaves	30-50	Spherical	Rout <i>et al</i> ; 2013
<i>Datura metel</i>	Leaves	16-40	Quasilinear superstructures	Kesharwani <i>et al</i> ; 2009
<i>Eclipta prostrate</i>	Leaves	35-60	Triangles, pentagons, hexagons	Rajakumar <i>et al</i> ; 2011
<i>Ficus carica</i>	Leaves	13	-	Geetha <i>et al</i> ; 2014

<i>Garcinia mangostana</i>	Leaves	35	-	Veerasamy <i>et al</i> ; 2010
<i>Moringa oleifera</i>	Leaves	57	-	Prasad <i>et al</i> ; 2011
<i>Teucrium polium</i>	Leaves	70-100	Spherical	Hashemi <i>et al</i> ; 2020
<i>Peganum harmala</i>	Leaves	184	Spherical	Alomar <i>et al</i> ; 2020
<i>Tagetes erecta</i>	Flowers	24-29	Spherical	Katta <i>et al</i> ; 2021
<i>Withania coagulans</i>	Leaves	14	Spherical	Tripathi <i>et al</i> ; 2019
<i>Zephyranthes rosea</i>	Flowers	10-30	Spherical	Maheshwaran <i>et al</i> ; 2020

Due to their size, features, and advantages over available chemical imaging drug agents and drugs, biologically synthesized metallic nanoparticles have been examined as potential tools for medical imaging as well as for treating diseases. Metallic nanoparticles

have been widely used for cellular delivery due to their versatile features like wide availability, rich functionality, good compatibility, and capability of targeted drug delivery and controlled release of drugs (Xu *et al*; 2009). Figure 1.2 represents the green synthesis and applications of metallic nanoparticles in biomedical and environmental fields.

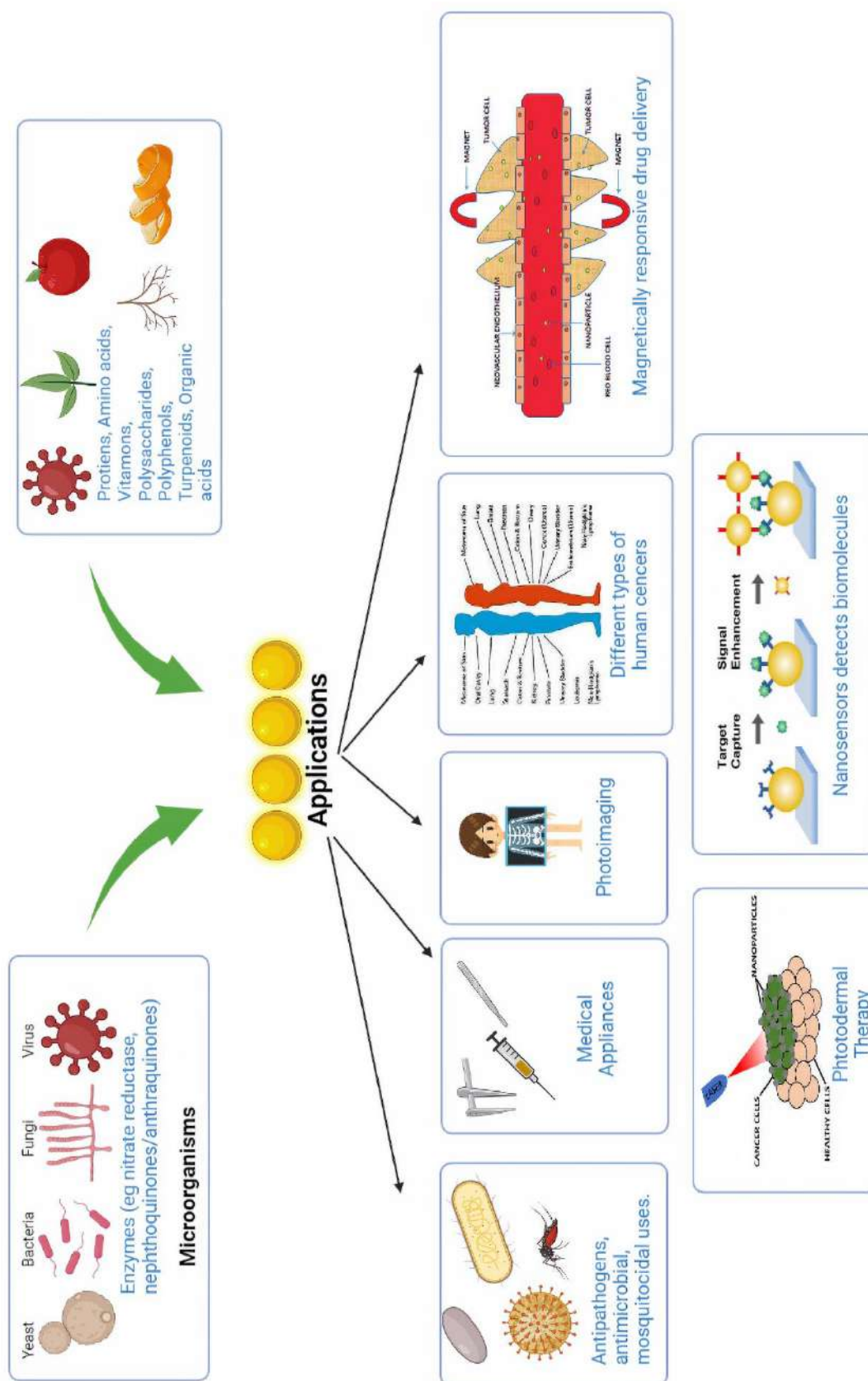


Figure 1.2: Green synthesis and applications of metallic nanoparticles in different fields

1.4.1 Need for green synthesis

Biosynthesis of nanoparticles is a kind of bottom-up approach where the main reaction occurring is reduction/oxidation. The need for the biosynthesis of nanoparticles rose as the physical and chemical processes were costly. Often, the chemical synthesis method leads to the presence of some toxic chemical absorbed on the surface that may have adverse effects in medical applications (Parasharu *et al*; 2009). This is not an issue when it comes to biosynthesized nanoparticles via the green synthesis route. So, in the search for cheaper pathways for nanoparticle synthesis, scientists used microbial enzymes and plant extracts (phytochemicals). With their antioxidant or reducing properties, they are usually responsible for the reduction of metal compounds into their respective nanoparticles. Green synthesis provides advancement over chemical and physical methods as it is cost-effective, environment friendly, easily scaled up for large-scale synthesis and in this method, there is no need to use high pressure, energy, temperature, and toxic chemicals (Begum *et al*; 2009).

1.4.2 Benefits of green synthesis of nanoparticles

Biological methods of synthesis have thus paved the way for the “greener synthesis” of nanoparticles and these have proven to be better methods due to slower kinetics (Qais *et al*; 2020). They offer better manipulation, control over crystal growth, and stabilization. This has motivated an upsurge in research on the synthetic routes that allow better control of shape and size for various nanotechnological applications. The use of environmentally benign materials like plant extracts, bacteria, fungi and enzymes (Tamilarasi *et al*; 2020) for the synthesis of silver nanoparticles offer numerous benefit listed as:

- Eco-friendly
- Simple and cheap
- Good Yield
- No hazardous waste
- Safe, effective and energy efficient
- Low cost of production and regulation (Sahayaraj *et al*; 2020).

1.5 Green synthesis of silver nanoparticles using plant extracts

The plant extract has been used in the production of silver nanoparticles and has drawn attention due to its rapid, eco-friendly, non-pathogenic, and providing a single-step technique for the biosynthetic processes. The biomolecules present in the plant extract such as proteins, amino acids, enzymes, polysaccharides, alkaloids, tannins, phenolics, saponins, terpenoids, and vitamins are responsible for the reduction and stabilization of silver ions.

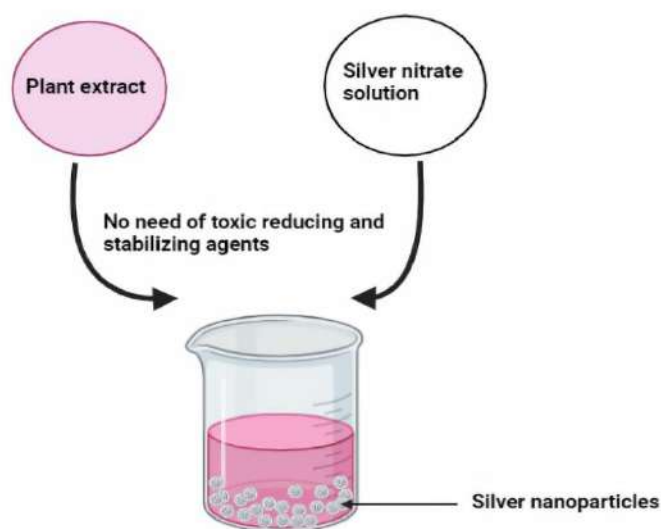


Figure 1.3: Synthesis of Silver nanoparticles using plant extract

1.5.1 Nanosilver

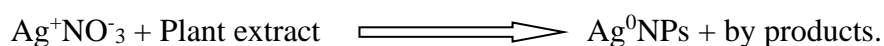
One of the substances used in nanoformulation is silver (nanosilver). Due to its antimicrobial properties, silver has also been incorporated in filters to purify drinking water and clean swimming pool water. Earlier, the antifungal properties of silver and silver nitrate were well incorporated in the field of medical science. Also, the medicinal importance of innumerable plants and plant parts was known. But the plant-mediated silver nanoparticle is a relatively newer concept. Nanobiotechnology and their derived products are unique not only in their treatment methodology but also due to their uniqueness in particle size, physical, chemical, biochemical properties, and the broad range of applications as well. This current emerging field of nanobiotechnology is at the primary stage of development due to the lack of implementation of innovative techniques on a large industrial scale and yet has to be improved with modern technologies. Hence, there is a need to design an economic, commercially feasible as well environmentally sustainable route of synthesis of Ag NPs to meet its growing demand in diverse sectors (Banerjee *et al*; 2014).

1.5.2 Bio-reduction mechanism of AgNP synthesis

Plant crude extract contains novel secondary metabolites such as phenolic acid, flavonoids, alkaloids, and terpenoids in which these compounds were mainly responsible for the reduction of ions into bulk metallic nanoparticles formation. These primary and secondary metabolites present have hydroxyl and ketonic groups which can bind to the metals and reduce the metal salt and provide stability against agglomeration. The extract from the plant releases proteins and enzymes into the silver nitrate solution in which the Ag⁺ ions combine with the enzyme to form an enzyme-substrate complex. The enzymes act on the

silver ions and silver nanoparticles are released. The silver nanoparticles combine with the protein released from the extract and there is a formation of protein capped silver nanoparticles (Yu *et al*; 2013). The reduction mechanism takes place as follows. When the precursor is added, it first forms a complex by breaking the –OH bond and forming a partial bond with the metal ion. The transfer of electrons takes place next, reducing the metal ions to nanoparticles (Tamilarasi *et al*; 2020).

The biochemical reaction of AgNO₃ reacts with plant broth leads to the formation of AgNPs by following reaction (Tripathy *et al*; 2019).



1.5.3 Plants are better synthesizers for NPs

Metal nanoparticles preparation using plants (inactivated plant tissue, plant extracts, and living plants) is an important branch of biosynthesis processes. It has long been known that plants have the potential to reduce metal ions both on their surface and in various organs and tissues remote from the ion penetration site (Makarov *et al*; 2014). Biomolecules existing in plant extracts including enzymes, proteins, amino acids, vitamins, polysaccharides, and organic acids such as citrates are potentially able to reduce metal ions. In this regard, in vitro approaches have been successfully developed in recent years, in which plant extracts are used for the bio-reduction of metal ions to form their nanoparticles. The extract of various parts of plants such as leaves, flowers, seeds, barks, and roots have been applied for the synthesis of AgNPs (Bar *et al*; 2009; Marambio and Hoek; 2010;

Velayutham *et al*; 2013). The plant's extracts may work both as reducing and capping agents in AgNPs synthesis.

In the present scenario of nanotechnology, plants are better synthesizers as compared to the other biological methods. The advantages of using plant extracts over microorganism, sugars are:

- The rate of synthesis is faster
- Provide a highly desirable system for nanoparticle synthesis because plants produce a wide range of secondary metabolites with strong reducing potential.
- Less sensitive to metal toxicity compared to algae and bacteria
- Control the size and shape of nanoparticles by providing capping layers to nanoparticles

1.5.3.1 Different parts of the plant used to produce metallic NPs

Recently, the plant-mediated nanomaterial has drawn more attention due to its vast application in various fields due to its physic-chemical properties. The different metallic nanoparticles such as gold, silver, platinum, zinc, copper, titanium oxide, magnetite, and nickel were synthesized from natural resources and have been studied exclusively. The different parts of plants such as stem, root, fruit, seed, callus, peel, leaves, and flowers are used to synthesize metallic nanoparticles in various shapes and sizes by biological approaches. Biosynthesis reactions can be altered by a wide range of metal concentrations and amount of plant extract in the reaction medium, which may transform the shapes and sizes of the nanoparticles (Chandran *et al*; 2006; Dubey *et al*; 2010).

1.6 AgNP characterization

Nanoparticles are generally characterized by their size, shape, surface area, and dispersity (Mittal *et al.*, 2013). The common techniques to evaluate nanoparticle characteristics can be classified into two main groups namely; quantitative and qualitative. These methods include a range of various sophisticated techniques like dynamic light scattering (DLS), scanning electron microscopy (SEM), energy dispersive spectroscopy (EDS), UV Vis spectroscopy, transmission electron microscopy (TEM), X-ray diffraction (XRD), Fourier transform infrared spectroscopy (FT-IR), Surface Enhanced Raman spectroscopy (SERS), atomic force microscopy (AFM), high angle annular dark-field (HAADF), atomic absorption spectroscopy (AAS), inductively coupled plasma (ICP) and X-ray photoelectron spectroscopy (XPS) (Rajasekharreddy *et al.*; 2010; Mittal *et al.*; 2015). AgNP characteristics can be studied using some of these techniques which in turn, are helpful to resolve diverse parameters such as particle size, shape, crystallinity, fractal dimensions, pores size, and surface area (Ingale and Chaudhari; 2013).

1.7 Wound healing potential of silver nanoparticles

Wound healing is a multifaceted process, consisting of coagulation, inflammation, tissue formation, and epithelialization (Tian *et al.*; 2007). The normal wound-healing process involves inflammation at the injury site, angiogenesis followed by granulation, tissue growth, connective tissue, and epithelium repair along with remodeling to heal the wound completely. Inflammatory pathways and cytokine modulation influence the healing process, and many immunological mediators and microbial colonization can slow the repair of an injured site (Atiyeh *et al.*; 2007). While early inflammatory effects help in abolishing

microbial infection, prolonged inflammatory responses can lead to tissue damage. Microbial pathogens in the wound fluid produce toxins and enzymes that prolong the inflammatory responses and hence delay the wound recovery. Rapid wound repair with minimal scarring is essential to avoid these complications (Wright *et al*; 1998).

Topical antimicrobials offer a prophylactic answer to some of these issues but, with the risk of resistance, are less helpful in wound therapy. Conventionally, silver-based products containing silver compounds were recommended in wound management for their bactericidal properties. However, high application frequency has led to reports of inflammatory effects and cosmetic defects (Atiyeh *et al*; 2007). With the aid of nanotechnology, the solubility and surface properties of silver can be improved by the formation of silver nanoparticles (AgNPs). AgNPs display distinguishing physicochemical and biological properties on account of tailored surface and size characteristics (Rai *et al*; 2009). AgNPs have a higher surface area and can markedly increase the release rate of singly charged silver, the soluble and most biologically active form of silver.

The AgNPs have multiple antimicrobial mechanisms. On exposure to moisture or wound fluid at the wound surface, AgNPs are oxidized and release charged silver ions. The charged form of silver causes cell membrane damage by interacting with cell surface proteins of pathogenic microorganisms and penetrating inside the cell (Wong *et al*; 2010). Intracellular charged AgNPs prevent DNA replication, inactivate the bacterial respiratory enzymes and impede cell division, resulting in cell lysis. Additionally, charged AgNPs are capable of generating free radicals with remarkable bactericidal potential (Anisha *et al*; 2013 and Liu *et al*; 2013). This leads to enhanced antimicrobial efficacy demonstrated by

AgNPs. On the other hand, the improved surface features of AgNPs also carry the risk of aggregation owing to instability. Unstable AgNPs interact with or accumulate in normal cell organelles, leading to cytotoxicity (Moulton *et al*; 2010) Thus, it becomes imperative to balance the wound healing efficacy of AgNPs against their toxicity.

The activity and toxicity of nanoparticulate systems are associated with their synthesis method, reducing agent, nature, concentration, and physicochemical characteristics (Mijnendonckx *et al*; 2013). Nanoparticles are synthesized and stabilized via physicochemical methods: electrochemical, reduction, vapor deposition, and a microwave-assisted process. However, contamination from precursors, use of toxic solvents, hazardous byproducts, and environmental concerns limit the application of these techniques. Green synthesis is a well-established route of nanoparticulate synthesis that is safe because it eliminates the toxicity arising from physicochemical approaches (He *et al*; 2013). Green synthesis employs plants, algae, fungi, yeasts, bacteria, and their products to synthesize nanoparticles. Plants and plant extracts are preferred for the green synthesis of nanoparticles over others as they are easy to handle, readily available, and economical (Iravani *et al*; 2011).

Potentilla fulgens Wall. ex Hook (Rosaceae) is a short, slender herb that is commonly used as medicine by various tribes of the Northern and North-Eastern states of India. It is commonly called ‘Himalayan Cinquefoil’ (English), ‘Bajradanti’ (Assamese and Hindi), and ‘Lynniangbru’ (Khasi tribes of Meghalaya). The roots are used traditionally to treat various diseases, ailments such as gastric ulcers, mouth ulcers, diabetes, diarrhea, gingivitis, and also to cure mouth and gum problems (Laloo *et al*; 2013). In northern parts

of India (Uttarakhand), the roots of the plant are commonly used to treat wounds and tiger bites (Kaul *et al*; 2011). Hence, based on the evidence of such traditional practice as medicine, the present study was designed to scientifically validate the *in vivo* wound healing efficacy of topical AgNPs synthesized with roots of *Potentilla fulgens*.

CHAPTER-2

LITERATURE REVIEW

2.0 Literature Review

In this era, nanotechnology is one of the most interesting areas which are used to describe the creation and utilization of materials with structural features between those of atoms and bulk materials with at least one dimension in the nano range. Processes used for nanoparticle synthesis are chemical, physical, and a recently developed biological method. The biological method has an advantage over chemical and physical methods of nanoparticle synthesis, as it is cost-effective and environmentally friendly (Nabhikha *et al*; 2009). The major biological systems involved in this are bacteria, fungi, and plant extracts (Prabhu and Poulose; 2012). In recent years, the biosynthesis of nanoparticles using plant extracts has gained more importance. The synthesis and applications of silver nanoparticles from several plants have been studied by many researchers (Kumar *et al*; 2010; Saxena *et al*; 2010; Ahmad *et al*; 2010).

In recent years, the use of ethnobotanical information in medicinal plant research has gained considerable attention in some segments of the scientific community. These medicinal plants are considered a rich resource of phytochemicals that can be used in drug development and synthesis. Bioresources are primary (carbohydrates, proteins, and amino acids) and secondary metabolites (steroids, flavonoids, phenolics, glycosides, saponins, tannins, terpenoids, and coumarins) that impart medicinal properties to the plants (Ayyanar *et al*; 2011).

2.1 Plant Profile: *Potentilla fulgens* Wall. ex Hook.

2.1.1 Taxonomical Classification (Tantawy *et al*; 2003)

<i>Kingdom</i>	: Plantae
<i>Phylum</i>	: Magnoliophyta
<i>Class</i>	: Angiospermae
<i>Order</i>	: Rosales
<i>Tribe</i>	: Potentilleae
<i>Subfamily</i>	: Rosoideae
<i>Genus</i>	: <i>Potentilla</i>
<i>Species</i>	: <i>fulgens</i>

2.1.2 Vernacular Names (Panigrahi and Dixit, 1980; Manandhar *et al*; 2002)

- ✓ **English** : Himalayan Cinquefoil
- ✓ **Sanskrit** : Vajradant
- ✓ **Hindi** : Bajradanti
- ✓ **Assamese** : Bajradanti
- ✓ **Khasi** : Lymniang bru or Lymniang kynthai
- ✓ **Bengali** : Bhuitara
- ✓ **Uttarakhand** : Akanada or Dentamanjari
- ✓ **Tibetan** : San ge zil pa
- ✓ **Nepali** : Ganephul or Dentamanjari

2.1.3 General description and geographical distribution

Potentilla fulgens Wall. (Figure 2.1) is a herb that is used as medicine in higher and sub-Himalayan regions. It is found to be well distributed mostly in Asian countries such as India, China, Nepal, Tibet, Bhutan, Korea, and Japan. In India, the plant is found mainly in

the Northern part viz. Jammu and Kashmir, Himachal Pradesh, Uttarakhand, West Bengal, and North Eastern regions of India such as Sikkim, Assam, Meghalaya, Nagaland, Manipur, and Arunachal Pradesh (Figure 2.2). The plant grows well in temperate, higher Himalaya, and alpine regions up to an altitude of 1800–4350 m ASL. The species was found mostly in open meadows and grassy slopes of the Himalayas growing along with oaks and *Rhododendron campanulatum* trees (Panigrahi and Dixit; 1980). The plant can be reproduced and cultivated by both sexual (seeds) and asexual (underground parts) methods (Bliss *et al*; 1971). In extreme rainfall and wild habitats of the state Meghalaya the plant grows vigorously and was reported to have a symbiotic association with an endophytic fungus *Pennicilium verruculosum*. The fungal endophyte is being explored for the early establishment of its seedlings and successful micropropagation (Bhagobaty *et al*; 2010). According to Pokhriyal *et al*; 1990, *Potentilla fulgens* was placed under the class of non-leguminous nitrogen-fixing plant since the roots were found to bear nodules on its surface. Throughout the Northeastern regions of India, the whole plant is valued for its potent ethnomedicinal properties and is receiving much attention for its domestication and commercialization, since the species is listed under the endangered category due to over-harvesting and deforestation from natural habitats (Laskar *et al*; 2005).

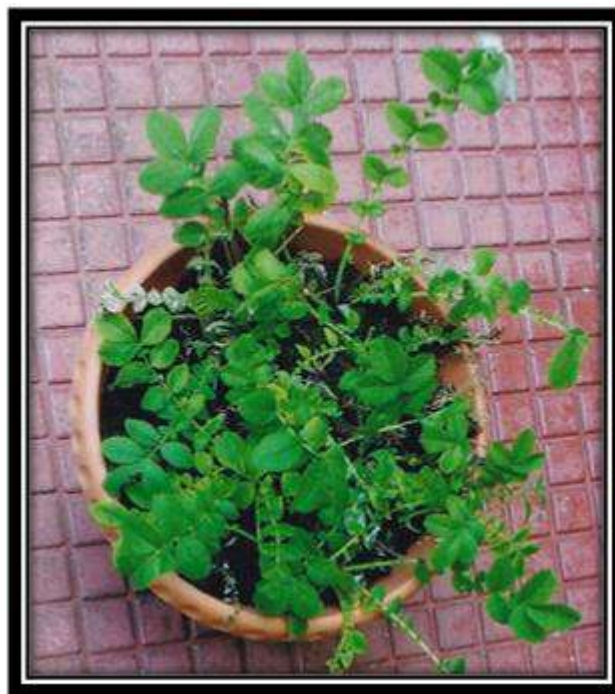


Figure 2.1: *Potentilla fulgens* Wall. ex Hook. Plant



Figure 2.2: Distribution of *Potentilla fulgens* in India and the state of Meghalaya

2.1.4 Taxonomical and Botanical description

The plant is an erect perennial herb, 15–75 cm high, with a thick rootstock, pinnate leaves, and yellow flowers (Panigrahi and Dixit; 1980; Gaur *et al*; 1999). It possesses both radical and cauline leaves. Radical leaves are 4–30 cm long, possessing 5–13 pairs of leaflets which are alternately large and small and diminish in size from uppermost and downwards; terminal leaflets are oblong or broadly obovate, 1.5–4 x 0.8–1.5cm in size, with closely and sharply toothed margins and silky tomentose abaxial surface. Cauline leaves are also abaxially white and sericeous; the leaf blade resembles that of radical leaves but has fewer pairs of leaflets. Flowers 1–2 cm in diameter are crowded in terminal corymbs. The floral pedicel is 2–4 cm long and bears gland-tipped multicellular and unicellular hairs. Sepals have entire margins, epicalyx segments are either entire or with 3–6 teeth, and the outer surface of the calyx lobe is silvery and silky. Petals are yellow, obovate with a rounded apex. Styles are subbasal and achenes glabrous. In western Himalaya the plant growth initiates in May, followed by flowering in June–July, fruiting in July–August, and senescence in September (Kaul *et al*; 2011). The plant grows on acidic soil (pH 6.0 ± 0.5), reddish-brown loamy soils (Laskar *et al*; 2005).

2.1.5 Ethnomedicinal uses

The rootstock and the whole herb of *Potentilla fulgens* are used as a potent medicine by many tribes of the higher and sub-Himalayan regions (Table 2.1). The plant is used in the treatment of various disease ailments such as diarrhea, stomach problems, mouth ulcers, cough, cold, diabetes mellitus, cancer, gum infection, tooth ailments (pyorrhea, toothache, and caries), astringent, and as a tonic. In medieval ages *Potentilla* extracts (water, milk,

CHAPTER-2 | LITERATURE REVIEW

honey, and alcoholic) were used for curing toothache, throat inflammations, wound–healing, jaundice, mouth ulcers, dysentery, and as homeostatic (Tomczyk and Latte; 2009). The root powder is an effective anthelmintic and is used for toothache and stomach problems. Root juice is taken for the treatment of peptic ulcers and other gastrointestinal problems and the root paste is used for controlling tooth infections. Twigs and leaves are chewed and used as a toothbrush by Bhutias in Uttarakhand, India. Hence, the drug is popularly known under the name Bajradanti ‘Vajra meaning hard’ and ‘danti meaning teeth’. The species is utilized commercially by Vicco Laboratories in India for the manufacture of Vicco tooth powder and paste (**Vicco Vajradanti™**) (Panigrahi and Dixit; 1980; Farooqui *et al*; 1998; Farooqui *et al*; 2001).

Table 2.1: Ethnomedicinal and traditional uses of *P. fulgens* in the higher and lower Himalayan regions

Country/State	Parts used	Ethnomedicinal uses	References
<i>Northeastern India</i>			
Meghalaya	Fresh roots	Diabetes mellitus, stomach disorder, gastric problems, mouth ulcer, cancer, diarrhea, high blood pressure, dentifrice.	Kundu <i>et al</i> ; 2016

CHAPTER-2 | LITERATURE REVIEW

Assam	Whole herb	Gums and tooth ailments (Pyorrhea, toothache, and caries), diarrhea, stomach problems, cough and cold, diabetes mellitus, cancer.	Roy <i>et al</i> ; 2010
Manipur	Roots	Burns and Toothache	Pfoze <i>et al</i> ; 2012
Sikkim	Plant juice Root powder	Stomach trouble, cough, and cold. Toothache, pyorrhea, and gingivitis.	Kaul <i>et al</i> ; 2011
<i>Northern India</i>			
Uttarakhand	Twigs and leaves Whole plants Roots	Used as a toothbrush. Stomatitis and aphthae. Wounds, tiger bites, and mouth ulcers.	Pala <i>et al</i> ; 2010
Ladakh	Leaf paste	Stomach pain, cough, cold, sore throat, and ulcer.	Kumar <i>et al</i> ; 2009

Other countries			
Nepal and Bhutan	Plant juice	Stomach problems, cough, and cold.	Laloo <i>et al</i> ; 2013
	Root powder	Toothache, stomach disorders, anthelmintic.	
	Fresh root	Cough and cold, diarrhea, diabetes mellitus, cancer, and strengthening gums.	
		Tooth infections.	
	Root juice	Peptic ulcer and masticated for Pyorrhea.	
	Root paste	Respiratory complaints.	
	Leaves/whole plant		

2.1.6 Chemical constituents

The genus *Potentilla* is chemically well known throughout the world for the diversity of active phytoconstituents such as tannins which have astringent effects and medicinal value (Tomczyk and Latte; 2009). However, based on the recent studies, most of the researchers have concentrated on triterpenoid structures present in the species. To date, *Potentilla erecta* (aerial and underground parts) is the leading species from the genus *Potentilla* with the highest number of constituents that have been reported so far *i.e.* altogether 68 structures, followed by *Potentilla anserine* (aerial and the underground parts altogether 37 compounds). *Potentilla fulgens* in the present situation are also finding an attractive platform in regards to the chemical nature of the compounds isolated either from the roots or aerial parts. The preliminary phytochemical testing reveals that both the aerial and underground parts of the plant were found to contain various phytoconstituents such as tannins, flavonoids, phenolics, proanthocyanidins, triterpenes, steroids, and saponins. So far 12 compounds have been isolated from this species including two novel triterpenoidal and one bioflavonoidal component. The plant is rich in polyphenolics components which are composed mainly of tannins and other major phenolic classes. Phytochemical investigation of the aerial parts led to the isolation of two novel triterpenes components *viz.* Potentene A (30-methyl-17 α -hopan-12-ene-3-one) and potentene B (3-O- β -D-gluconopyranosyl-(1,2)- β -D-glucuronopyranosylhopan-12-eno-11-oxo-28oic acid) (Jaitak et al., 2010b). Moreover, three well-known compounds such as rutin, epiafzelchin, and afzelchin-4- α - \rightarrow 8'' catechin were also reported from the aerial parts of the plant. The underground (root) portion was reported to contain a novel bioflavonoidal component Potifulgene (Epiafzelchin-6-o-8'' epiafzelchin) and a major component (-) epicatechin which belongs to flavonoidal class (Jaitak et al; 2010). In addition, five known

terpenes namely hyptadienic acid, tormentic acid, rosamultic acid, 2a, 19a-dihydroxy-3-oxo-12-ursen-28-oic acidb-D-glucopyranoside ester and kajiichigoside were also recently isolated from the root portion of the plant (Kumar *et al*; 2013).

2.1.7 Pharmacological activity

The scientific world's particular interest in the genus *Potentilla* and its curative properties originated from the realm of traditional medicine. Ethnic medicine has come to be an irreplaceable source of knowledge of medicinal plants and their curative qualities, as well as creating clues for scientific research, which usually confirms the legitimacy of their usage. Modern pharmacological studies have scientifically confirmed and validated the traditional usage of various *Potentilla* species in the treatment of diverse disease ailments. The reason behind such potent activities was mainly attributed to the presence of a high amount of tannins and phenolics components in the genus (Tomczyk and Latte; 2009). *Potentilla fulgens* Wall. has quite a broad spectrum of pharmacological activities in preclinical studies. Some of the pharmacological studies reported are shown below:

(a) Toxicity study

Acute toxicity study of the methanolic root extract of *P. fulgens* was tested in mice at a dose level of 450 mg/kg, p.o. The results showed that no adverse effects up to 4 weeks were observed during the experiment which signifies that the extract was safe up to the tested dose.

(b) Antineoplastic activity

The anti-neoplastic activity of the methanolic root extract of *Potentilla fulgens* L. was reported to have significant activity against certain tumor cells in mice (Syiem *et al*; 2003). In the study, approximately 1×10^6 Dalton's lymphoma (DL) cells were transplanted intraperitoneally into swiss–albino mice. The treated/control value was reported to be 154% (250mg/kg) when the animals were treated on the 1st, 3rd, 5th and 7th day after transplantation. The result indicated that the methanolic extract of the plant showed potent antitumor activity on DL cells. Rosangkima *et al*; 2004; also showed that the aqueous root extract of the herb of *Potentilla fulgens* was active against neoplastic tumors murine ascites Dalton's lymphoma (DL) in rodents.

(c) Antihyperglycemic activity

Hypoglycemic and antihyperglycemic activities of the methanolic extract of *P. fulgens* were evaluated in normal and alloxan-induced diabetic mice. Normal and diabetic mice were administered with the extract at doses of 150–450 mg/kg, i.p. The blood glucose levels were measured at different time intervals up to a period of 5 days. The results showed that the blood glucose level was reduced to 31% in normal and 63% in alloxan-induced mice, following the administration of the effective dose. A prolonged antihyperglycemic activity was reported in the diabetic mice and glucose level was found 79 % low in comparison to control even on the 3rd day. The results were compared with that of insulin, glibenclamide, and metformin, clearly indicating significant hypoglycemic and antihyperglycemic activities (Syiem *et al*; 2002).

(d) Antihyperlipidemic activity

The effect of *P. fulgens* root extract on lipid and carbohydrate profiles was evaluated in alloxan-induced diabetic mice. Standard drugs used during the experiment were metformin (i.p.), glibenclamide (i.p.), and insulin (s.c.). The methanolic extract (250 mg/kg, p.o.) was administered to diabetic mice on alternate days for a period of one week. On day 8th the blood samples were collected for the estimation of cholesterol, triglyceride, and HDL cholesterol levels. The results showed that treatment with *P. fulgens* methanolic extract (250 mg/kg, p.o. and i.p.) maintains the lipid profile in treated groups when compared to the control diabetic group. A significant reduction in the cholesterol and triglyceride level by 72% and 81% was observed respectively, whereas HDL level was found to increase significantly only with the i.p. treated group. Glycolytic enzymes such as glucokinase and hexokinase were also assayed in the same study. Methanolic extract of *P. fulgens* (250 mg/kg) when given by i.p. route selectively enhanced the hepatic hexokinase activity, whereas oral administration did not produce any effect. In addition, no significant effect was observed in the liver glucokinase (GK) and hexokinase skeletal muscle (HK) levels when the animals were administered with the same dose of the extract (Syiem *et al*; 2009).

(e) α -glucosidase inhibitory activity

The mechanistic antidiabetic activity of *P. fulgens* methanolic root extract, its ethyl acetate fraction, and some important isolated components from ethyl acetate fraction was reported *via*. inhibiting the α -glucosidase enzyme (Kumar *et al*; 2013). Inhibitors of α -glucosidase constitute an important class of anti-diabetic drugs that prevent the sudden rise in postprandial hyperglycemia by inhibiting the hydrolysis of oligosaccharides into absorbable monosaccharides. Five components including terpenoids were isolated from the ethyl

acetate fraction using column chromatography, purified by HPLC methods, and characterized by NMR and mass spectrophotometric techniques. Terpenoids such as hyptadeinic acid, tormentic acid, rosamultic acid, 2a, 19a-dihydroxy-3-oxo-12-ursen-28-oic acid β -D-glucopyranoside ester and Kajiichigoside F1 were isolated and tested for α -glucosidase inhibitory activity. Among these hyptadienic acid, which possess an A-ring contracted triterpenoid, was reported to be the most potent against α -glucosidase enzyme. The IC_{50} value with the highest α -glucosidase inhibitory activity was represented as ethyl acetate fraction ($12.79 \pm 2.68 \mu\text{g/mL}$) > methanolic extract ($38.32 \pm 3.22 \mu\text{g/mL}$) > hyptadeinic acid ($39.67 \pm 1.88 \mu\text{M/mL}$) > Rosamultic acid ($52.35 \pm 4.14 \mu\text{M}$) > Tormentic acid ($80.58 \pm 4.77 \mu\text{M/mL}$) > n-butanol fraction ($85.37 \pm 5.53 \mu\text{g/mL}$) > 2a, 19a-dihydroxy-3-oxo-12-ursen-28-oic acid β -D-glucopyranoside ester ($91.07 \pm 2.54 \mu\text{g/mL}$) > Kajiichigoside F1 ($151.38 \pm 2.17 \mu\text{M/mL}$). The results revealed that the A-ring contracted triterpenes may serve as a class of triterpenes with α -glucosidase inhibitory activity. Also, identification of enzyme inhibitory activity of these constituents justified the traditional use of *P. fulgens* in the management/treatment of diabetes (Syiem *et al*; 2009).

(f) Antihelmintic activity

Roy *et al*; 2010; reported the anthelmintic activity of the ethanolic root extract of *P. fulgens* against the cestode parasite, *Raillietina echinobothrida*, and the trematode, *Gastrothylax crumenifer*. The parasites were incubated in 1, 5, 10, 20, 50 and 100 mg crude alcoholic extract per mL of phosphate-buffered saline (PBS) at a temperature of $37 \pm 1^\circ\text{C}$. Paralysis and death were observed at 2.00 ± 0.05 and 2.80 ± 0.06 h for the cestode and 1.21 ± 0.06 and

2.18±0.04 h for the trematode parasites at the highest test concentration of the plant extract. The commercial anthelmintic, Praziquantel (PZQ) showed significant activity at the tested concentration (0.02 mg/mL). To further investigate the efficacy of the plant extract, vital tegumental enzymes of the parasite viz. acid phosphatase (AcPase), Alkaline phosphatase (Alk-Pase), and Adenosine triphosphatase (ATPase) were studied. Quantitatively, the total enzyme activity of AcPase, AlkPase, and ATPase was found to be reduced significantly by 69.20, 66.43, and 29.63 % for *R. echinobothrida* and 47.96, 51.79, and 42.63% for *G. crumenifer*, respectively compared to the respective controls; the histochemical study also showed reduction in the visible staining of the enzymes. The reference drug, PZQ also showed a more or less similar effect to that of the plant extract. The result suggested that *P. fulgens* have potent anthelmintic activity against the tested strains.

(g) Antioxidant activity

Jaitak *et al*; 2010; studied the *in vitro* antioxidant activity of *Potentilla fulgens* extract, fractions, and isolated components using three *in vitro* experiments, namely, 2,2'-azino-bis (3-ethylbenzothiazoline-6-sulfonic acid) (ABTS), 1,1-Diphenyl-2-picrylhydrazyl (DPPH), and ferric-reducing antioxidant power (FRAP) assay. Among the three fractions (ethyl acetate, butanol, and water fraction) and the total aqueous methanolic extract, the butanol fraction exhibited a significant scavenging response measured in terms of TEAC (mM Trolox equivalent/mg extract). The butanol fraction was found to possess strong antioxidant activity (2.54 ± 0.69 , 2.41 ± 0.53 , 3.57 ± 0.05 mM Trolox equivalent/mg extract) with ABTS, DPPH and FRAP assays, respectively. The chemical composition of extracts, studied in terms of total polyphenol content (TPC), was found in the range of

20.61±0.38 to 33.28±0.11 mg/g gallic acid equivalent. A significant correlation was observed between total polyphenolics and antioxidant activity, indicating the participation of phenolics in antioxidant activities of extract and fractions. In the same study, two components that were isolated from *P. fulgens* viz. biflavanoid (Potifulgene) and epicatechin were also studied for antioxidant activity. As compared to epicatechin, Potifulgene was found to have higher antioxidant activity with IC₅₀ of 6.85±0.38, 4.24±0.41, 5.35±0.53 for ABTS, DPPH, and FRAP assays respectively, whereas the IC₅₀ of epicatechin was found to be 2.13±0.05, 1.50±0.02, 1.57±0.03 respectively. A study on the aerial parts of *P. fulgens* was also performed by Jaitak et al., 2010b. Phytochemical investigation of the aerial parts of *P. fulgens* led to the isolation of two new triterpenes, potentene A and potentene B. In addition, three known compounds afzelchin-4α→8"-catechin, epiafzelchin, and rutin were isolated. The structures of all these compounds were elucidated by spectroscopic techniques. From all the five isolated components the maximum antioxidant activity for scavenging of 1,1, diphenyl-2-picrylhydrazyl radical was observed with that of afzelchin-4α→8"-catechi followed by epiafzelchin and rutin with IC₅₀ values of 1.21, 2.88, and 5.20 mg/mL, respectively; the known standard antioxidant, vitamin C, had an IC₅₀ value of 0.44 mg/mL.

(h) Sorbitol dehydrogenase inhibitory activity

Methanolic extract of *P. fulgens* was reported to inhibit sorbitol dehydrogenase (SDH), the enzyme responsible for the conversion of sorbitol to fructose in the polyol pathway (Syiem and Majaw; 2010). Polyol pathway is one of the intracellular events that occur in the presence of high glucose ambience and results in cellular abnormalities due to altered

NADH/NAD⁺ ratio. Alteration in such pathways results in the major microvascular complications of diabetes including nephropathy, neuropathy, and retinopathy. In the study, the SHD levels were estimated in liver, kidney, and eyeballs of swiss albino mice induced with alloxan monohydrate. The result showed that the methanolic extract of *P. fulgens* at a dose level of 150–350 mg/kg in both oral and i.p. treated animals showed significant dose-dependent inhibition of SDH level in the liver. The kidney SDH level was also reported to be significantly reduced at doses 50–350 mg/kg (both p.o. and i.p.). However, the SDH level in the eye was found to be significantly lowered only at higher doses of 150 and 250 mg/kg (p.o. and i.p.).

(i) Antimicrobial activity

Zuo *et al.*, 2008; had performed the antibacterial screening of 19 Chinese medicinal plants extract (including *P. fulgens* fruit extract) for inhibition against clinical isolates of methicillin-resistant *Staphylococcus aureus* strain (MRSA). The minimal inhibitory concentrations (MICs) and minimal bactericidal concentrations (MBCs) were determined in the setting of clinical MRSA isolates. Antibacterial susceptibilities were screened for inhibitory zone and MICs/MBCs determined by serial dilution with a standardized microdilution broth methodology. Vancomycin was used as a positive control. All the presented 19 plants showed positive anti-MRSA activity with MIC values ranging between 1.25–3.07mg/ml. The MICs value (expressed as Mean \pm S.E.M., mg/ml) of *P. fulgens* fruit extract was reported to be 3.07 ± 0.48 which is the least effective anti-MRSA as compared to all the tested plants extract. The most effective anti-MRSA activity in the study was reported with that of *Dendrobenthamia capitata* with the MICs value of 1.25 ± 0.18 .

(j) Wound healing activity

Kundu *et al*; 2016; reported the wound healing activity of root extract of *Potentilla fulgens* on experimental rats. Wounds were inflicted on animals by using both excision and incision models. The wounded animals were treated for 16 days with EPF (oral: 200–400 mg/kg and topical: 5–10% w/w) and PFEA (oral: 75 mg/kg; topical: 1.75% w/w). Various physical (wound contraction, epithelialization rate, tensile strength) and biochemical parameters (hydroxyproline, hexosamine, proteins, DNA) were examined during the study. Oxidant product (lipid peroxidase), antioxidant enzymes (catalase, superoxide dismutase), and reduced glutathione were determined. Morphological and histopathological studies of the skin tissues were monitored. A significant ($p < 0.05$) wound healing property was observed when the animals were treated topically with EPF (10% w/w) and PFEA (1.75% w/w). A significant ($p < 0.05$) increase in the levels of hydroxyproline, hexosamine, protein, and DNA up to 59.22, 70.42, 61.01, and 60.00% was observed, respectively. This effect was further demonstrated by the morphological and histopathological representation, thus showing significant ($p < 0.05$) re-epithelialization on the healing area. EPF and PFEA also showed significant ($p < 0.05$) antioxidant activity.

2.2 Green synthesis of plant-mediated silver nanoparticles

Umoren *et al*; 2014; reported a simple and effective eco-friendly approach for the synthesis of silver nanoparticles (AgNPs) using *Malus domestica* (red apple) fruit. The fruit extract acts as both reducing and capping agents. The synthesized AgNPs were characterized using various instrumental techniques including ultraviolet-visible spectroscopy (UV-vis), Fourier transform infrared spectroscopy (FTIR), x-ray diffraction (XRD), scanning electron

microscope (SEM), energy dispersive spectroscopy (EDS), and dynamic light scattering (DLS). Surface Plasmon Resonance (SPR) for AgNPs was observed at 422 nm. FTIR spectroscopy is useful for identifying the chemical composition present on the surface of silver nanoparticles and to identify the capping agents. The experiment was continuously observed the color change as well as with UV–vis spectrophotometer. The effects of different parameters such as (i) concentration of silver nitrate, (ii) concentration of *Malus domestica* extract, and (iii) reaction time on nanoparticle formation were examined. The SEM images showed flower-like shaped structures. The zeta potential of the synthesized AgNPs was determined in water as a dispersant. The zeta potential was found to be -65.07 mV. The high value confirms the repulsion among the particles and thereby increases instability of the formulation and the average size of silver nanoparticles is 150 nm. The crystalline nature of AgNPs was confirmed by the analysis of the XRD pattern; the synthesized silver nanoparticles were found to be stable at room temperature as revealed by the negative value of zeta potential due to the presence of natural products.

Banerjee *et al*; 2014; reported the leaf extract mediated green synthesis of silver nanoparticles from three widely available Indian plants- *Musa balbisiana* (banana), *Azadirachta indica* (neem), and *Ocimum tenuiflorum* (black tulsi). In their study, AgNPs were prepared by the reaction of 1 mM silver nitrate and 5% leaf extract of each type of plant separately. Biosynthesized AgNPs were duly characterized and tested for their antibacterial activity and toxicity. The AgNPs were characterized by UV-visible spectrophotometer, particle size analyzer (DLS), scanning electron microscopy (SEM), transmission electron microscopy (TEM), and energy-dispersive spectroscopy (EDS). Fourier transform infrared spectrometer (FTIR) analysis was carried out to determine the

nature of the capping agents in each of these leaf extracts. AgNPs obtained showed significantly higher antimicrobial activities against *Escherichia coli* (*E. coli*) and *Bacillus sp.* in comparison to both AgNO₃ and raw plant extracts. Additionally, a toxicity evaluation of these AgNPs containing solutions was carried out on seeds of Moong Bean (*Vigna radiata*) and Chickpea (*Cicer arietinum*). Results showed that seeds treated with AgNP solutions exhibited better rates of germination and oxidative stress enzyme activity nearing control levels, though detailed mechanisms of uptake and translocation are yet to be analyzed. In totality, the AgNPs prepared are safe to be discharged in the environment and possibly utilized in processes of pollution remediation. AgNPs may also be efficiently utilized in agricultural research to obtain better health of crop plants as shown by the study.

Wilson *et al*; 2015; focuses on the green synthesis of silver nanoparticles (CANPs) by utilizing the reducing activity of *Centella asiatica* and exploring the anti-diabetic property exhibited by CANPs carried out by in vitro antidiabetic tests such as glucose Uptake by Yeast Cells, non-enzymatic glycosylation of hemoglobin assay, Inhibition of alpha-amylase enzyme assay, followed by UV-Visible spectrophotometry, X-Ray Diffraction (XRD) analysis and Scanning electron microscope (SEM) for characterization. The shape and size of CANPs were studied using Transmission electron microscopy (TEM). UV-Visible spectrophotometry showed the plasmon resonance peak at 430 nm. The antioxidant and anti-diabetic property of CANPs was determined. These results indicate that CANPs possess effective anti-oxidant and anti-diabetic properties. In their entirety, the silver nanoparticles prepared are safe to be free in the environment and perhaps utilized for industrial and remedial purposes.

Ali *et al*; 2016; reported the green synthesis of silver nanoparticles using *Artemisia absinthium* aqueous extract. They e investigated the reducing potential of aqueous extract of *Artemisia absinthium* L. for synthesizing silver nanoparticles (AgNPs). Optimal synthesis of AgNPs with desirable physical and biological properties was investigated using ultraviolet-visible spectroscopy, dynamic light scattering (DLS), transmission electron microscopy (TEM), and energy-dispersive X-ray analysis (EDX). To determine their appropriate concentrations for AgNP synthesis, two-fold dilutions of silver nitrate (20 to 0.62 mM) and aqueous plant extract (100 to 0.79 mg ml⁻¹) were reacted. The results showed that silver nitrate (2 mM) and plant extract (10 mg ml⁻¹) mixed in different ratios significantly affected the size, stability, and yield of AgNPs. Extract to AgNO₃ ratio of 6:4 v/ v resulted in the highest conversion efficiency of AgNO₃ to AgNPs, with the particles in an average size range of less than 100 nm. Furthermore, the direct imaging of synthesized AgNPs by TEM revealed polydisperse particles in the size range of 5 to 20 nm. Similarly, nanoparticles with the characteristic peak of silver were observed with EDX. This study presents a comprehensive investigation of the differential behavior of plant extract and AgNO₃ to synthesize biologically stable AgNPs.

He *et al*; 2017; reported the biosynthesis of silver nanoparticles using seed extract of *Alpinia katsumadai*, and their antioxidant, cytotoxicity, and antibacterial activity. UV-visible spectroscopy, FETEM, EDX, SAED, XRD, DLS, and FT-IR analysis were used to characterize the morphology and crystalline phase of AgNPs. The FETEM and DLS analysis showed AgNPs were quasi-spherical in shape, with an average diameter of 12.6 nm for the size distribution. The SAED spectrum of the AgNPs indicated their crystalline nature, which was further confirmed by the XRD studies. The FT-IR spectra revealed that

phytochemicals from *Alpinia katsumadai* seed extract act as a capping and reducing agent for AgNP formation. The AgNPs showed distinctive free radical scavenging, potent antibacterial activity against different types of bacteria, and cytotoxicity activities. The results confirmed that *Alpinia katsumadai* is a potential bio-resource/biomaterial for synthesizing AgNPs with applications in antibacterial and antioxidant agents.

In the study by Rasheed *et al*; 2017; the reducing potential of *Artemisia vulgaris* leaves extract (AVLE) was investigated for synthesizing silver nanoparticles without the addition of any external reducing or capping agent. The appearance of blackish brown color evidenced the complete synthesis of nanoparticles. The synthesized silver nanoparticles were characterized by UV-visible spectroscopy, scanning electron microscope (SEM), energy-dispersive X-ray spectroscopy (EDX), transmission electron microscope (TEM), atomic force microscopy (AFM) and Fourier transforms infrared spectroscopy (FT-IR) analysis. UV–Vis absorption profile of the bio-reduced sample elucidates the main peak around 420 nm, which corresponds to the surface plasmon resonance of silver nanoparticles. SEM and AFM analyses confirmed the morphology of the synthesized nanoparticles. Similarly, particles with a distinctive peak of silver were examined with EDX. The average diameter of silver nanoparticles was about 25 nm from Transmission Electron Microscopy (TEM). FTIR spectroscopy scrutinized the involvement of various functional groups during nanoparticle synthesis. The green synthesized nanoparticles presented more effective antibacterial activity against pathogenic bacteria than AVLE alone. In-vitro antioxidant assays revealed that silver nanoparticles (AV-AgNPs) exhibited promising antioxidant properties. The nanoparticles also displayed a potent cytotoxic effect against HeLa and MCF-7 cell lines. In conclusion, the results supported the advantages of

employing a bio-green approach for developing silver nanoparticles with antimicrobial, antioxidant, and antiproliferative activities in a simple and cost-competitive manner.

A study by Shankar *et al*; 2017; reported the biosynthesis of silver nanoparticles using the fruit extract of *Capsicum frutescence* (Sweet pepper). The fruit extract was exposed to silver ions and the resultant biosynthesized silver nanoparticles characterized by UV–Vis spectrophotometry indicated the surface plasmon resonance band at 385–435 nm. X-ray diffraction spectrum showed crystalline structure while scanning electron microscope analyses exposed the monodisperse distribution and particle size of 20–25 nm. The elemental analysis displayed a strong signal at 3 keV that agrees to silver ions and confirms the presence of metallic silver. The antibacterial activity of silver nanoparticles was determined by the agar well diffusion method against gram-positive and gram-negative bacteria. Maximum and minimum zones of inhibition were renowned against *Escherichia coli* (11.5 mm) and *Bacillus subtilis* (10.5 mm), respectively. This study exposed that silver nanoparticles retained good bactericidal activity at 80 µg/ml concentration.

Intending to synthesize silver nanoparticles, Sudha *et al*; 2017; used the aerial parts of *Lippia nodiflora* and evaluated the antioxidant, antibacterial and cytotoxic properties. The biosynthesized AgNPs were characterized by UV–Visible Spectroscopy, Fourier-Transform Infrared Spectroscopy (FTIR), and X-Ray Diffraction (XRD) analysis. The AgNPs were found to be stable at –25.2 mV through zeta potential study. The morphology and size of synthesized silver nanoparticles were confirmed by Scanning Electron Microscope with energy dispersive spectra (SEM-EDX) and Transmission Electron Microscopy (TEM) analysis with a size range from 30 to 60 nm. Biosynthesized AgNPs

exhibited strong antioxidant activity as well as showed potent antibacterial activity against human pathogenic bacteria. The cytotoxicity study of AgNPs was also revealed against MCF-7 breast cancer cell lines in a dose-dependent manner. The recognized bioactivity confirmed by the synthesized AgNPs directs towards the clinical use as an antioxidant, antibacterial and cytotoxic agent.

In the study by Raj *et al*; 2018; the facile green synthesis of silver nanoparticles (AgNPs) using aqueous leaf extract of *Enicostemma axillare* (Lam.) has reported. The size and shape of Ag nanoparticles were characterized by XRD, TEM, and SEM-EDS. The formation and stability of the reduced silver nanoparticles in the colloidal solution were monitored by UV Vis spectrophotometer analysis. Zeta potential was confirmed by a DLS study. The mean particle diameter of silver nanoparticles was calculated from the TEM, SEM and the size of the particles was measured between 15 and 20 nm. TEM analysis revealed the spherical shape of the particles. The crystalline nature of the nanoparticles in the face-centered cubic structure is confirmed by the peaks in the XRD pattern corresponding to (111), (200), (220) and (311) planes. This study showed the biogenic, environmentally friendly, and cost-effective synthesis and characterization of the silver nanoparticles.

Zangeneh *et al*; 2019; used the flowers of *Stachys lavandulifolia* for the biosynthesis of silver nanoparticles. They also reported the cytotoxicity, antioxidant, antibacterial and cutaneous wound-healing properties of the synthesized nanoparticles. These AgNPs were characterized using Fourier transform-infrared spectroscopy, field emission-scanning electron microscopy, energy-dispersive X-ray spectroscopy,

transmission electron microscopy, and ultraviolet-visible spectroscopy. The synthesized AgNPs had great cell viability dose-dependently [investigating the effect of the plant on human umbilical vein endothelial cell line] and indicated this method was non-toxic. In the study, the 2,2-diphenyl-1-picrylhydrazyl (DPPH) free radical scavenging test was carried out to examine antioxidant properties, which revealed similar antioxidant properties for AgNPs and butylated hydroxytoluene. Agar diffusion tests were applied to determine the antibacterial characteristics. The macro broth tube test was run to determine minimum inhibitory concentration. All data of antibacterial and cutaneous wound-healing examinations were analyzed by SPSS 21 software (Duncan post hoc test). AgNPs showed higher antibacterial properties than all standard antibiotics ($p \leq 0.01$). Also, AgNPs prevented the growth of all bacteria at 2–8 mg/ml concentrations and destroyed them at 2–16 mg/ml concentrations ($p \leq 0.01$). For the in vivo experiment, after creating the cutaneous wound, the rats were randomly divided into six groups: untreated control; treatment with Eucerin basal ointment; treatment with 3% tetracycline ointment; treatment with 0.2% AgNO₃ ointment; treatment with 0.2% *S. lavandulifolia* ointment; and treatment with 0.2% AgNPs ointment. These groups were treated for 10 days. For histopathological and biochemical analysis of the healing trend, a 3 × 3-cm section was prepared from all dermal thicknesses at day 10. Use of AgNPs ointment in the treatment groups substantially reduced ($p \leq 0.01$) the wound area, total cells, neutrophil, macrophage, and lymphocyte, and remarkably raised ($p \leq 0.01$) the wound contracture, hydroxyproline, hexosamine, hexuronic acid, fibrocyte, and fibrocytes/fibroblast rate compared with other groups. Seemingly, AgNPs can be used as a medical supplement owing to their non-cytotoxic, antioxidant, antibacterial and cutaneous wound-healing properties.

Behravan *et al*; 2019; reported the green synthesis of silver nanoparticles using *Berberis vulgaris* leaf and root aqueous extract and its antibacterial activity. After collection, identification, and extraction of *Berberis vulgaris* was performed production of silver nanoparticles. In the study effect of parameters such as AgNO₃ concentration (0.5, 1, 3, 10 mM), aqueous extract (3, 5, 10, 15, 30 mL), and contact time (1, 2, 6, 12, 24 h) were investigated in the synthesis of nanoparticles and also the antibacterial effect of these nanoparticles was studied on *Escherichia coli* and *Staphylococcus aureus* bacteria by Disk diffusion test and Minimum Inhibitory Concentration test (MIC). According to XRD results and analysis of TEM, nanoparticles have spherical shapes and sizes of 30 to 70 nm. On the other hand, antibacterial tests showed these nanoparticles have more antibacterial activity than other extracts. The result showed the biosynthesis of silver nanoparticles using an aqueous extract of *Berberis vulgaris* is a clean, inexpensive, and safe method that has not been used any toxic substance and consequently does not side effects and this nanoparticle has high antibacterial activity.

Jemilugba *et al*; 2019; reported A simple, green, cost-effective and environmentally benign method for the synthesis of silver nanoparticles (AgNPs) using aqueous extract of *Combretum erythrophyllum* plant leaves as both the reducing and capping agents is herein reported for the first time. The as-prepared Ag-NPs were characterized using Ultraviolet-Visible (UV–Vis) absorption spectroscopy, transmission electron microscopy (TEM), Fourier transform infrared spectroscopy (FTIR), X-ray diffraction (XRD), and dynamic light scattering (DLS) techniques. The TEM image showed that the particles are spherical in shape, and well dispersed with an average particle diameter of 13.62 nm. The as-synthesized Ag-NPs showed efficient antibacterial activities against pathogenic Gram-

positive *Staphylococcus aureus* (ATCC 25923) & *Staphylococcus epidermidis* (ATCC 12228), and Gram-negative *Escherichia coli* (ATCC 10536) & *Proteus vulgaris* (33420). Compared to the streptomycin drug, which was ineffective against *S. epidermidis*, the as-synthesized Ag-NPs were effective against *S. epidermidis* and other *Staphylococcus* species that are implicated in different dermatological infections.

In the study by Tripathi *et al*; 2019; AgNPs have been synthesized utilizing in-vitro grown leaf extract of anti-diabetic medicinal plant *Withania coagulans* Dunal by the reduction of silver nitrate solution. *W. coagulans* synthesized silver nanoparticles (WcAgNPs) were characterized by UV–visible spectroscopy, scanning electron microscopy, energy dispersive X-ray analysis, transmission electron microscopy, X-ray powder diffraction, and Fourier transform Infra-Red spectroscopy. All cumulative results showed that WcAgNPs were ~14 nm in size having a spherical shape with face-centered cubic structure. High-performance liquid chromatography confirmed the involvement of withanolides in AgNPs synthesis as a reducing/capping agent. Synthesized WcAgNPs showed greater antioxidative potential when compared with *W. coagulans* leaf extract. WcAgNPs have efficient antimicrobial potential and suppress the growth of both gram-positive and gram-negative bacteria. In our finding, we also observed cytotoxicity of WcAgNPs against SiHa (cervical cancerous, hyper-triploid) cell lines and apoptosis in SiHa cells after 48-hour incubation with 13.74 $\mu\text{g ml}^{-1}$ (IC₅₀) concentration of WcAgNPs. As results suggest, this is the first report which explains that *W. coagulans* leaf extract has potential as a bio-reducing agent for the synthesis of silver nanoparticles, which can be exploited as an antioxidant, antimicrobial and anticancer agent and depicting an effective

way for utilizing bioactive resources in the restoration of medicinal properties of this plant with high efficacy.

Jebril *et al*; 2020; reported the green synthesis, characterization, and antifungal activities of silver nanoparticles (AgNPs). The synthesis of AgNPs has been produced by mixing silver nitrate solution with aqueous *Melia azedarach* leaf extract as a reducing and stabilizing agent for AgNPs. After only 10 min of reaction, the light yellow color of the *M. azedarach* leaf extract was changed to brown due to the reduction of silver ions to AgNPs, under ambient conditions. The growth of biosynthesized AgNPs was monitored by UV–Visible spectroscopy complemented by dynamic light scattering technique (DLS), zeta potential, scanning electron microscopy (SEM), energy-dispersive X-ray spectroscopy (EDS), X-ray diffraction (XRD) and Fourier transform infrared spectroscopy (FTIR). The peak absorbance of the UV–vis spectra was at 400 nm confirming the formation of silver nanoparticles. SEM analysis shows the existence of small spherical nanoparticles with a size ranging from 18 to 30 nm (average 23 nm). XRD analysis shows that the AgNPs were face-centered cubic (FCC) lattices. The EDS analysis displays intense signals of the silver element. FTIR analysis demonstrated that the hydrolyzable tannic acid involved in *M. azedarach* leaf extract is responsible for the bioreduction and stabilization of AgNPs. The stability of AgNPs was confirmed by zeta potential analysis. A negative zeta potential value of AgNPs reduces the *Verticillium* wilt severity and relative vascular discoloration, respectively, by 87% and 97%, as compared to inoculated and untreated control. The antifungal activity carried out in this work opens up an important perspective of the biosynthesized AgNPs.

Alomar *et al*; 2020; focused on a green chemistry approach to synthesize eco-friendly AgNPs using an aqueous extract of *Peganum harmala* leaves. The formed AgNPs were characterized using different spectroscopic and microscopic analyses: ultraviolet-visible spectrophotometry (UV–Vis), Fluorolog 3 spectrometry, transmission electron microscopy (TEM), dynamic light scattering (DLS), and Fourier transform infrared spectroscopy (FTIR), techniques using a Zetasizer. The resulting nanoparticles were screened for their biomedical and pharmaceutical properties. They investigated antimicrobial activity against various strains of bacteria and fungi. The synthesized AgNPs showed a higher antibacterial potential against Gram-negative pathogen *E. coli* with an inhibition zone of 65 mm rather than Gram-positive pathogens *S. aureus* and *B. cereus* of inhibition zone 50 mm. Meanwhile, no inhibition zone was observed for *E. faecalis*. Furthermore, the formed AgNPs were applied to enhance the sensitivity and selectivity of the spectrophotometric determination of the antibiotic Rifaximin in bulk powder or tablet form with a λ_{max} of 340 nm. The proposed spectrophotometric technique for determining Rifaximin in the presence of silver nanoparticles showed a linear relationship in the concentration ranges of 5–80 $\mu\text{g/mL}$ and followed the linear regression equation $A = 0.039C - 0.166$ ($r = 0.9997$), with low limits of detection and quantification of 1.75 and 5.0 $\mu\text{g mL}$. According to the ICH guidelines, the proposed technique was validated.

In the study by Hashemi *et al*; 2020; an eco-friendly method to produce stable silver nanoparticles using the leaf extract of a medicinal plant of *Teucrium polium* (*T. polium*) was reported. The green synthesized silver nanoparticles (*T. polium*-AgNPs) were characterized by UV Visible spectroscopy, X-ray diffraction (XRD) study, Fourier transform infrared spectroscopy (FTIR) and scanning electron microscopy (SEM). The

biosynthesized nanoparticles exhibited significant anticancer activity against MNK45 human gastric cancer cell line. The data obtained in the study shows the potent therapeutic value of *T. polium*-AgNPs and the scope for further development of anticancer drugs.

Hekmati *et al*; 2020; used the aerial parts of *Allium rotundum* L, *Falcaria vulgaris* Bernh. and *Ferulago angulate* Boiss. were used for the synthesis of silver nanoparticles (Ag NPs). Ag NPs were characterized by UV–vis spectrophotometer, X-ray diffractometer (XRD), and Transmission electron microscopy (TEM). The formation and stability of the reduced silver nanoparticles were checked by UV–vis spectrophotometer analysis. The average particle diameter of silver nanoparticles was calculated from the XRD pattern according to Scherrer's equation. The antimicrobial, synergistic effects of synthesized nanoparticles and ethanolic extracts of plants were studied alone and in combination with *Pseudomonas aeruginosa* PAO1 and *Staphylococcus aureus* ATCC 25923 using disk diffusion method and the diameter of the zone of inhibition compared to the Tetracycline, Kanamycin, and Cefpirome. The minimum inhibitory concentration (MIC) of bacteria was determined using micro broth dilution. The XRD spectroscopy of synthesized nanoparticles showed the face-centered cubic structure. Also, TEM showed the formation of silver nanoparticles with an average size of 20.5 nm. The diameter of the inhibition zone of synthesized silver nanoparticles in the MIC of the mixture of plant extracts and silver nanoparticles was 21, and 25 (mm) for *P. aeruginosa*, and *S. aureus*, respectively. Obtained results showed that the bio-synthesized silver nanoparticles have an antibacterial effect on both *P. aeruginosa* and *S. aureus*.

Manik *et al*; 2020; studied the effect of two different plant's leaf extract i.e., *Artocarpus heterophyllus* and *Azadirachta indica* as reducing and stabilizing agent on silver nanoparticles synthesis. The obtained silver nanoparticles are studied using an X-ray diffraction spectrum to confirm its orientation and crystal structure. Shape, average size, and crystalline nature are investigated and estimated using scanning electron microscope images and transmission electron microscopy with selected area diffraction patterns. The possible bio-reducing agents within the leaf extracts are confirmed using FTIR analysis. This study provides a chemical-free synthesis method to produce silver nanoparticles and provides a better approach to produce the nanoparticles which can be used for medical as well as cosmetic purposes.

Panda *et al*; 2020; used aqueous leaf extract of *Symplocos racemosa* for the synthesis of silver nanoparticles (AgNPs) by adding 1mM AgNO₃ as a reducing agent. Silver nanoparticles (AgNPs) from aqueous leaf extract and 1 mM AgNO₃ are successfully synthesized here. The characterization of the silver nanoparticles was carried out by UV–visible spectroscopy, XRD (X-Ray Diffraction), FTIR (Fourier Transform Infrared Spectroscopy) and Transmission Electron Microscopy(TEM), FE-SEM (Field Emission Scanning Electron Microscope), EDX (Energy Dispersive X-Ray Spectroscopy) and Transmission Electron Microscopy(TEM). The limit of UV–visible spectroscopy at 422 nm supported the reduction of AgNO₃ to AgNPs. Analysis of FTIR showed that secondary metabolites are responsible for bio-reduction in silver nanoparticles of silver nitrate. The antimicrobial activity of synthesized silver nanoparticles has been studied on *Pseudomonas aeruginosa*.

Sahayraj *et al*; 2020; reported the green synthesis of silver nanoparticles using dry leaf aqueous extract of *Pongamia glabra* Vent (Fab.) and evaluation of its phytofungicidal activity. From 3.0 to 5.0 ml, PG-AgNPs drastically and significantly reduced *Rhizopus nigricans* mycelia weight, reduced spore count when compared to a crude extract of *P. glabra* shows the efficacy of bio nanosilver ions. The results confirmed that the *P. glabra* dry leaves extracts are an excellent eco-friendly, and reliable source for the synthesis of AgNPs as compared to the conventional methods. *Pongamia glabra* is a medicinal as well as a pesticidal plant having diverse phytochemicals. The synthesized silver nanoparticles' physical nature, structure, size were characterized. They hypothesized that PGDL aqueous extract was found to produce stable silver nanoparticles at room temperature having antimicrobial activity useful in post-harvest against seeds infecting pathogenic bacteria. Maximum absorbance was observed at 430 nm and synthesis takes place within 60 min and took 3 h for stabilization. Bionano ions size is in the range between 6.60–52.2 nm with an average size of 29 nm. Amines are responsible for the reduction process whereas amides as capping agents. Therefore, *P. glabra* leaves provide future opportunities in nano-fungicide by tagging nanoparticles.

Tamilarasi *et al*; 2020; synthesized silver nanoparticles using silver nitrate as the precursor and an aqueous extract of fresh leaves of *Gomphrena globosa* (Globe amaranth) as the reducing and stabilizing agent. The active phytochemicals present in the leaves cause a quick reduction of silver ions (Ag^+) to metallic silver nanoparticles (Ag^0). The formation of Ag nanoparticles was initially confirmed by visual observation through the color change of the mixture. The silver nanoparticles obtained were characterized using UV–visible absorption spectroscopy, X-ray diffraction (XRD), Fourier transform infrared

spectroscopy (FTIR), Scanning electron microscopy (SEM), Energy dispersive X-ray analysis (EDAX), High-Resolution transmission electron microscopy (HR-TEM), and Selected area electron diffraction (SAED) analysis. The synthesized silver nanoparticles show excellent antibacterial activity against three gram-positive bacteria (*Staphylococcus aureus*, *Bacillus subtilis*, *Micrococcus luteus*) and three gram-negative bacteria (*Escherichia coli*, *Pseudomonas aeruginosa*, and *Klebsiella pneumoniae*).

Qais *et al*; 2020; synthesized silver nanoparticles from an aqueous extract of *Carum copticum* and characterized using UV–vis absorption spectroscopy, Fourier-transform infrared spectroscopy (FTIR), X-ray diffraction (XRD), transmission electron microscopy (TEM), and scanning electron microscopy (SEM). Synthesized nanoparticles were checked for their ability to inhibit quorum sensing-mediated virulence factors and biofilms against three test pathogens at sub-MIC values. There was ~75% inhibition of violacein production by synthesized nanoparticles against *C. violaceum*. The *P. aeruginosa* virulence factors such as pyocyanin production, pyoverdinin production, exoprotease activity, elastase activity, swimming motility, and rhamnolipid production were inhibited by 76.9, 49.0, 71.1, 53.3, 89.5, and 60.0% at sub-MIC. Moreover, virulence factors of *S. marcescens* viz. prodigiosin production, exoprotease activity, and swarming motility was reduced by 78.4, 67.8, and 90.7%. The nanoparticles also exhibited broad-spectrum antibiofilm activity with 77.6, 86.3, and 75.1% inhibition of biofilms of *P. aeruginosa*, *S. marcescens*, and *C. violaceum* respectively. The biofilm formation on glass coverslip was reduced remarkably as evident from SEM and CLSM analysis. The findings revealed the in vitro efficacy of silver nanoparticles against bacterial pathogens and can be exploited in the development of alternative therapeutic agents in management of bacterial infections for topical application,

mainly wound infection, or coating of surfaces to prevent bacterial adherence on medical devices.

2.3 Mechanism of formation of silver nanoparticles

Silver ions are reduced by the various plant metabolites including terpenoids, polyhydroxyphenols, carbohydrates, alkaloids, phenolic compounds, and proteins, etc. Fourier transform infrared spectroscopy (FTIR) has been used to demonstrate the biomolecules present in the extract which are responsible for the synthesis of nanoparticles. One of the biomolecules which majorly participate is terpenoids. Terpenoids are also known as isoprene, a naturally occurring organic compound in plants, which contains five-carbon isoprene units. It has been explored by some researchers that Geranium leaf extract contains terpenoids, which act as a major player in the biosynthesis of AgNPs (Shankar *et al*; 2003).

Cinnamomum zeylanicum (cinnamon) extracts contain eugenol which might be responsible for the reduction of silver nitrate to AgNPs. Based on FTIR spectroscopy data, it has been proposed that the deprotonation of the hydroxyl ion of eugenol leads to the formation of resonance stabilized structures which can be further oxidized, by reducing metal ions into its nano range (Sathishkumar *et al*; 2009). Another major class of plant metabolites is flavonoids. Flavonoids are a group of polyphenolic compounds containing 15 carbon atoms and are water-soluble. Flavonoids can be classified into isoflavonoids, bioflavonoids, and neoflavonoids, which can act as chelating and reducing agents for metal ions. The functional groups present in flavonoids are solely responsible for nanoparticle formation.

The transition of flavonoids from the enol to the keto may lead to the reduction of metal ions to form nanoparticles (Makarov *et al*; 2014).

Ahmad *et al*; 2010; reported that *Ocimum basilicum* (sweet basil) extract contains flavonoids, eugenol, and polyphenols that play a key role in the formation of AgNPs from silver ions by tautomerization of enol to keto form. Several studies have been shown that flavonoids can act as chelating agents for example quercetin is a flavonoid that can chelate at three positions involving the carbonyl and hydroxyls at the C3 and C5 positions and the catechol group. This helps in understanding that flavonoids are involved in the initiation of nanoparticle formation (nucleation) and further aggregation, in addition to the bioreduction stage. For example, *Lawsonia inermis*, a good source of apiin (apigenin glycoside) was used for the biosynthesis of quasi-spherical AgNPs having an average diameter of 21-30 nm (Kasthuri *et al*; 2009).

It has been observed from FTIR spectroscopy that a carbonyl group has been attached to the nanoparticles, which shows that the sugars present in plant extracts are participating in the reduction and stabilization of metal ions into nanoparticles. Glucose, linear monosaccharides having a free aldehydic group, can directly act as reducing agents whereas fructose which contains a keto-group can act as antioxidants if tautomeric transitions occur from ketone to an aldehyde. It has been reported that when glucose was used as a reducing agent the nanoparticles with different morphologies were observed whereas with fructose only monodispersed nanoparticles were observed. It has been postulated that aldehydic group of carbohydrate gets oxidized into a carboxylic group via

the nucleophilic addition of OH⁻, which ultimately lead to the reduction of metal ions and synthesis of nanoparticles (Makarov *et al*; 2014).

There are three main phases included in the plant-mediated synthesis. The initial phase is also known as the activation phase during which metal ions get reduced and the reduced metal atoms get nucleated; another is the growth phase in which spontaneous aggregation of small adjacent nanoparticles occurs to form particles of a larger diameter, which are thermodynamically more stable; the last phase is the termination phase which determines the final shape of the nanoparticles (Makarov *et al*; 2014; Si and Mandal; 2007). An increase in the growth phase leads to aggregation of nanoparticles into nanotubes, nanorods, and nano triangles, etc (Makarov *et al*; 2014). In the termination phase, nanoparticles undergo a conformational change which is thermodynamically stable, which confirms the role of plant extract that stabilizes metal nanoparticles.

2.4 Pharmacological applications of plant-mediated metallic nanoparticles

Silver nanoparticles are mostly used in the medical field due to their antimicrobial effect, while zinc and titanium nanoparticles are used in cosmetics. Silver, zinc, and other metal nanoparticles are also used in food packaging, wound dressings, catheters for drug delivery, and so on due to the broad range of antimicrobial effects. The second application area of biological nanoparticles is the development of sensors for various biomolecules related to environmental factors and agriculture. Furthermore, nanoparticles are also used in gene delivery and cell labeling in plants and medicine. Some applications of metal nanoparticles are still in development, such as photoimaging, photothermal therapy, and magnetically responsive drug delivery.

(a) Anti-oxidant activity

Antioxidant agents including enzymatic and non-enzymatic substances regulate the free radical formation. Free radicals are causing cellular damage including brain damage, atherosclerosis, and cancer. The free radicals are generated by reactive oxygen species (ROS) such as superoxide dismutase, hydrogen peroxides, and hydrogen radicals. Biomolecules such as proteins, glycoproteins, lipids, fatty acids, phenolics, flavonoids, and sugars strongly control free radical formation (Marambio-Jones and Hoek; 2010). The scavenging power of enzymatic and non-enzymatic antioxidants is useful for the management of various chronic diseases such as diabetes, cancer, AIDS, nephritis, metabolic disorders, and neurodegenerative. The antioxidant effect of silver nanoparticles was stronger than other synthetic commercial standards e.g. ascorbic acid and so on (Reichelt *et al*; 2012).

(b) Anti-bactericidal activities of metallic nanoparticles

The AgNPs were effectively disrupting the polymer subunits of cell membranes in pathogenic organisms. The reciprocal action of nanoparticles subsequently breaks the cell membrane and disturbs the protein synthesis mechanism in the bacterial system (Sondi and Salopek-Sondi; 2004). The increasing concentrations of silver nanoparticles have faster membrane permeability than the lower concentrations and consequently rupture the cell wall of bacteria (Kasthuri *et al*; 2009). The maximum conductivity was observed in *Rhizophora apiculata* reduced silver nanoparticles which shown a low number of bacterial colonies in the experimental plate compared with AgNO₃ treated cells, which may be due to the smaller size of the particles and larger surface area which leads to the increase of

membrane permeability and cell destruction (Antony *et al*; 2011). The interactions of bacteria and the metallic silver and gold nanoparticles have been bonded with active sites of cell membranes to inhibit the cell cycle functions (Kim *et al*; 2007). The biosynthesized silver nanoparticles were achieved in a single-step procedure by using *Citrus sinensis* peel extract as a reducing and a capping agent. *C. sinensis* peel extract reduced silver nanoparticles effectively and the activity against *Escherichia coli*, *Pseudomonas aeruginosa* (gram-negative), and *Staphylococcus aureus* (gram-positive) has been proved (Kaviya *et al*; 2011).

Similarly, Krishnaraj *et al*; 2010; reported that *Acalypha indica* plant leaf synthesized silver nanoparticles effectively and control the water-borne pathogenic bacteria with lower concentrations of 10 µg/ml. The antimicrobial activity of metallic nanoparticles justifies its wound healing potential.

(c) Anti-fungicidal activities of metallic nanoparticles

The fungicidal mechanism of biosynthesized metallic nanoparticles has more potential than commercial antibiotics like fluconazole and amphotericin. The plant-derived Ag nanoparticles have clearly shown the membrane damage in *Candida* y cell function was destroyed (Logeswari *et al*; 2012). Most of the commercial antifungal agents have limited applications clinically and in addition, there are more adverse effects and less recovery from microbial disease. Subsequently, the commercial drugs induce side effects such as renal failure, increased body temperature, nausea, liver damage, and diarrhea after using the drugs. Nanoparticles were developed for novel and effective drugs against microbes. The fungal cell wall is made up of a high polymer of fatty acid and protein. The multifunctional

AgNPs have promising activity against spore-producing fungus and effectively destroy fungal growth. The significant changes were observed in the fungal cell membrane by treating it with metallic nanoparticles (Torresdey *et al*; 2002).

(d) Antiplasmodial activity of metallic nanoparticles

Currently, the most common diseases are spreading everywhere by the vectors. Vector control is a serious requirement in epidemic disease situations. The advanced antiplasmodial species-specific control method is less effective. This method has been more economical but less effective to control the target organisms in the health care sector (Gnanadesigan *et al*; 2011). Hence, effective and affordable antimalarial drugs are urgently required to control the plasmodial activity. In the last few decades, plants have been used as traditional sources of natural products and having enough sources for drug development for the antimalarial disease. The plant-derived chemical constituents such as quinine, artemisinin, and aromatic compounds have been successfully used against resistant strains of malaria parasites (Jayaseelan *et al*; 2011). Due to the high resistance of parasites, an alternative drug is needed for controlling the resistant strains. The plants developed metallic nanoparticles such as silver, platinum, and palladium nanoparticles effectively control the malarial population in the environment. Also, the biogenic synthesis of metallic silver nanoparticles from plant extract has been used to suppress the number of malarial productions.

(e) Anti-inflammatory action of metallic nanoparticles

Anti-inflammatory is a significant wound healing mechanism. Anti-inflammatory is a cascade process that produces immune-responsive compounds such as interleukins and cytokinins which can be produced by keratinocytes including T lymphocytes, B lymphocytes, and macrophages (Jacob *et al*; 2012). Certain inflammatory mediators such as enzymes, antibodies are secreted from the endocrine system. Other potential anti-inflammatory agents such as cytokines, IL-I, IL-II are secreted from the primary immune organs. These anti mediators induce the healing process (Satyavani *et al*; 2011). Also, the inflammatory mediators are involved in biochemical pathways and control the expansion of diseases. Biosynthesized gold and silver nanoparticles achieved positive wound repair mechanism and tissue regeneration in inflammatory function (Gurunathan *et al*; 2009). The studies proved that biosynthesized gold and silver nanoparticles are alternative sources for treating inflammation in a natural process.

(f) Anticancer studies on plant-mediated nanoparticles

Cancer is an uncontrolled cell proliferation with hysterical changes of biochemical and enzymatic parameters, which is the universal property of tumor cells. The overexpression of cellular growth will be arrested and regulated with systematic cell cycle mechanisms in cancerous cells by using bio-based nanoparticles as novel controlling agents (Akhtar *et al*; 2013). Also, the plant-mediated nanoparticles have a great effect against various cancer cell lines such as MCF 7, Hep 2, HCT 116, and Hela cell lines. Recently, many studies reported that plant-derived nanoparticles have the potential to control tumor cell growth. The improved cytotoxic effect is due to the secondary metabolites and other non-metal compositions in the synthesizing medium (Raghunandan *et al*; 2011; Das *et al*.; 2013).

The plant-derived silver nanoparticles regulate the cell cycle and enzymes in the bloodstream (Alt *et al*; 2004). Moreover, the plant synthesized nanoparticles relatively control the free radicals formation from the cell. Free radicals commonly induce cell proliferation and damage normal cell function. The moderate concentration of gold nanoparticles induces the apoptosis mechanism in malignant cells (Dipankar and Murugan; 2012). Similarly, Ag nanoparticles treated MCF-7 cancer cell line have retained the concentration of the biomolecules in the cells, and subsequently the cell metabolism was regulated (Das *et al.*, 2011). The metallic nanoparticles have proved their novel applications in the medical field to diagnose and treat various types of cancer and other retroviral diseases. The biobased nanoparticles are new and revolutionized to treat malignant deposits without interfering with normal cells. Suman *et al*; 2013 reported that the green synthesis of silver nanoparticles exhibited a significant cytotoxic effect in HeLa cell lines compared to other chemical-based synthetic drugs.

(g) Antiviral effects of metallic nanoparticles

Plants-mediated nanoparticles are the alternative drugs for treating and controlling the growth of viral pathogens. The entry of viruses into a host is very reckless and it is involved in the faster translational process to multiply their colony numbers. Biosynthesis of AgNPs nanoparticles can act as potent broad-spectrum antiviral agents to restrict virus-cell functions. Suriyakalaa *et al*; 2013 studied the bio-AgNPs that have persuasive anti-HIV action at an early stage of reverse transcription mechanism. The metallic NPs are strong antiviral agents and inhibit viral entry into the host system. The biosynthesized metallic nanoparticles have multiple binding sites to bind with gp 120 of the viral

membrane to control the function of the virus. The bio-based nanoparticles are acting as effective virucidal agents against cell-free virus and cell-associated virus (Sun *et al*; 2005). In addition, the silver and gold nanoparticles are constantly inhibiting post-entry stages of the HIV-1 life cycle. Therefore, the metallic nanoparticles will act as promising antiviral drugs against retroviruses.

(h) Antidiabetic management of metallic nanoparticles

Diabetes Mellitus (DM) is a group of metabolic dysfunction in which a person has uncontrolled sugar levels in the blood. Certain foods and balanced diets or synthetic insulin drugs can prevent diabetes at certain levels, but the complete treatment of DM is a big challenge. However, the biosynthesized nanomaterials could be an alternative treatment for its cure. Daisy and Saipriya's ; 2012 results showed that gold nanoparticles have good therapeutic effects against diabetic models. Gold nanoparticles significantly decline the level of liver enzymes such as alanine transaminase, alkaline phosphatase, serum creatinine, and uric acid in treated diabetes mice. The gold nanoparticles treated diabetic model showed a decrease of HbA (glycosylated hemoglobin) level which is maintaining the normal range. Swarnalatha *et al*; 2012; explored the *Sphaeranthus amaranthoides* biosynthesized silver nanoparticles inhibited α -amylase and acarbose sugar in diabetes-induced animal models. α -amylase inhibitory components are present in the ethanolic extract of *S. amaranthoides* (Manikanth *et al*; 2010). Likewise, Pickup *et al*; 2008; studied that nanoparticles are potent therapeutic agents to control diabetes. The clinical studies in mice successfully control the sugar level of 140 mg/dl in silver nanoparticles treated groups.

CHAPTER-3

AIM AND OBJECTIVES

3.0 Aim and Objectives

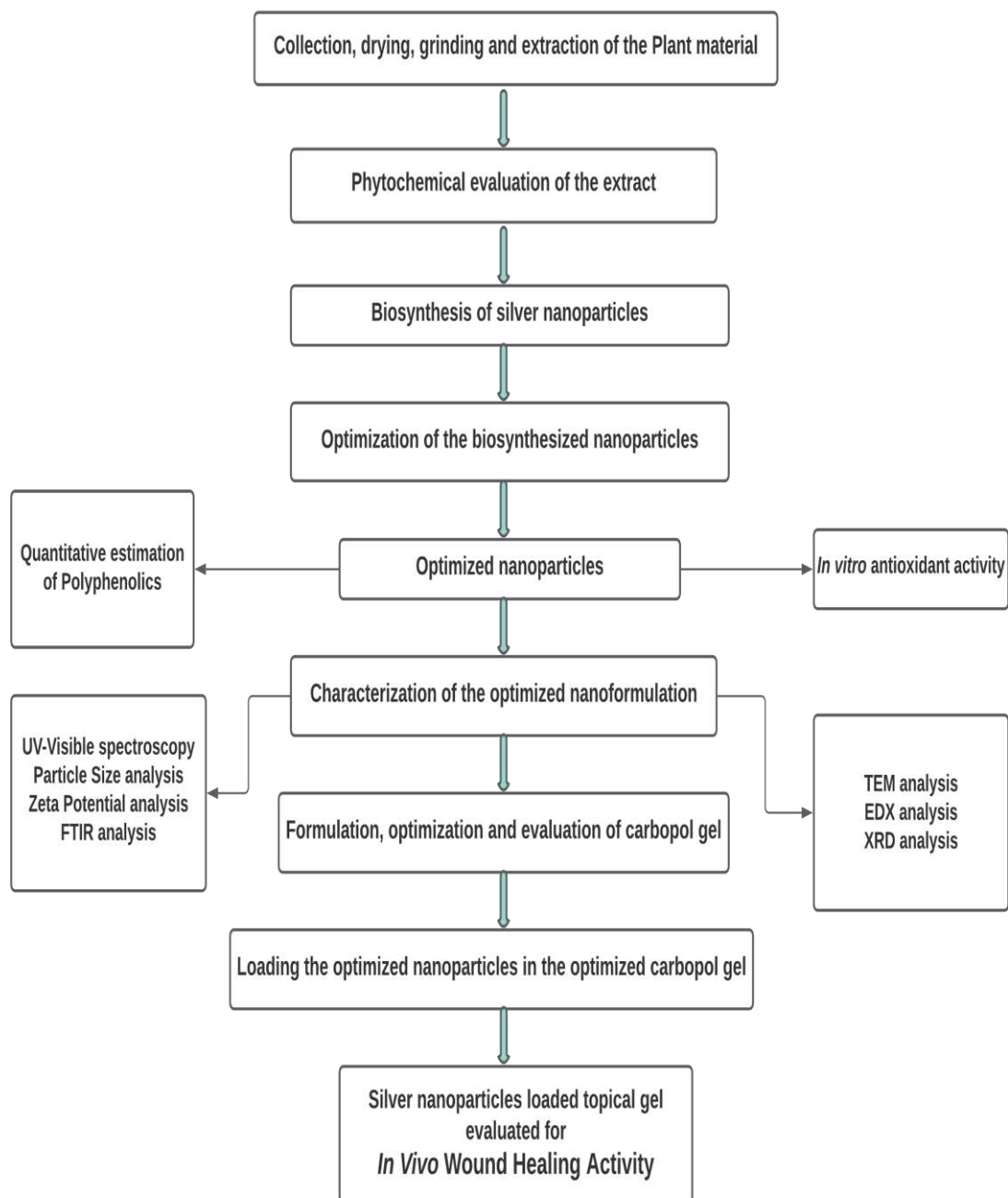
3.1 Aim: To perform the green synthesis, characterization, and evaluation of *in vitro* antimicrobial, antioxidant, and *in vivo* wound healing activity of silver nanoparticles loaded in topical gel using hydroalcoholic root extract of *Potentilla fulgens*.

3.2 Research Objective

Following are the main objectives of the present study:

- ✓ To carry out the extraction and phytochemical evaluation of *Potentilla fulgens* root.
- ✓ To carry out the optimization and synthesis of silver nanoparticles using the plant extract.
- ✓ Characterization of the biosynthesized silver nanoparticles.
- ✓ To study the *in vitro* antioxidant property and antibacterial activity of the synthesized silver nanoparticles.
- ✓ To quantitatively estimate the content of major polyphenolics in the biosynthesized nanoparticles.
- ✓ To carry out the formulation, optimization, and pharmaceutical evaluation of topical gel with and without biosynthesized nanoparticles.
- ✓ Evaluation of the *in vivo* wound healing activity using excision wound model.
- ✓ To perform the histopathological and biochemical estimations.

3.3 Plan of Work



CHAPTER-3

MATERIAL AND METHODS

4.0 Materials and Methods

4.1 Collection of Plant material

The plant material (root portion) was collected during daytime in the month of October-November 2020 from the Shillong region (25.5788° N, 91.8933° E) of the East Khasi Hills District, Meghalaya, Northeast India. The botanical authentication of the specimen was already done by Dr. N. Odyuo (Scientist C), Botanical Survey of India, Shillong, Meghalaya (Letter no.: BSI/ERC/2010/Plant identification/281).

4.2 Chemicals and equipment

Table 4.1: List of chemicals used

CHEMICALS AND REAGENTS USED	SOURCE
Ethanol	Nucleus Scientific
Silver nitrate(AgNO_3)	FINAR
Sodium Hydroxide(NaOH)	Sigma Aldrich
Dimethyl sulfoxide (DMSO)	MERCK
Wagners reagent	-
Mayers reagent	-

Dragendroff's reagent	-
Fehling's solution A	-
Fehling's solution B	-
Benedict reagent	-
Sulphuric acid (concentrated)	NICE
Lead acetate	Sigma Aldrich
Hydrochloric acid	NICE
Alpha naphthol	FINAR
Pyridine	HiMedia
Sodium nitroprusside	Nucleus Scientific
Ferric chloride	Nucleus Scientific
Lead acetate	HiMedia
Millon's reagent	-
Copper sulfate	MERCK
Barfoed's reagent	-
Ninhydrine	MERCK

Folin-ciocalteu (FC) reagent	HiMedia
Sodium carbonate	Sigma Aldrich
Polyvinyl pyrrolidone (PVPP)	MERCK
Tannic acid	Sigma Aldrich
Quercetin dihydrate	Sigma Aldrich
Aluminum trichloride	MERCK
Glacial acetic acid	MERCK
Methanol	FINAR
DPPH	Sisco Research Laboratories Pvt. Ltd
Ascorbic acid	Sigma Aldrich
Carbopol 940	Sigma Aldrich
Triethanolamine	EMPARTA

Table 4.2: List of major instruments and equipment used

INSTRUMENTS AND EQUIPMENT	MODEL AND MAKE
Digital Balance	DENVER

Thermostat water bath	I-therm AI-7981
pH meter	Systronics, 361
Hot Air Oven	HiMedia
Brookfield Viscometer	BROOKFIELD, LVDV-E
Lyophilizer (Freeze Dryer)	IIC Industrial Corporation
Homogenizer	IKA RW20
Ultra sonicator	PCI Analytics, 3-SL-100
Cooling Centrifuge	REMI
Heating mantle	PERFIT INDIA
Tray dryer	PERFIT INDIA
UV-Vis Spectrophotometer	SHIMADZU, UV-1800
Fourier Transformed Infra-Red Spectrometer	BRUKER, Alpha-E
Texture Analyzer	Stable Micro System, FD/1-077
Zetasizer	Malvern, NANO-S90
Transmission Electron Microscopy	TEM-2100 Plus

X-Ray Diffraction	Bruker D8 Advanced
Magnetic stirrer	IKA big squid
Rotary Vapor Evaporator	BUCHI, V-700
Binocular Microscope	LABOMED

4.3 Preparation of plant extract

4.3.1 Drying and Pulverizing: After collection of the plant material, it was initially surface cleaned with running tap water to remove the debris and other contaminated organic matter and then twice with deionized water and allowed to dry in a tray dryer (PERFIT INDIA) at a temperature not exceeding 40° C. The dried roots were pulverized well to powder form and kept in a well-closed container in a dry place.

4.3.2 Preparation of hydroalcoholic extract of *Potentilla fulgens*

50 gm of the powdered root was macerated thrice with 500 ml of hydro alcoholic solvent (350 ml ethanol and 150 ml water) with slight heating. The mixture was kept for 24 hours. After 24 hours, the extract was filtered with Whatman No.1 filter paper. The solvent was evaporated using a rotary vacuum evaporator (Buchi, Switzerland) under reduced pressure at 45 °C followed by lyophilization to acquire pure extract that was refrigerated at 4 °C till further analysis.

4.4 Preliminary phytochemical screening of the extract

The preliminary phytochemical screening based on qualitative analysis of the extracts will be tested as per the standards methods available in the literature (Laloo *et al*; 2020). Qualitative

tests were screened for various phytochemical classes such as alkaloids, glycosides, phenolics, tannins, flavonoids, steroids/triterpenes, saponins, mucilages, proteins, amino acid, and carbohydrates components.

4.4.1 Test for alkaloids

- **Wagner's Reagent Test:** To 2-3 ml of extract, a few drops of Wagner's reagent were added by the side of the test tube. The formation of reddish-brown ppt. indicates the test as positive and ensures the presence of alkaloids.
- **Mayer's Reagent Test:** To 2-3 ml of extract, a few drops of Mayer's reagent was added by the side of the test tube. A white or creamy ppt. indicates the test as positive.
- **Dragendorff's test-** To 2-3 ml of extract, a few drops of Dragendorff reagent was added.. The formation of orange to reddish color precipitate ensures the presence of alkaloids.

4.4.2 Test for carbohydrates

- **Molisch's Test:** To 2-3 ml of extract, a few drops of alcoholic solution of alpha naphthol was added. The mixture was then shaken well and 1 ml of concentrated H_2SO_4 was added along the side of the test tube. A violet ring formed at the junction of two liquids indicates the presence of carbohydrates.
- **Fehling's Test:** 1 ml of both Fehling's A and Fehling's B solution was mixed, boiled for 1 minute. An equal volume of test solution was added to the mixture. The mixture was then heated in a boiling water bath for 5 min. Initially yellow and then brick red ppt. indicates the presence of carbohydrates.

- **Benedict's Test:** Equal volume of Benedict's reagent and test solution was mixed in a test tube and heated in a boiling water bath for 5 min. Solution appearing green, yellow, or red depending on the amount of reducing sugar present in the test solution indicates the presence of carbohydrate.

4.4.3 Test for glycosides

- **Cardiac glycoside**
 - **Legal Test:** To alcoholic extract, 1 ml of pyridine and 1 ml sodium nitroprusside was added. The appearance of pink to red color indicates the presence of glycosides.
- **Anthraquinone Glycoside**
 - **Borntrager's Test:** To 3 ml of extract, dilute H_2SO_4 was added. The mixture was boiled and filtered. To the cold filtrate, an equal volume of benzene or chloroform was added, shaken well. If the ammoniacal layer turns pink or red in addition to ammonia it indicates the presence of glycosides.

4.4.4 Test for steroid

- **Salkowski Reaction:** To 2 ml of extract, 2 ml of chloroform, and 2 ml of concentrated H_2SO_4 was added and well shaken. If the chloroform layer appears red and the acid layer shows greenish-yellow fluorescence it indicates the presence of steroids.

4.4.5 Test for tannins and phenolics

- **Ferric Chloride Test:** To 2-3 ml of extract, a few drops of 5% ferric chloride solution was added. A deep blue-black color indicates the presence of tannins and phenolic compounds.

4.4.6 Test for flavonoids

- **Lead acetate test-** To 2-3 ml of extract, lead acetate solution was added. The formation of orange-brown precipitate residues signifies the presence of flavonoids.

4.4.7 Test for proteins

- **Biuret Test:** To 3 ml of test solution, 4% sodium hydroxide, and few drops of 1% copper sulfate solution were added. The appearance of violet or pink color indicates the presence of proteins.
- **Millon's Test:** 3 ml of test solution was mixed with 5 ml of Millon's reagent. The appearance of white ppt. indicates the presence of proteins.

4.4.8 Test for amino acids

- **Ninhydrin test:** 3 ml of plant extract was heated with 5% Ninhydrin solution (prepared in butanol) in a boiling water bath for 10 minutes. The appearance of purple or bluish color indicates the presence of proteins.

4.4.9 Test for tannins

- The plant extract was dissolved in methanol followed by the addition of 10% lead acetate. The appearance of white precipitate indicated the presence of tannins.

4.4.10 Test for monosaccharides

- **Barfoeds test:** Equal volume of Barfoeds reagent and extract solution was mixed followed by heating for 1-2 minutes in a water bath. After cooling, the appearance of reddish color indicates the presence of monosaccharides.

4.5 Biosynthesis of silver nanoparticles

Silver nanoparticles were synthesized following the previously reported method with slight modification. To synthesize silver nanoparticles, a stock solution of *P. fulgens* dried extract was prepared with a concentration of 1mg/ml. Then 1, 2, 3, 4, and 5 mL of plant extract was added separately to 49, 48, 47, 46, and 45 ml of silver nitrate solution respectively keeping its concentration at 1 mM. Silver nanoparticles were also synthesized by varying concentrations of AgNO₃ (1 mM- 5 mM) keeping extract concentration constant (1 mL). This setup was incubated at 200 rpm for 1 hour in a dark chamber to minimize the photo-activation of silver nitrate. The reduction of Ag⁺ to Ag⁰ was initially confirmed by visual inspection of color change from colorless to brown and then by spectrophotometric absorption at 400–420 nm. Various reaction parameters (concentrations of plant extract, concentrations of metal ions and pH,) were optimized to enhance the yield of nanoparticles. The nanoparticles were harvested by centrifugation (REMI) to remove unreacted phytochemicals from the reaction medium at 18,000 rpm for 30 min and the pellet was thoroughly washed with deionized water. The resulting

suspension was dried in a lyophilizer (IIC Industrial Corporation) and then further characterized (Ahmed *et al*; 2016).

4.6 Selection criteria for the optimized formulation

For optimizing the best formulation, different concentrations of the plant extract were allowed to react with different concentrations of silver nitrate solution. Initially, 1 mg of the plant extract was allowed to react with 1-5 mM of silver nitrate solution. Similarly, 2.5 mg, 5 mg, 10 mg of plant extract were allowed to react with 1-5 mM of silver nitrate. Thus, a total of 20 different nanoparticle formulations were synthesized. Out of the 20 different nanoparticle formulations, selection of the optimized formulation was done based on UV-visible spectroscopy, particle size, and polydispersity index (PDI). And thus, the nanoformulation, showing a broader peak in UV-vis spectroscopy, and with comparatively higher particle size and polydispersity index are rejected. While, 6 formulations having very sharp peaks depicted in UV-visible spectroscopy and a comparatively lower particle size and polydispersity index (PDI) (measured using dynamic light scattering), are selected. Out of the 6 formulations, the best and optimized formulation was selected based on zeta potential.

4.7 Optimization of certain parameters for the synthesis of nanoparticles

Various parameters such as concentrations of plant extract, the concentration of metal ions, pH of the reaction mixture, and reaction time were optimized to increase the yield of nanoparticles. The ratio of metal ions to reducing agents affects the rate of synthesis as well as the size, shape, and yield of nanoparticles. Then different amounts (1 to 5 mg) of plant extract were added to

water (50 mL). Metal salt was added to these dilutions and reaction mixtures were continuously stirred at 200 rpm maintaining dark conditions. The absorbance of the resultant solutions was measured by a UV–vis spectrophotometer (SHIMADZU, UV-1800) periodically. To optimize the metal ion concentration, a fixed concentration of plant extract was added to various flasks containing different concentrations of silver nitrate (1-5 mM). This setup was also maintained at the dark condition with a 200 rpm stirring speed. The pH in all the cases was measured. To optimize reaction time, in terms of yield and properties of nanoparticles, samples were collected at various time intervals and subjected to characterization. The nanoparticle colloidal solution and their lyophilized form (nanopowder) were kept in dark condition at room temperature for about 9 months to check their stability. The stability of the particles was periodically checked by UV–vis spectral analysis (Mittal *et al*; 2015).

4.8 Characterization of the optimized nanoparticles

Characterization of silver nanoparticles was carried out by using various analytical techniques like UV–Visible spectroscopy, Dynamic Light Scattering (DLS) X-Ray Diffraction (XRD), Fourier Transform Infrared Spectroscopy (FTIR), Energy-dispersive X-ray spectroscopy (EDX), Transmission Electron Microscopy (TEM) (Panda *et al*; 2021).

4.8.1. UV–vis spectra analysis

The UV–vis absorbance spectra were used for the preliminary identification of silver nanoparticle formation. An absorption band near 400–450 nm indicated the formation of silver nanoparticles (Cheng *et al*; 2015). For this purpose, 300 μ L of silver nanoparticles were taken in a quartz cell of 1.0 cm path length and brought the volume up to 2 mL by the addition of

deionized water. Sample absorbance was recorded in the wavelength ranging from 300-700 nm using a UV spectrophotometer (SHIMADZU, UV-1800) at different time intervals (Rashhed *et al*; 2017)

4.8.2 Size and zeta potential analysis

Dynamic light scattering (DLS) or zeta-sizer is a technique used to measure the size and size distribution of very small particles dispersed in a liquid. To estimate the particle size and zeta potential, a dilute suspension of nanoparticles was prepared in deionized water and sonicated (for removing aggregation) at 35 °C for 30 min and subjected to DLS analysis. The average particle size and zeta potential of nanoparticles were estimated by Zetasizer Nano ZS (Malvern Instruments, Malvern, UK) (Manik *et al*; 2020).

4.8.3 FTIR analysis of Ag nanoparticles

FTIR spectroscopy was performed to identify the functional groups capped on the surface of nanoparticles. The functional groups of the synthesized nanoparticles were identified using FTIR (BRUKER, Alpha-E) spectroscopy. The bio-reduced colloidal nanoparticle solution was centrifuged at 15,000 RPM for 30 min and the pellets were thoroughly washed with deionized water. The resulting suspension was completely dried in a freeze dryer and analyzed by FTIR spectroscopy (Qais *et al*; 2020).

4.8.4 Transmission electron microscopy (TEM) analysis

Transmission electron microscopy (TEM) analysis of the nanoparticles was carried out by TEM-2100 Plus electron microscope using 200 kV. The TEM sample was prepared by a drop of reaction sample on a carbon-coated copper grid and the excess solution was removed by blotting

followed by drying under a mercury lamp. The drop on the TEM grids was allowed to leave for 2 min and the grid was allowed to dry. The synthesized silver nanoparticles were analyzed for their size (Jebril *et al*; 2020).

4.8.5 Energy dispersive X-ray analysis (EDX)

The elemental composition of nanoparticles was determined using energy dispersive X-ray analysis (EDX) attached with the TEM instrument.

4.8.6 X-ray diffraction analysis (XRD)

X-ray diffraction (XRD) analysis, carried out on an XRD instrument operating at 45 kV and a current of 40 mA with CuK α radiation, was performed to determine the nature of nanoparticles. The instrument was operated over the 2θ range of 30–80° (Bruker D8 Advanced) (Mittal *et al*; 2015).

4.9 Determination of total phenolics and simple phenolics (Makkar *et al.*, 2000)

4.9.1 Reagent preparation

- **Preparation of 1N Folin-Ciocalteu (FC) reagent:** 1 ml of commercially available FC reagent (2N) was diluted with 1 ml of distilled water and transferred to a brown bottle and refrigerated (4°C).
- **Preparation of sodium carbonate solution (20%):** For the preparation of 20% sodium carbonate solution, 2 gm of sodium carbonate was weighed and dissolved in 10 ml of distilled water.

- **Insoluble polyvinyl pyrrolidone (polyvinyl polypyrrolidone, PVPP):** This is commercially available from Sigma.
- **Standard tannic acid solution (0.1 mg/ml):** 25 mg tannic acid (TA, Merck) was dissolved in 25 ml distilled water and then diluted 1:10 in distilled water.

4.9.2 Preparation of standard calibration curve: For the preparation of the standard calibration curve, tannic acid (0.00, 0.02, 0.04, 0.06, 0.08, and 0.10 mg/mL) was initially taken in different eppendorf tubes adjusting the volume to 0.5 ml with distilled water. It was followed by the addition of 0.25 ml of Folin– Ciocalteu's phenol reagent (1N). To its tube, 1.25 ml of sodium carbonate solution (20%) was added and the resultant mixture was incubated at room temperature for 40 minutes which was further vortexed and recorded absorbance at 725 nm.

4.9.3 Procedure for estimation of total phenolics (Makkar *et al*, 2000)

For the estimation of total phenolics, A sample of nanoparticles (0.1 ml, 1mg/ml) was taken in an eppendorf tube and the volume was adjusted to 0.5 ml with distilled water. It was followed by the addition of 0.25 ml of Folin– Ciocalteu's phenol reagent (1N). To the mixture, 1.25 ml of sodium carbonate solution (20%) was added and the resultant mixture was incubated at room temperature for 40 minutes. After 40 minutes, the tube was vortexed and the absorbance was recorded at 725 nm. The tannic acid was used as a standard for the calculation of total phenolic content and calculated as tannic acid equivalent from the above calibration curve.

4.9.4 Estimation of simple phenolics (Makkar *et al*, 2000)

PVPP binds tannins. Initially, take 100 mg of PVPP in an eppendorf tube and dissolve in 1 ml of distilled water. AgNPs (1 ml, 1mg/ml) were added to the tube and vortexed. After vortexing, the

resulting tube was kept at 4°C for 15 minutes. It was again vortexed and then centrifuged (3000 RPM for 10 minutes) to collect the supernatant. The supernatant has only simple phenolics other than tannins. The phenolic content of the supernatant was measured as the earlier method i.e. determination of total phenolics.

Total tannin can be calculated by the following formula:

$$\text{Total tannin content} = \text{Total phenols} - \text{Simple phenols}$$

4.10 Determination of total flavonoid content (Kumaran *et al*; 2005)

4.10.1 Preparation of standard calibration curve using quercetin:

A stock solution of quercetin 1 mg/ml was prepared in distilled water. From the stock solution, 5, 10, 25, 50, and 100 µl of quercetin was taken in different test tubes and the volume was adjusted to 100 µl in each test tube with distilled water. To each test tube, 100 µl aluminum trichloride (20% in H₂O) was added followed by the addition of 1 drop of glacial acetic acid. The resultant mixtures were diluted with ethanol up to 5 ml. The absorption at 415 nm was recorded after 40 minutes and the calibration curve was plotted.

4.10.2 Estimation of total flavonoid content:

AgNP (100 µl, 1mg/ml) was taken in a test tube and 100 µl aluminum trichloride (20% in H₂O) was added to it. This was followed by the addition of 1 drop of glacial acetic acid. The resultant mixture was diluted with ethanol up to 5 ml and recorded absorbance at 415 nm after 40 minutes. m. A blank sample was prepared using 100µl of methanol in place of AgNP.

The number of flavonoids in AgNPs in quercetin equivalents (QE) was calculated by the following formula:

$$\text{Total Flavonoid} = (A.m_0) / (A_0.m)$$

where A represents the absorbance of the AgNPs,

A_0 is the absorbance of the standard quercetin

m is the weight of AgNPs

m_0 is the weight of quercetin in solution, mg.

4.11 *In vitro*-antioxidant activity

The radical scavenging activity had been determined using DPPH free radical assay with some modification. Initially, a stock solution of 1 mg/ml of AgNPs was prepared and 25, 50, 100, 200, 400 $\mu\text{g/mL}$ of the various concentrations of plant extracts in methanol were added to 5 mL of 100 μM solution of DPPH in methanol. After 30 minutes of incubation, absorbance has been read against blank taken as methanol at 517 nm and the percentage inhibition activity can be calculated from the following equation:

$$\% \text{ Inhibition} = [(A_0 - A_1) / A_0] \times 100 \dots\dots\dots(i)$$

Where A_0 is the absorbance of the control, and A_1 is the absorbance of the extract/ standard. Here Ascorbic acid was used as a standard. All the readings were performed in triplicates (Braca *et al*; 2001).

All the values of the experimental results were expressed as mean \pm standard error of the mean (SEM). For the evaluation of anti-oxidant activity, student t-test was done. GraphPad Prism 5.0 software (GraphPad Software, Inc., La Jolla, CA) was used for all statistical analyses. A difference in the mean values of $p < 0.05$ was considered to be statistically significant.

4.12 Preparation of topical gel

4.12.1 Preparation of plain gel

For the preparation of plain gel, carbopol 940 was dissolved in demineralized water with continuous stirring till it dissolves completely. A sufficient amount of triethanolamine was added dropwise to the carbopol solution with constant stirring until a clear consistent gel was obtained. The prepared gel was evaluated for different physicochemical parameters (Aiyalu *et al*; 2016).

4.12.2 Optimization of plain gel

For optimizing the gel preparation, 0.1, 0.2, 0.3, 0.4, and 0.5 % of carbopol 940 were dissolved in demineralized water with continuous stirring. During stirring, a sufficient amount of triethanolamine was added dropwise to each carbopol solution with constant stirring until a clear consistent gel was obtained. The prepared gels were evaluated for different physicochemical parameters. And the optimization of the gel was based on the physicochemical parameters (Aiyalu *et al*; 2016).

4.12.3 Pharmaceutical evaluation of the gel

4.12.3.1 . Sensory properties and physical observation of oral gel formulations

Prepared gel formulations were visually inspected for clarity, color, homogeneity, consistency, and presence of particles. To investigate the consistency of the formulations, a small quantity of gel was pressed between the thumb and the index fingers, and the consistency of the gel was noticed (Alam *et al*; 2020).

4.12.3.2 Appearance and Homogeneity

The physical appearance and homogeneity of the prepared gels were evaluated by visual perception. They were tested for their appearance and presence of any aggregates (Aiyalu *et al*; 2016).

4.12.3.3 Grittiness

All the formulations were evaluated microscopically for the presence of any appreciable particulate matter which was seen under a light microscope. Hence obviously they gel preparation fulfills the requirement of freedom from particular matter and form grittiness (Kaur *et al*; 2013)

4.12.3.4 pH measurement

pH measurement of the gel was carried out using a digital pH meter by dipping the glass electrode completely into the gel system to cover the electrode. The measurement was carried out in triplicate and the average of the three readings was recorded (Queiroz *et al*; 2009).

4.12.3.5 Determination of viscosity

The viscosity of the gel formulations was determined using Brookfield viscometer (S-64, model BROOKFIELD, LVDV-E) at 25 °C with a spindle speed of the viscometer rotated at 1-20 rpm (Nayak *et al*; 2005). Evaluations were done in triplicates and mean viscosities were calculated.

4.12.3.6 Spreadability

Two sets of glass slides of standard dimensions were taken. The gel formulation was placed over one of the slides. The other slide was placed on the top of the gel, such that the gel was sandwiched between the two slides in an area occupied by a distance of 7.5 cm along with the slides. A hundred-gram weight of gel was placed on the upper slides so that the gel was between the two slides was pressed uniformly to form a thin layer. The weight was removed and the excess of gel adhering to the slides was scrapped off. The two slides in position were fixed to a stand without the slightest disturbance and in such a way that only upper slides could slip off freely by the force of weight tied on them. A 20 g weight was tied to the upper slide carefully. The time taken for the upper slide to travel the distance of 7.5 cm and separated away from the lower slide under the influence of the weight was noted. The experiment was repeated three times and the meantime was taken for calculation (Aiyalu *et al*; 2016).

Spreadability was calculated by using the following formula:

$$S = m \times l/t$$

where, S= spreadability,

m-weight tied to upper slides (20 g),

l- length of the glass slide (7.5 cm),

t- time taken in sec.

4.12.3.7 Gel strength

The strength of the gel formulations was determined using a texture profile analysis (Stable Micro System, FD/1-077). The experiment was done by placing the gels in standard beakers below the probe. In this, an analytical probe is then immersed into the sample. The Texture Analyzer was set to the 'gelling strength test' mode or compression mode with a test speed of 1.0 mm/s. An acquisition rate of 50 points per second and a trigger force of 5 g were selected. An aluminum probe of 7.6 cm diameter was used for all the samples. The study was carried out at room temperature. The force required to penetrate the gel was measured as gel strength in terms of grams (Harish et al; 2009).

4.12.4 Loading of AgNPs in gel

After optimization of the plain gel, 20 mg of synthesized AgNPs were added to the optimized gel formulation (10 gm, 0.2 %) and was constantly stirred mechanically for 30 minutes till uniform distribution of the AgNPs.

4.13 Experimental setup and treatment protocol for wound healing activity

Albino Wistar rats of either sex (220 ± 10 g) were used for the study after receiving approval from the Institutional Animal Ethical Committee, Girijananda Chowdhury Institute of Pharmaceutical Science, Guwahati (Project Proposal approval no. GIPS/IAEC/M.PH/PRO/01/2021). The rats were housed under standard laboratory conditions and were fed with commercial rat feed and water ad libitum. The animals were divided into 5 groups with six animals in each group ($n = 6$) as shown below. All the standard and tested drugs

were administered to the animal for a period of 16 days. Animals were fasted for 18 h (with free access to water ad libitum) before the commencement of the experiment.

- **Group I (normal group):** This group received a normal diet and water ad libitum. No wound was induced in this group.
- **Group II (Untreated group):** This group received a normal diet and water ad libitum + induction of open wound.
- **Group III (Treated with the plain gel):** This group received a normal diet + water ad libitum + induction of open wound + treatment with plain gel without drug.
- **Group IV (Standard Control):** This group received a normal diet and water ad libitum + induction of open wound + treatment with marketed silver nitrate gel (0.2 % w/w).
- **Group V:** This group received a normal diet and water ad libitum + induction of open wound + treatment with 0.2 % w/w formulated topical gel.

4.14 Acute dermal toxicity studies

Healthy young female adult rats (220±10 g), nulliparous and non-pregnant were selected for conducting the acute dermal toxicity studies. The animals were acclimatized to the laboratory conditions for seven days prior to the start of the study, using group caging for welfare reasons. The acute dermal toxicity testing of the tested drugs was performed by applying the topical AgNP gel on the shaved backs of the rats. The animals were then monitored for any sign of dermal toxicity as per the methods described in OECD/OCED guideline no. 402 (Acute dermal toxicity 2017).

4.15 Wound healing activity using excision wound model

The experimental animals were divided into 5 groups with six animals in each group (n=6) and were anesthetized using ketamine (40 mg/kg) [IP] anesthesia, before the creation of the wound. The particular skin area was shaved 1 day prior to the experiment. An excision wound was inflicted by cutting away the skin measuring 30 mm² full thickness and 2mm depth from a predetermined shaved area. The wounds were left undressed to the open environment and the animals were carefully observed for any infection. Hemostasis was achieved by blotting the wound with a cotton swab soaked in normal saline solution. The wounded animals were housed separately in different cages. The wound area was measured instantly using Android software, ImitoMeasure (available in google play store). The wound area was measured out on respective days (0th, 5th, 7th, 10th, 14th, and 21st day) and the percentage wound contraction was calculated as shown below (Zangeneh *et al*; 2019).

$$\% \text{ Wound contraction} = \frac{\text{Wound area on day '0'} - \text{Wound area on day 'n'}}{\text{Wound area on day '0'}} \times 100$$

Wound area on day '0'

The period of epithelialization was calculated as the number of days required for falling off of the dead tissue remnants without any residual raw wound. For the determination of the epithelialization period, animals (n=6) will be divided into 5 separate groups in a similar way in the excision wound model (Kundu *et al*; 2016)

4.15.1 Measurement of wound contraction area

Measurements of wound area using tracing papers is tedious and there is a high possibility of errors since it is manual. So, today researchers are searching for an alternative. And obviously, the alternative is the use of sophisticated software. For the very first time, in the present study, **ImitoMeasure**, an android software, freely available on google play store is used for measuring the wound contraction area. This software uses specific calibrated markers for measuring the wound area and provides accurate results.

4.16 Histopathological studies

On the 21st postoperative day, a fraction of the excision skin tissues from all the normal, control, standard, and treated animals were processed for histopathological examination. All the samples were fixed in 10% buffered formalin, blocked with paraffin, and then sectioned into 5 μ m thickness. All the selected sections were processed and stained with hematoxylin and eosin (H–E) dye (Murthy *et al*; 2013). The stained tissues were examined and photographed.

4.17 Statistical analysis

All the values of the experimental results were expressed as mean \pm standard error of mean (SEM). For the evaluation of wound area, from post-operative day 0–21th, analysis of variance (ANOVA) was done, statistically by two-way ANOVA followed by Bonferroni's post-test for multiple comparisons between groups. GraphPad Prism 5.0 software (GraphPad Software, Inc., La Jolla, CA) was used for all statistical analyses. A difference in the mean values of $p < 0.05$ was considered to be statistically significant.

CHAPTER-5

RESULTS AND DISCUSSION

5.0 RESULTS AND DISCUSSIONS

5.1 Phytochemical evaluation

5.1.1 Extraction yield

The percentage yield of the *Potentilla fulgens* root extract obtained after maceration was found to be 3.07 %.

5.1.2 Preliminary phytochemical screening of the extract

From the preliminary phytochemical screening, it was observed that the roots of *Potentilla fulgens* showed the presence of active classes of phytochemicals which include polyphenolics (tannins, phenolics, and flavonoids), saponin glycoside, steroids, and carbohydrates. Whereas, alkaloids, coumarins, cardiac glycosides, and mucilage components seem to be absent. This confirms that the herb may be a good source of polyphenolics which are therapeutically active components of plants. Phytochemical screening only gives a preliminary idea about the qualitative nature of active phytoconstituents present in the plant material.

5.2 Biosynthesis of silver nanoparticles

Initially, the synthesized nanoparticles were identified by visually observing the color change of the reaction mixture. The addition of plant extract of *P. fulgens* into the beakers containing the aqueous solution of silver nitrate led to the change in the color of the solution from colorless to reddish-brown (shown in Fig 5.1) within reaction duration (Veerasamy *et al*; 2011). The color change in the reaction mixture indicated the formation of nanoparticles. The reaction color was due to the excitation of surface plasmon vibrations (essentially the vibration of the group conducting electrons) in the colloidal solution of nanoparticles (Mittal *et al*; 2012).



Fig 5.1: Biosynthesis of AgNPs using *P. fulgens* extract (color of silver nitrate and plant extract before and after the reaction)

5.3 Selection of the optimized formulation

For optimizing the best formulation, different concentrations of the plant extract were allowed to react with different concentrations of silver nitrate solution. Initially, 1 mg of the plant extract was allowed to react with 1-5 mM of silver nitrate solution. Similarly, 2.5 mg, 5 mg, 10 mg of plant extract were allowed to react with 1-5 mM of silver nitrate. Thus, a total of 20 different nanoparticle formulations were synthesized. Out of the 20 different nanoparticle formulations, selection of the optimized formulation was done based on UV-visible spectroscopy, particle size, and polydispersity index (PDI). And thus, the nanoformulation, showing a broader peak in UV- vis spectroscopy, and with comparatively higher particle size and polydispersity index are rejected. While, 6 formulations having very sharp peaks depicted in UV-visible spectroscopy and a comparatively lower particle size and polydispersity index (PDI) (measured using dynamic light scattering), are selected.

CHAPTER-5 RESULTS & DISCUSSION

Out of the 6 formulations, the best and optimized formulation was selected based on zeta potential. Table 5.1 represents the comparative data of UV spectroscopy, particle size analysis, polydispersity index (PDI), and zeta potential of the 6 formulations, which was used for the optimization of the biosynthesized silver nanoparticles.

Table 5.1: Comparative data of UV, PDI, Z-average after till 1month

Sample Code	UV				PDI				Z- average (nm)				Z- ptnl
	24 hrs	1 wk	3 wks	1 mnt h	24 hrs	1 wk	3 wk	1 mnth	24 hrs	1 wk	3 wks	1 mnt h	
1 mg + 4mM	NG	G	NG	NG	0.158	0.213	0.250	0.281	231	229	221	259	25.0
2.5 mg+ 4 mM	G & S	G & S	G & S	G & S	0.189	0.224	0.193	0.23	173	177	176	163	27.5
5 mg+ 4 mM	NG	NG	NG	NG	0.175	0.212	0.209	0.24	189	193	196	173	NG
2.5 mg+ 5 mM	VG & S	VG & S	VG & S	G & S	0.200	0.227	0.239	0.27	253	263	259	243	27.6
5 mg + 3 mM	VG & S	VG & S	VG & S	VG & S	0.207	0.210	0.220	0.20	154	152	153	137	25.5

10 mg	G	G	G	G	0.238	0.25	0.26	0.29	153	146	155	169	25.5
+ 2mM						2	8						

*G: Good; NG: Not good; VG: Very good and S: Sharp

5.4 Characterization of the optimized silver nanoparticles

5.4.1 Visual observation and UV-Vis spectroscopy

Silver nanoparticles were synthesized at different concentrations of the silver nitrate solution (1-5 mM) keeping the plant extract concentration constant (1mM). Plasmon resonance band observed at 436-446 nm similar to those reported in the literature (Obaid *et al*; 2015). There is an increase in the intensity of absorption peaks after regular intervals of time and the color intensity increases with the duration of incubation. It was also observed that the intensity of absorption peaks increases with an increase in the concentration of the silver nitrate salt. Parallel changes in color have been observed at different concentrations of plant extract (1mg, 2.5 mg, 5mg, and 10 mg) keeping the silver nitrate concentration constant.

In all the cases, an absorption band near 400-450 was observed which signifies the formation of silver nanoparticles.

Fig 5.2 represents the different UV-spectrum on varying the concentration of silver nitrate and the plant extract.

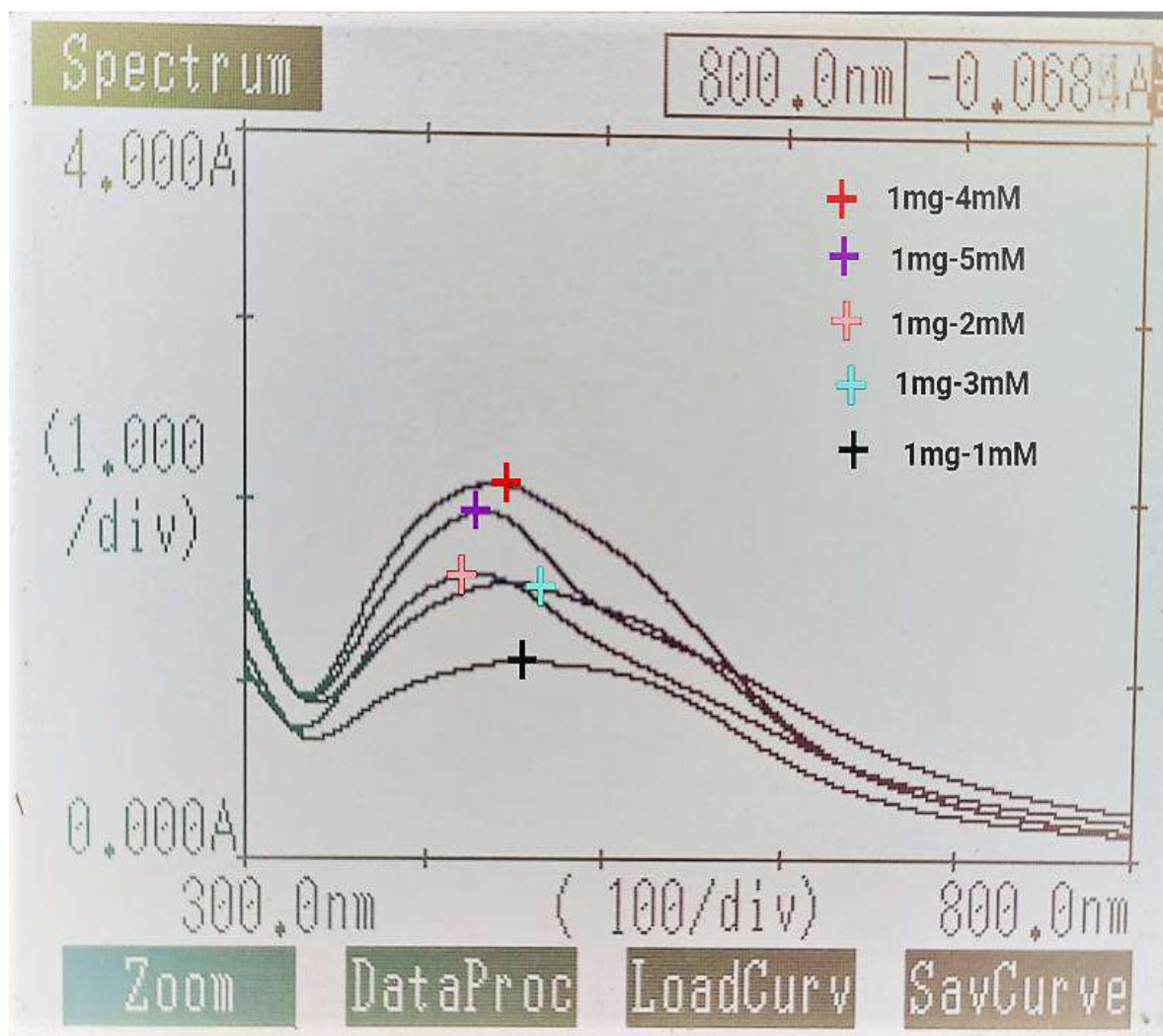


Fig 5.2 (a): UV spectrum of 1 mg of plant extract reacting with different concentration of silver nitrate

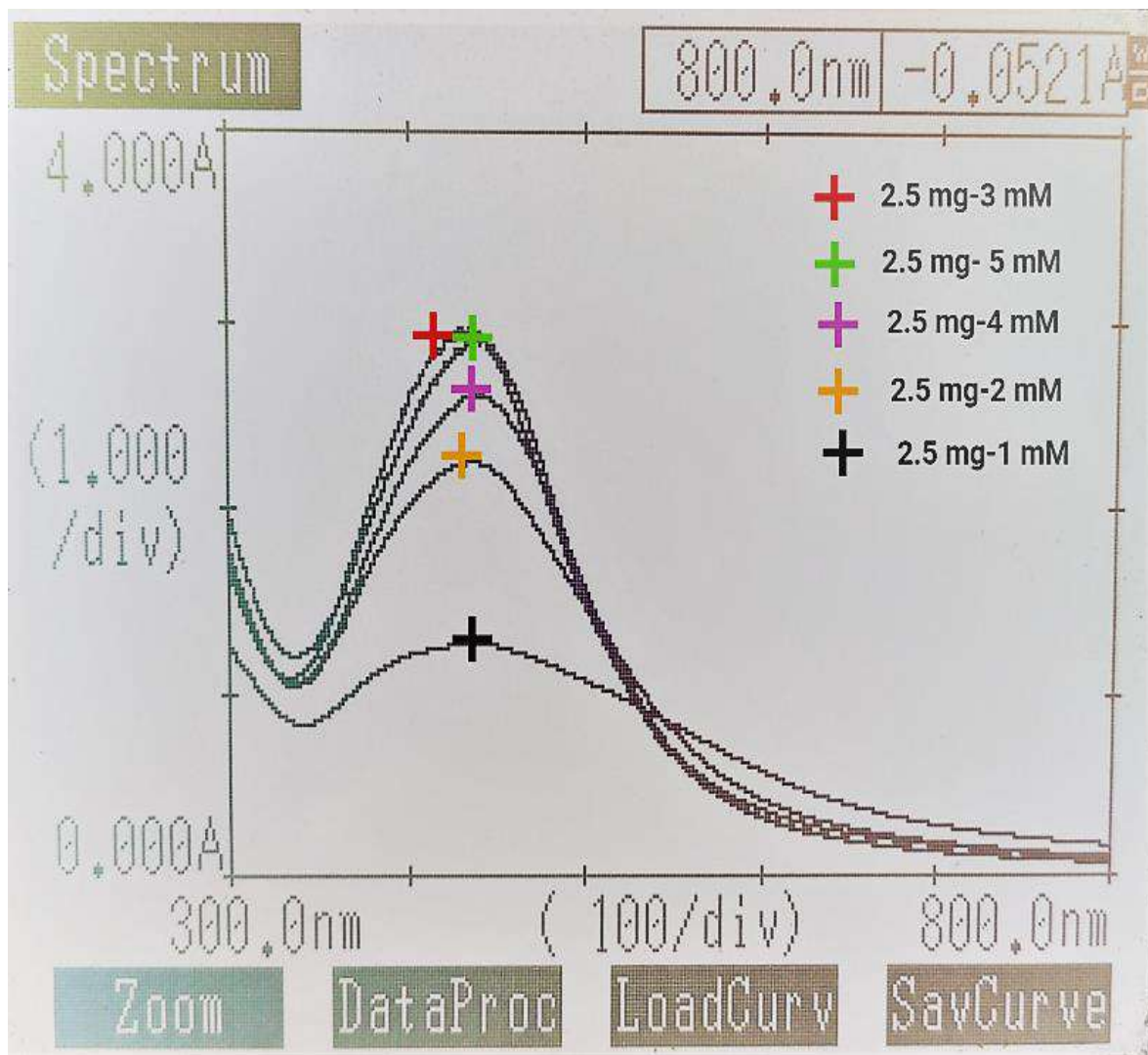


Fig 5.2 (b): UV spectrum of 2.5 mg of plant extract reacting with different concentration of silver nitrate

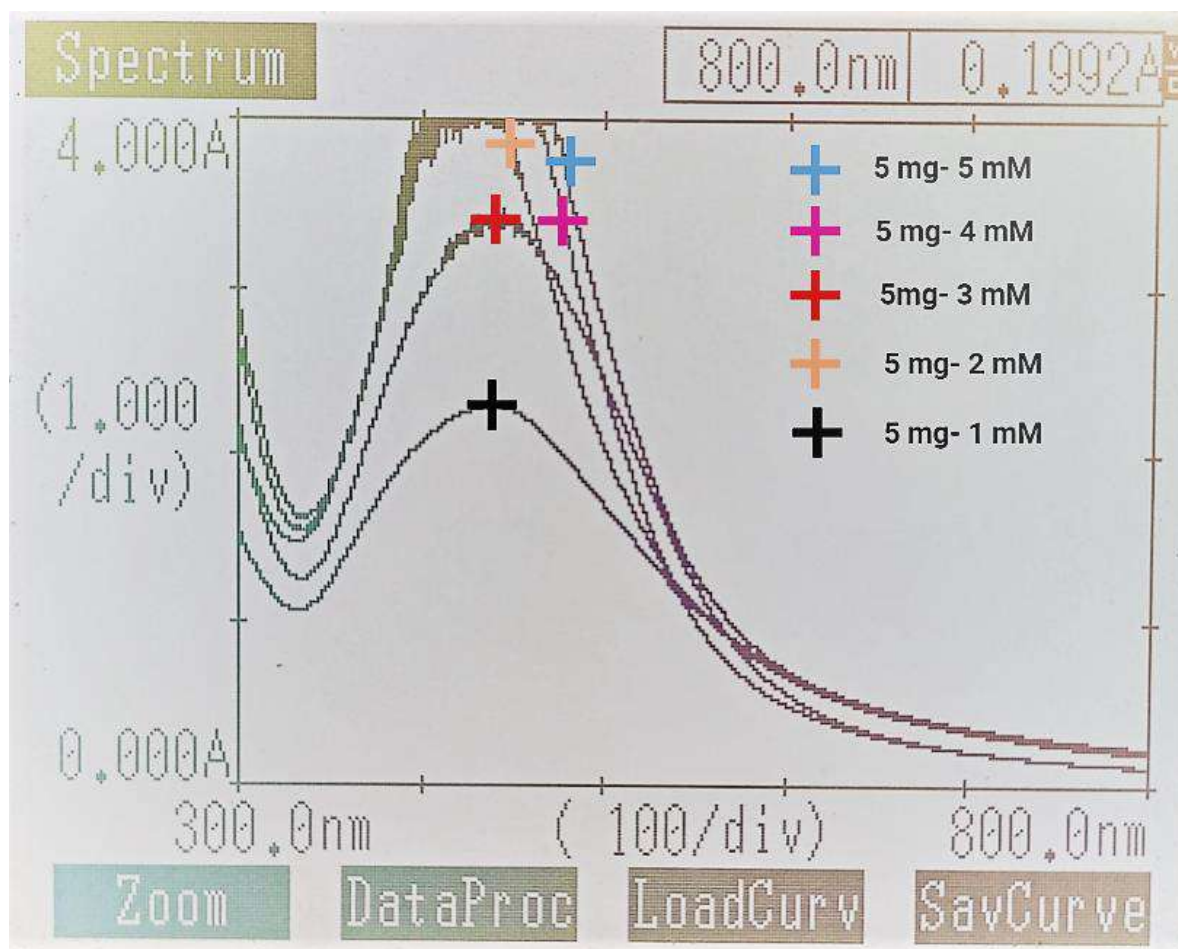


Fig 5.2 (c): UV spectrum of 5 mg of plant extract reacting with different concentration of silver nitrate

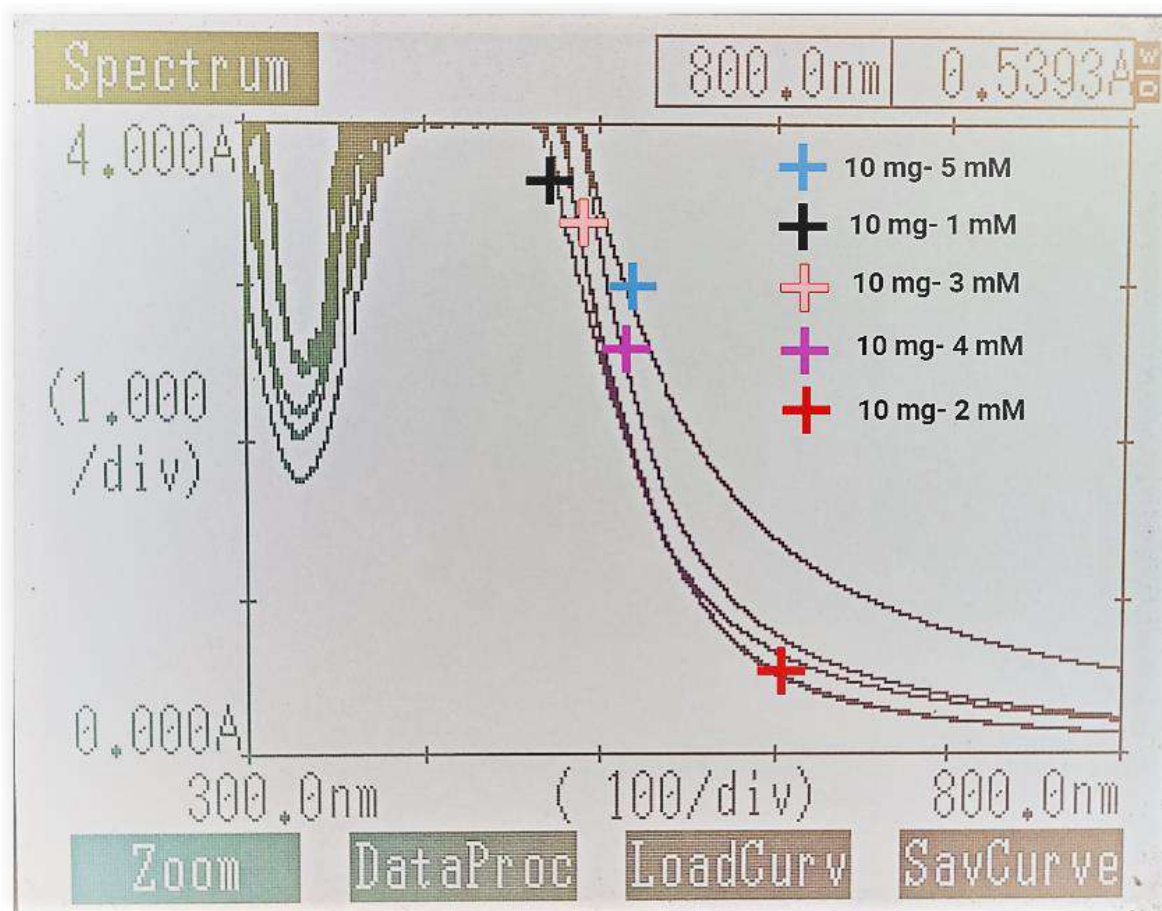


Fig 5.2 (d): UV spectrum of 10 mg of plant extract reacting with different concentrations of silver nitrate

5.4.2 Zeta sizer and zeta potential

Using dynamic light scattering, the average particle size (before sonication) was found to be 128 nm while the zeta potential was found to be -25.5 mV. A polydispersity index of 0.206 indicates the good mono-dispersity and -ve zeta potential indicates good stability with capping by negatively charged groups of nanoparticles. After sonication, the particle size was found to be 15-20 nm. Some distribution at a lower range of particle size indicates

that the synthesized nanoparticles are also in a lower range of particle size. Figure 5.3 (a), figure 5.3 (b), and figure 5.4 show the dynamic light scattering pattern and the zeta potential distribution of the synthesized AgNPs using hydroalcoholic extract of *P. fulgens*.

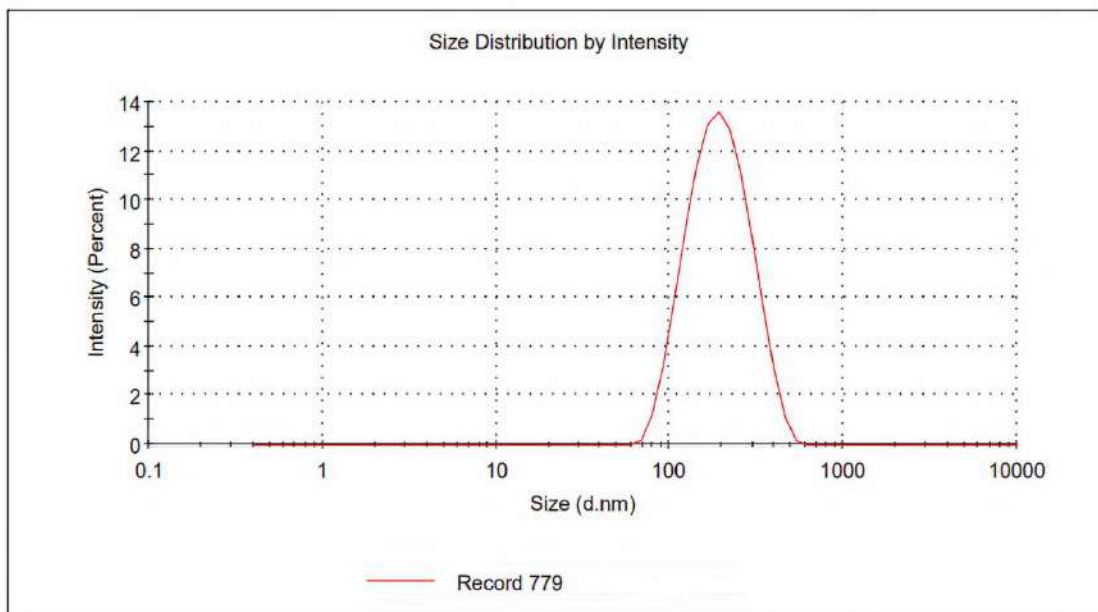


Figure 5.3 (a): Size distribution by intensity of the synthesized AgNPs-PF

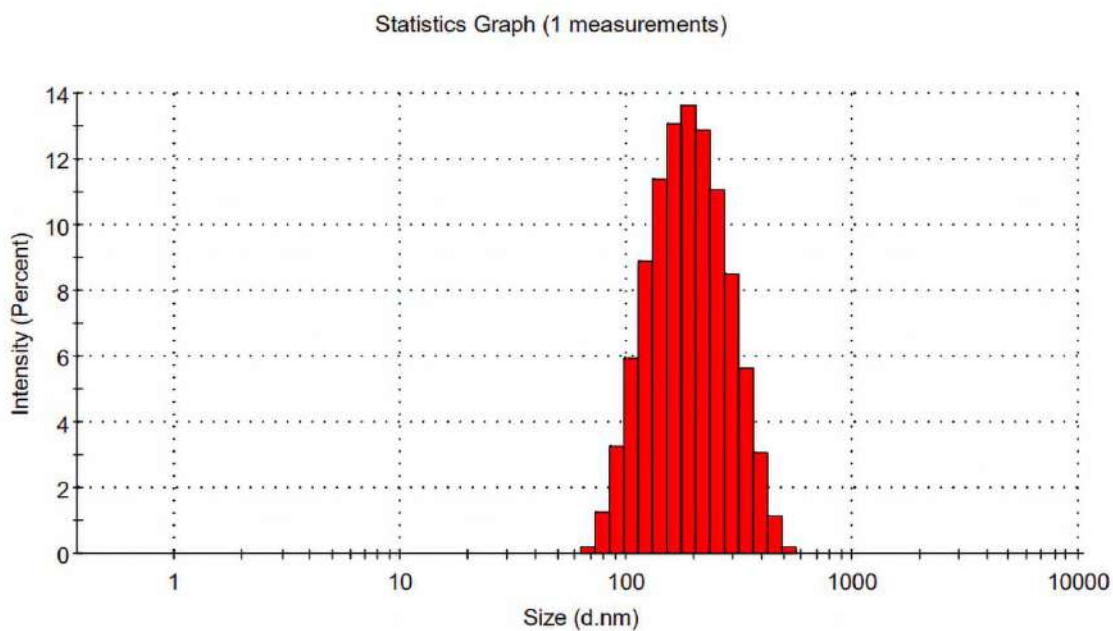


Figure 5.3 (b): Statistics graph of the synthesized AgNPs-PF

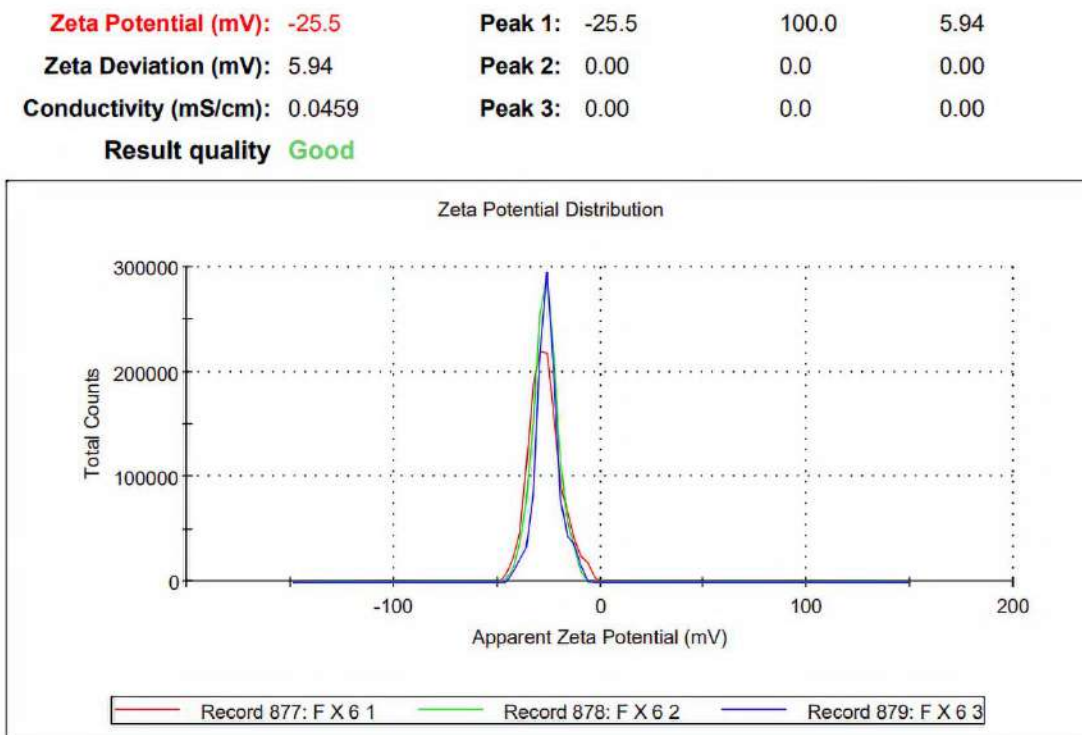


Figure 5.4: Zeta potential distribution of the synthesized AgNPs-PF

5.4.3 FTIR analysis

FTIR spectra were analyzed to investigate the possible reducing functional groups present in the *P. fulgens* root extract. Figure 5.5 shows the FTIR spectra of the synthesized silver nanoparticles. The nanoparticles capped with phytochemicals of *P. fulgens* showed the IR peaks at 3822, 1617, 1348, and 823 cm^{-1} regions. The FTIR spectrum of nanoparticles showed the involvement of O-H stretching, involvement of C=N in-plane vibrations of amino acids, corresponding to amides I, II, and III, aromatic rings, and ether linkages were found commonly present in the nanoparticles synthesized by the hydroalcoholic root extract of *P. fulgens*. These representative IR peaks suggested the presence of flavonoids, phenolics, and terpenoids capped on nanoparticles.

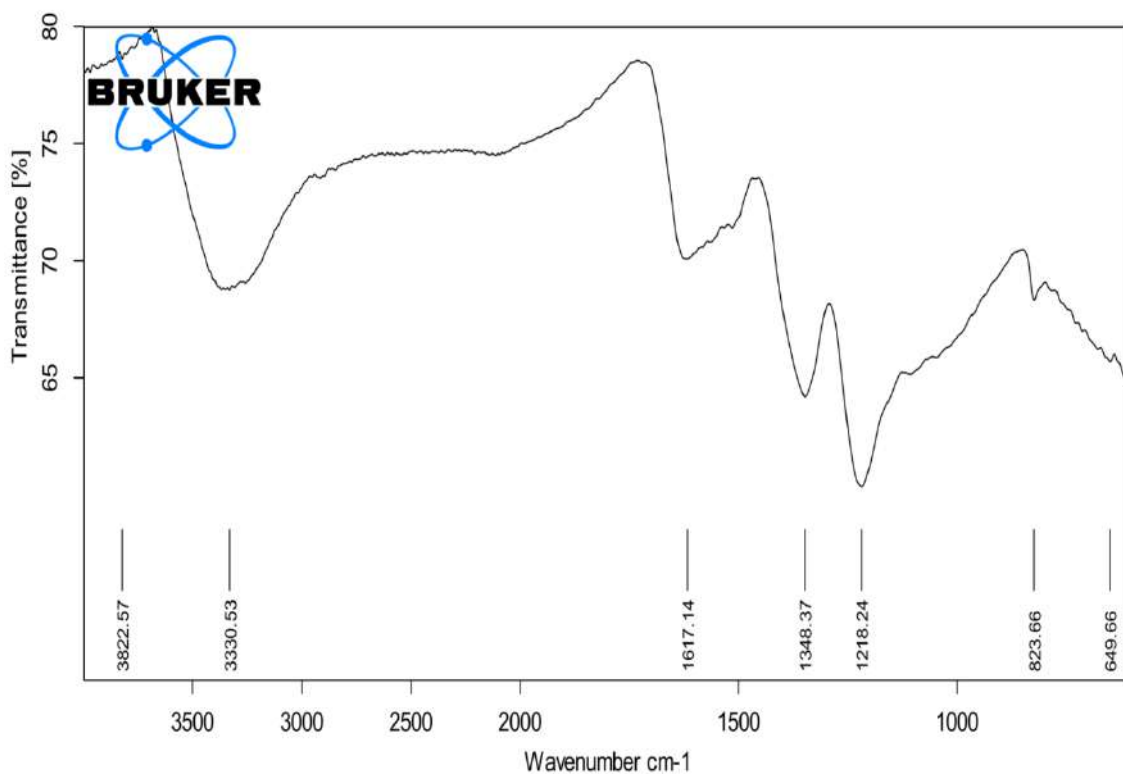


Figure 5.5: FTIR spectra of the synthesized AgNPs-PF

5.4.4 Transmission electron microscopy (TEM) analysis

Transmission electron microscopy (TEM) has been used to identify the size, shape, and morphology of nanoparticles. It reveals that the silver nanoparticles are well dispersed and predominantly spherical in shape. Fig. 5.6 shows the TEM micrograph of the silver nanoparticles synthesized by *P. fulgens* root extract indicating the spherical shape of the particles in the order of 15–20 nm.

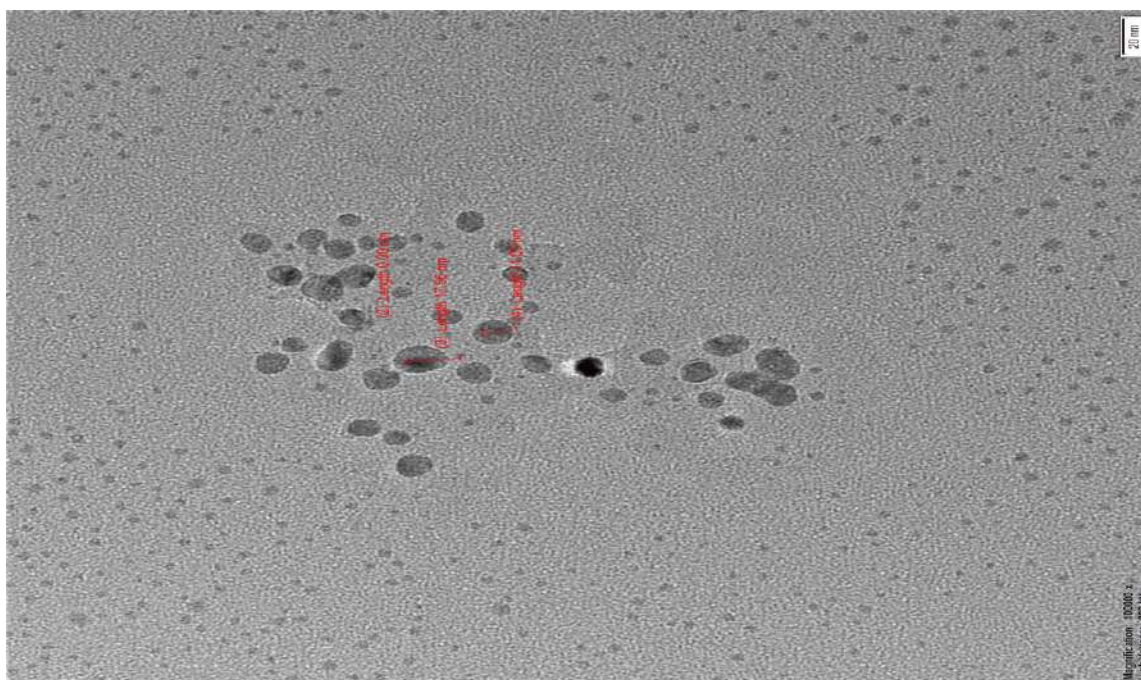
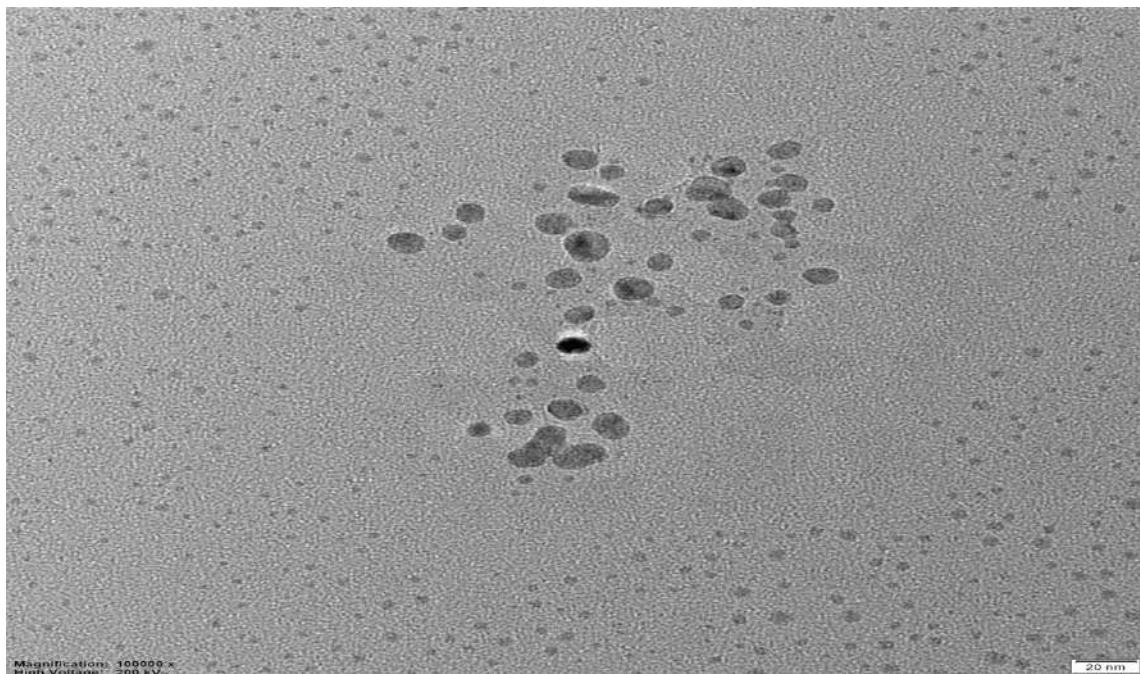


Figure 5.6: TEM micrograph of the AgNPs-PF

5.4.5 Energy dispersive X-ray analysis (EDX)

EDX was used to find elemental composition in the reaction mixture. The revealing of the strong signal by EDX (Figure 5.7) confirmed the presence of silver nanoparticles. EDX of AgNPs revealed the presence of pure silver (Ag 100 %) and was the major constituent element compared to carbon (0.00 %) as shown in figure 5.8.

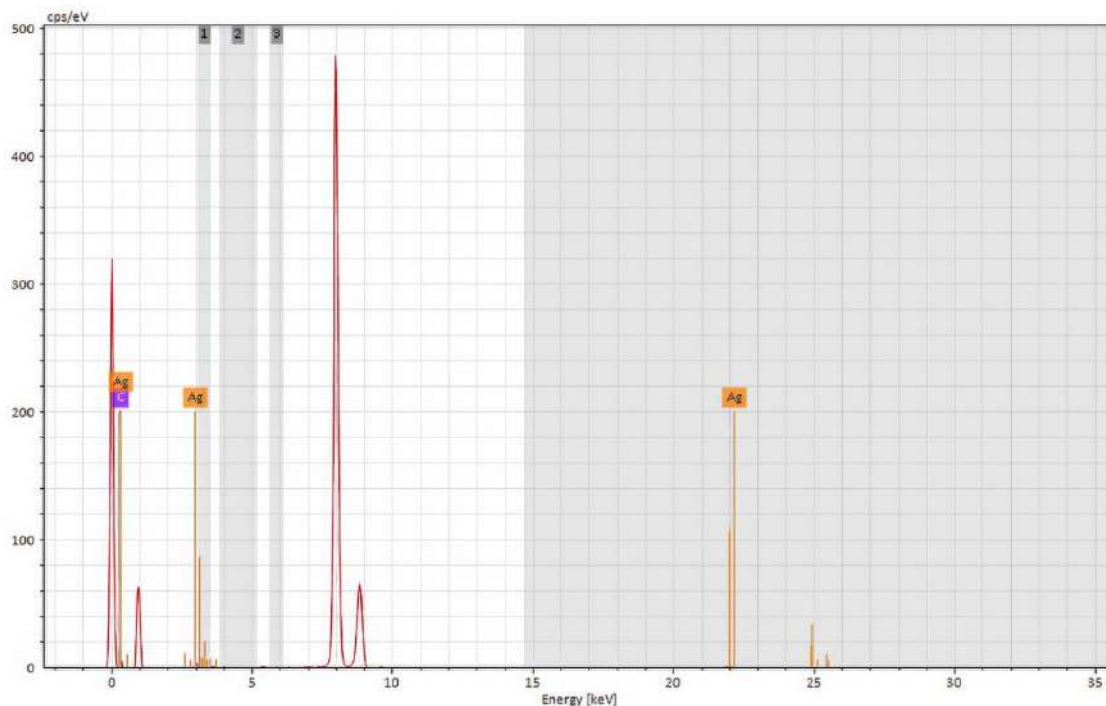


Figure 5.7: Energy-dispersive X-ray spectroscopy (EDX) micrograph of the AgNPs-PF

Element	At. No.	Netto	Mass [%]	Mass Norm. [%]	Atom [%]	abs. error [%] (1 sigma)	rel. error [%] (1 sigma)
Silver	47	227	100.00	100.00	100.00	7.90	7.90
Carbon	6	0	0.00	0.00	0.00	0.00	0.00
		Sum	100.00	100.00	100.00		

Figure 5.8: Percentage of elements present in the synthesized AgNPs-PF

5.4.6 X-ray diffraction analysis (XRD)

XRD is commonly used for determining the chemical composition and crystal structure of a material; therefore, detecting the presence of silver nanoparticles in plant tissues can be achieved by using XRD to examine the diffraction peaks of the plant. X-ray diffraction pattern of the biosynthesized silver nanoparticles from the root extract of *P. fulgens* is shown in Figure 5.9. The XRD pattern of silver nanoparticles illustrated that the synthesized nanoparticles are crystalline in nature. A number of Bragg reflections with 2θ values ranging from 26 to 80°, at 26, 32, 38, 47, 66, and 78, the pattern of reflection according to Bragg's equation of silver nanoparticles showing crystalline nature of nanomaterials (Sankar et al, 2019). These peaks of nanoparticles were matched with JCPDS databases of the standard silver (file No. 04-0783). It confirms that the resultant particles are face-centered cubic (FCC) in shape. The unassigned peaks could be due to the crystallization of the bioorganic phase that occurs on the surface of the nanoparticle. The noises were probably due to macromolecules present in the plant extract which may be responsible for the reduction of silver ions.

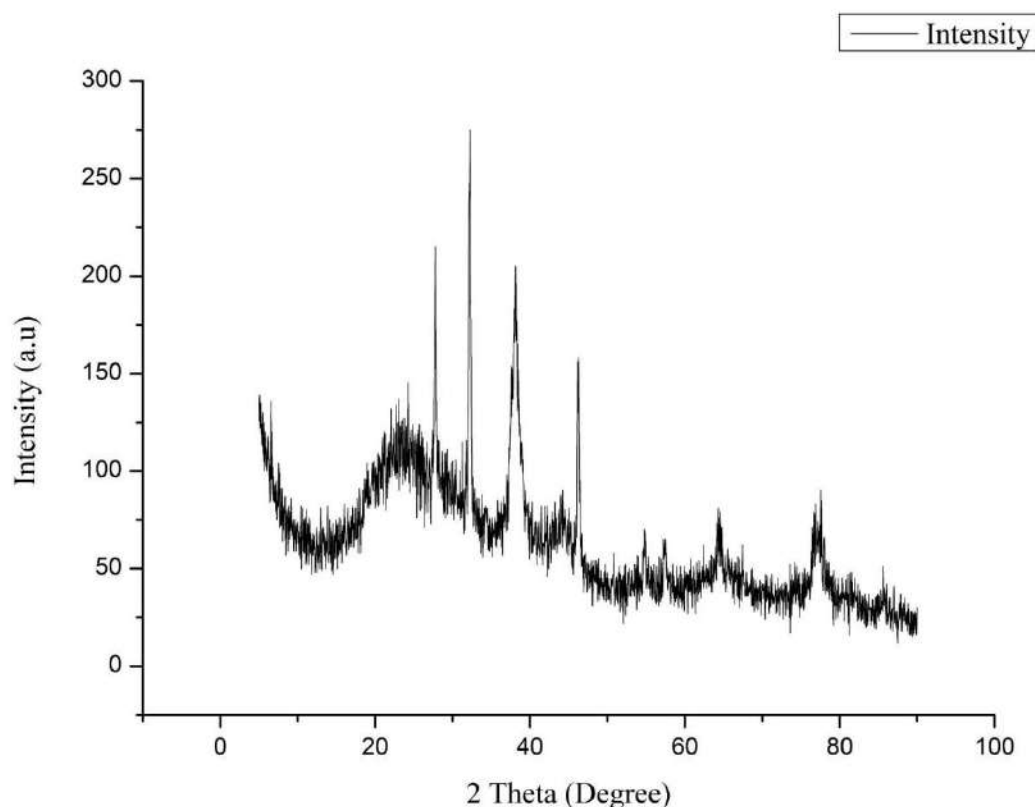


Figure 5.9: X-ray diffraction (XRD) spectra of AgNPs-PF

5.5 Optimization of certain parameters for nanoparticle synthesis

The nanoparticles were primarily characterized by UV–vis spectroscopy. Based on this, various physicochemical parameters (concentrations of plant extract, concentration of metal ions, pH, and reaction time) were optimized to enhance the yield of nanoparticle synthesis. The reaction mixture containing 5 mg plant extract and 3mM silver nitrate in 50 mL water was able to produce the maximum concentration of silver nanoparticles. The peak with 5 mg root extract was sharp as compared to other peaks, indicating the formation of relatively better-sized nanoparticles. The effect of silver nitrate concentration on the synthesis of silver nanoparticles (AgNPs) was studied by varying its concentration from 1mM to 5 mM using 1-5 mg root extract. The yield of silver nanoparticles increased with the increase of

metal salt concentration from 1mM to 4 mM, beyond which, there was again a fall in absorbance. The synthesis of nanoparticles to the desired size and shape by optimizing the plant extract and metal ions is also reported in the literature (Iravani *et al*; 2013; Veerasamy *et al*; 2011; Krishnaraj *et al*; 2012). The effect of pH on the synthesis of nanoparticles by the root extract and organic compounds was examined over a wide range of pH starting from pH 3 to 13. At acidic pH, larger size nanoparticles were formed, whereas, at alkaline pH, smaller size nanoparticles were observed. This was concluded based on UV–vis absorption spectra (narrow or broad peak). The effect of reaction pH on the synthesis and stabilization of metal nanoparticles as well as on their size and shape was also reported by various investigators (Sathishkumar *et al*; 2010; Selvakannan *et al*; 2004). Nanoparticle aggregation seems to outdo the nucleation process in acidic conditions, whereas at alkaline pH, a large number of nuclei formation, instead of aggregation, led to the synthesis of a higher amount of nanoparticles with a smaller diameter. Blueshift in the absorption pattern confirmed the formation of relatively smaller size nanoparticles. Gericke and Pinches reported the various manipulation methods to control the size and shape of gold nanoparticles synthesized by *Verticillium luteoalbum* (Gericke *et al*; 2006). They found that aggregation of NPs was observed after 36 h reaction, which is a sign of instability. The optimum time required for the synthesis of maximum nanoparticles by *P. fulgens* was found to be 24 hours. The stability results showed no alteration in the absorption peak at 420 nm up to 60 days, indicating good stability of synthesized silver nanoparticles. Lyophilized form of nanoparticle powder remained stable for more than 8 months when stored at room temperature.

5.6 Quantitative estimation of total polyphenolic content

The data revealed that there is quite a significant amount of polyphenolic components in the synthesized AgNP-PF which is calculated in terms of mg/g of AgNP-PF equivalent to standard tannic acid (for total phenolic and tannin) and quercetin (for total flavonoid). The result for total polyphenolic content (phenolic, tannin, and flavonoid) is represented in table 5.2.

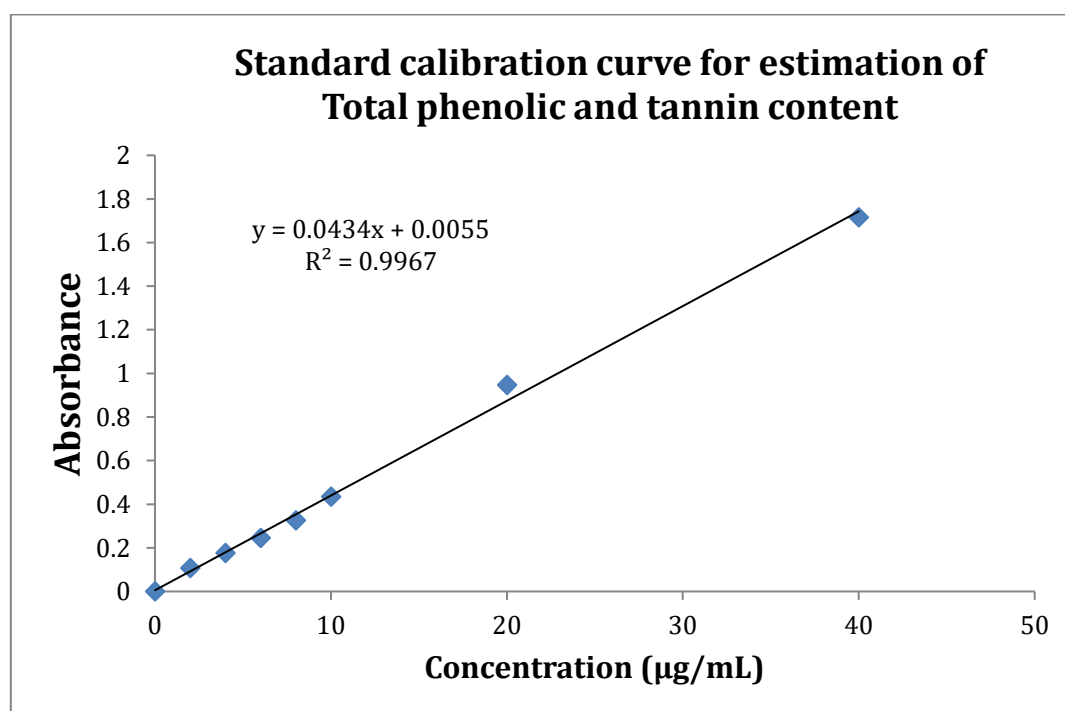


Figure 5.10: Standard calibration curve for the estimation of total phenolic, total simple phenolic, and total tannin content (results are expressed in mg/g of AgNP-PF equivalent to tannic acid).

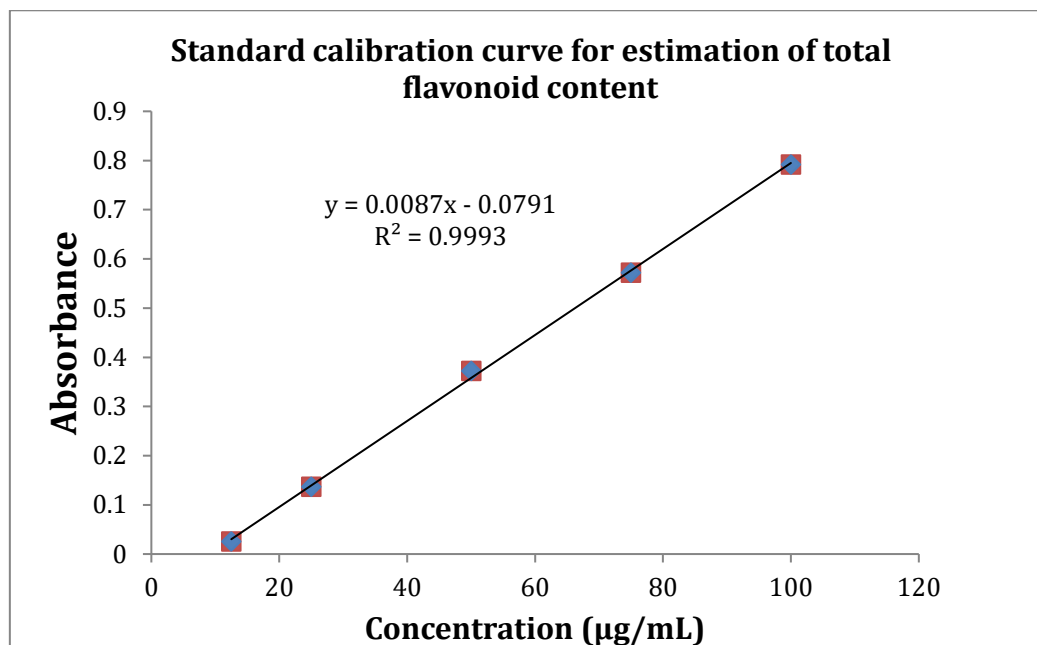


Figure 5.11: Standard calibration curve for the estimation of total flavonoid content
(results are expressed in mg/g of AgNP-PF equivalent to quercetin).

Table 5.2: Quantification of total major phenolic, simple phenolic, tannin, and flavonoid content in AgNP-PF

Sl.No	Phytochemical class	AgNP-PF
1.	Total major phenolic content (mg/g AgNP-PF equivalent to tannic acid) [A]	56 ± 1.45
2.	Total simple phenolic content (mg/g AgNP-PF equivalent to tannic acid) [B]	15 ± 1.25
3.	Total tannin content (mg/g AgNP-PF equivalent to tannic acid) [A-B]	41.2 ± 0.9
4.	Total flavonoid content (mg/g of AgNP-PF equivalent to quercetin)	13.15 ± 2.1

5.7 In vitro-antioxidant activity (DPPH radical scavenging activity)

Figure 5.12 represents the potential activity of AgNP-PF and standard quercetin (a flavonoid compound) to scavenge the oxidative radical (DPPH) at 517 nm. Result as shown in Table 5.3 revealed that even though at high concentration (100-400 $\mu\text{g/mL}$), AgNP-PF showed a marked reduction in the DPPH radical from purple to the yellow color formation, but when statistically (by student t-test) compared to the standard drug quercetin, the IC_{50} value showed significant effect ($*p<0.05$), which means that the tested AgNP-PF is not comparable to that of quercetin for scavenging of DPPH radical.

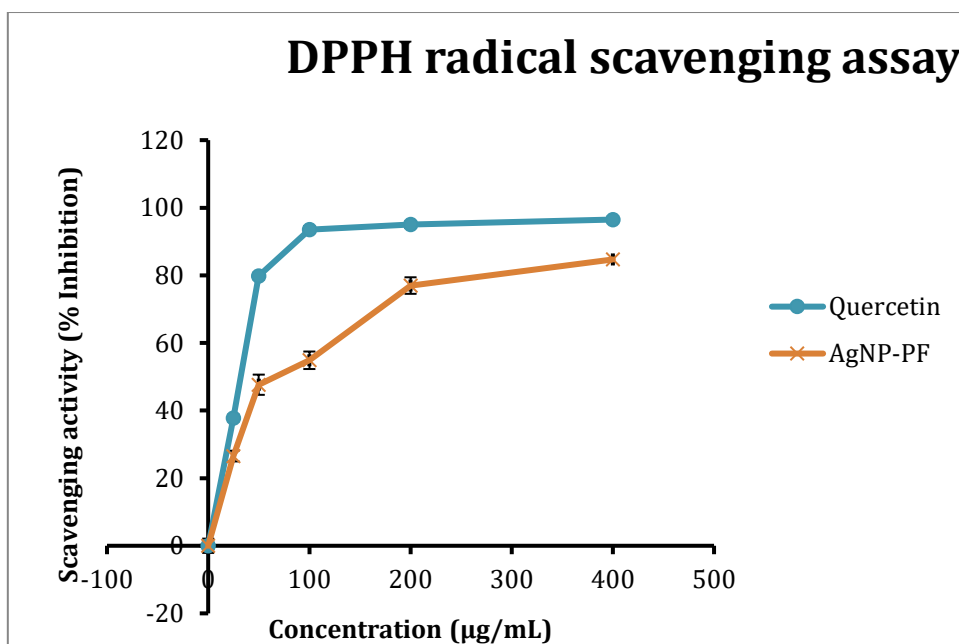


Figure 5.12: DPPH radical scavenging activity of standard quercetin and AgNP-PF synthesized from *P. fulgens*

Table 5.3: IC₅₀ values of standard quercetin and AgNP-PF

Tested sample	IC ₅₀ concentration in µg/mL
Quercetin	23.20 ± 5.21
AgNP-PF	119.51 ± 10.88 *

[All results are expressed as Mean ± S.E.M. Statistical comparison was determined by Students t-test followed by unpaired t-test (comparison with control taken as standard quercetin); **P* < 0.05, statistically significant compared to quercetin].

[**Statistical evaluation:** (**p* < 0.05) Statistical difference signifies lesser scavenging activity as compared to quercetin taken as standard. Whereas, statistical non-significant (^{ns}*p* < 0.05) reveal comparable scavenging activity as compared to standard quercetin]

5.8 Preparation and optimization of topical gel

In general, gel formulation is more preferred, among the other topical semisolid preparations, since it has a long residence time on the skin, high viscosity, moisturizing effect on flaky skin due to their occlusive properties, more bio adhesiveness, less irritation, independent of water solubility of the active ingredient, ease of application and better release characters (Loganathan *et al*; 2001). In the present study, carbopol gel of different concentrations (F1: 0.1%, F2:0.2%, F3:0.3%, F4:0.4% and F5:0.5%) were prepared. Carbopol 940 was used as a gelling agent in the formulation as they are biodegradable, bioadhesive, biocompatible, irritation-free, and not absorbed into the body. From the pharmaceutical evaluation of all the gel formulations, it was apparent that Formulation 3 (F3) with 0.3% carbopol 940 was found to be the best formulation.

5.8.1 Pharmaceutical evaluation of the plain gel formulations

Five gel formulations F1 to F5 prepared using carbopol 940 polymers were evaluated for sensory properties and physical appearance, grittiness, pH, viscosity, spreadability, net content, extrudability, and gel strength. Results of the study were within acceptable limits of the ICH guidelines and the details of the same are recorded in Table 5.4.

Table 5.4: Pharmaceutical evaluation of the plain gel formulation

Code	Poly mer Conc. (%)	Physical appearance	pH*	Viscosity * (poise)	Spreadabilit y* g cm/sec	Consi stency	Grittin ess
F1	0.1	Smooth, transparent clear, thin and homogeneous	7.57	0.1850	32	Low	No
F2	0.2	Smooth, transparent clear, thin and homogeneous	7.57	0.2462	56	Low	No

F3	0.3	Smooth, translucent, clear and homogenous	7.60	0.3873	64	Moderate	No
F4	0.4	Smooth, translucent clear, thick and homogeneous	7.79	0.5662	71	High	No
F5	0.5	Smooth, translucent clear, thick and homogeneous	7.88	0.7275	75	High	No

*Values mentioned are mean values (n=5)

5.8.2 Evaluation of the topical gel loaded with silver nanoparticles (AgNPs-PF)

After the preparation and optimization of the plain gel, synthesized AgNPs were loaded into the optimized plain gel formulation. The prepared nanogel formulation was further evaluated for different pharmaceutical parameters including, sensory properties, appearance, homogeneity, grittiness, pH, viscosity, and spreadability. Results of the study

were within acceptable limits of the ICH guidelines and the details of the same are recorded in Table 5.5.

Table 5.5: Evaluation of the topical gel loaded with silver nanoparticles (AgNPs)

Physical appearance	pH*	Viscosity* (poise)	Spreadability* g cm/sec	Consistency	Grittiness
Smooth, translucent, clear, and homogenous	7.55	0.3943	68	Good	No

*Values mentioned are mean values (n=5)

Figure 5.13 shows the topical gel formulation before and after loading the synthesized silver nanoparticles (AgNPs-PF).

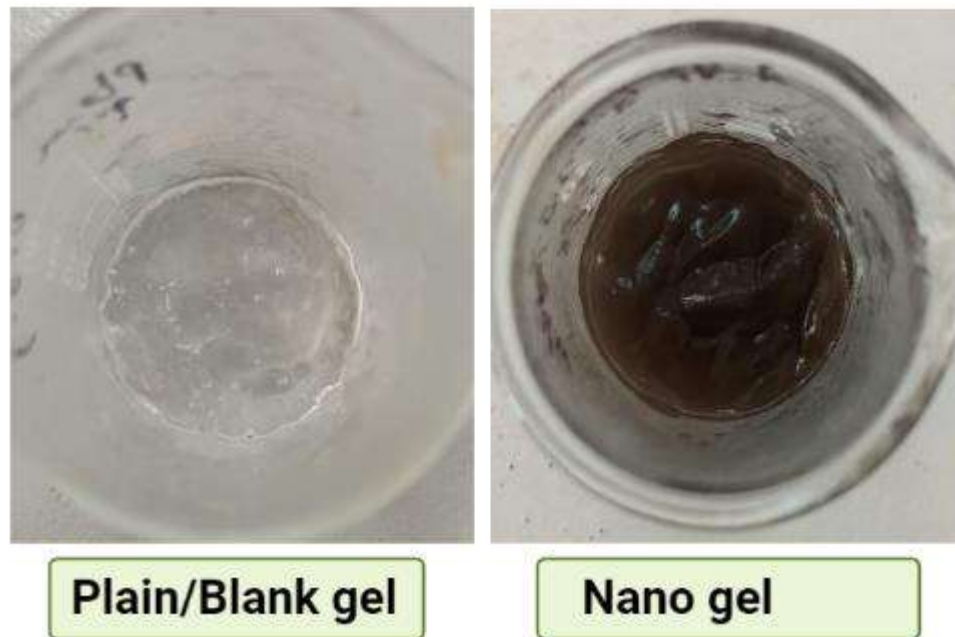


Figure 5.13: Topical gel formulation before and after loading the silver nanoparticles (AgNPs).

5.9 Acute dermal toxicity

Silver nanoparticle (AgNP-PF) topical gel applied to the shaved backs of the rat showed no sign of skin irritation, inflammation, swelling, or other changes. Hence, the toxicity testing showed the safety profile of the tested drug.

5.10 Cutaneous wound-healing potential of AgNPs-PF

5.10.1 Morphology of wound contraction

The result for the wound structural changes and healing effects from day 0 to day 21 after treating with tested samples is represented in Figure 5.14. Topically, groups treated with simple plain gel (carbopol gel) showed no significant difference ($p < 0.05$) in the wound contraction area when compared to the negative control group (untreated group). However,

CHAPTER-5 | RESULTS & DISCUSSION

topical treatment of the animal groups with commercially available silver nitrate gel (0.2% w/w) and AgNP-PF (0.2% w/w) on day 7, day 14, and day 21 depicted a significant (* $p < 0.05$) reduction in the wounded area when compared to the untreated control group. The percentage wound contraction (%) concerning plain gel control, standard control, and that of tested AgNP-PF is respectively shown in the suffix of table 5.6 data. The wounded area (in mm^2), percentage wound contraction, and epithelialization period are represented in Table 5.6 and Figure 5.14.

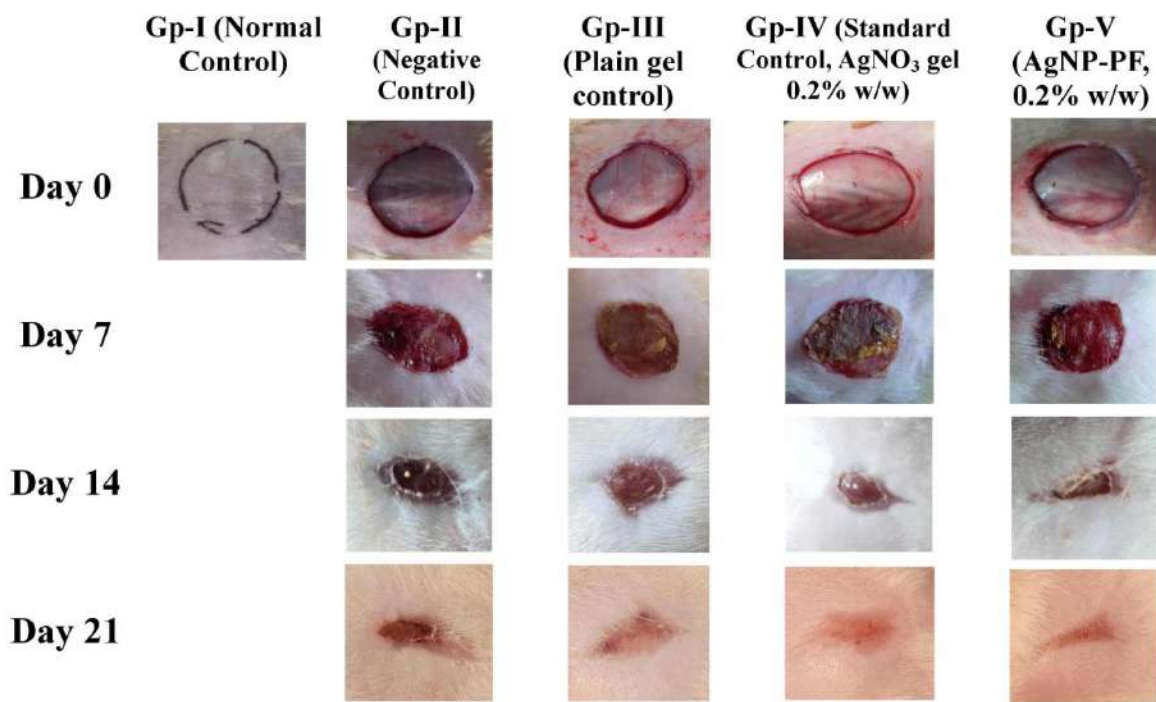


Figure 5.14: Wound structural changes and healing effects from day 0 to day 21 after treating with tested samples

CHAPTER-5 RESULTS & DISCUSSION

Table 5.6: Effect of topical treatment of 0.2% w/w AgNP-PF and standard 0.2% w/w AgNO₃ gel on wound contraction in 21 days excision wounded rats.

Experimental group / dose	Wound area (cm ²) and percentage of wound contraction			
	Day 0	Day 7	Day 14	Day 21
Gp-I: Normal Control	-	-	-	-
Gp-II: Negative Control (NgC)	3.05 ± 0.27	2.52 ± 0.30	1.30 ± 0.25	1.00 ± 0.15
Gp-III: Plain Gel Control (Carbopol gel)	3.06 ± 0.24	2.55 ± 0.25 (0% vs. Gp-II Day-7) (16.7% vs. Gp-III Day-0)	1.21 ± 0.19 (6.92% vs Gp-II Day-14) (60.5% vs. Gp-III Day-0)	0.90 ± 0.05 (10% vs Gp-II Day-21) (70.6% vs. Gp-III Day-0)
Gp-IV: Standard Control (0.2% AgNO ₃ Gel)	2.99 ± 0.30	1.70 ± 0.32 ^{a,b} (32.5% vs. Gp-II Day-7) (43.1% vs. Gp-IV Day-0)	0.52 ± 0.08 ^a (82.6% vs Gp-II Day-14) (60.0% vs. Gp-IV Day-0)	0.10 ± 0.01 ^{a,b} (90% vs Gp-II Day-21) (96.6% vs. Gp-IV Day-0)
Gp-V: AgNP-PF gel (0.2% w/w)	2.98 ± 0.11	1.75 ± 0.15 ^{a,b} (30.6% vs. Gp-II Day-7) (41.3% vs. Gp-V Day-0)	0.55 ± 0.11 ^a (57.7% vs Gp-II Day-14) (81.5% vs. Gp-V Day-0)	0.11 ± 0.05 ^{a,b} (89% vs Gp-II Day-21) (96.3% vs. Gp-V Day-0)

(1) All results are expressed as Mean \pm S.E.M ($n=6$ in each group). Statistical comparison was determined by two way ANOVA followed by the Bonferroni's post test. ^a $p < 0.05$, statistically significance as compared to Negative control; ^b $p < 0.05$, statistically significance as compared to Plain gel control.

(2) % wound contraction is calculated using the formula: % wound contraction =
$$\frac{(\text{Negative control} - \text{Treated control})}{\text{Negative control}} \times 100$$

5.10.2 Histopathology studies

The excised tissue obtained from the normal control group depicted well-organized epithelial cells (**E**) having well-characterized outer epidermis. Normal formation of collagen fibres (**CF**) and hair follicles (**HF**) was also observed (Figure 5.15 A). The excision tissue of the animals obtained from the 21st day, untreated groups (negative control) showed extreme damage to the epidermis (**DE**) and its epithelial cells with the destructive formation of collagen fibres (Figure 5.15 B). The same condition was also observed with that of the plain carbopol gel treated group even though there is a slight improvement on the epithelial layer (Figure 5.15 C). Rats treated topically with reference drug (0.2 % AgNO₃) and AgNP-PF (0.2%), produces a skin with significant healing property, followed by regeneration, re-epithelialization (**RE**) and improved reformation of collagen fibres (**CF**), fibroblast cells (**FC**) and inflammatory cells (**IFC**) (Figures 5.15 D & 5.15 E).

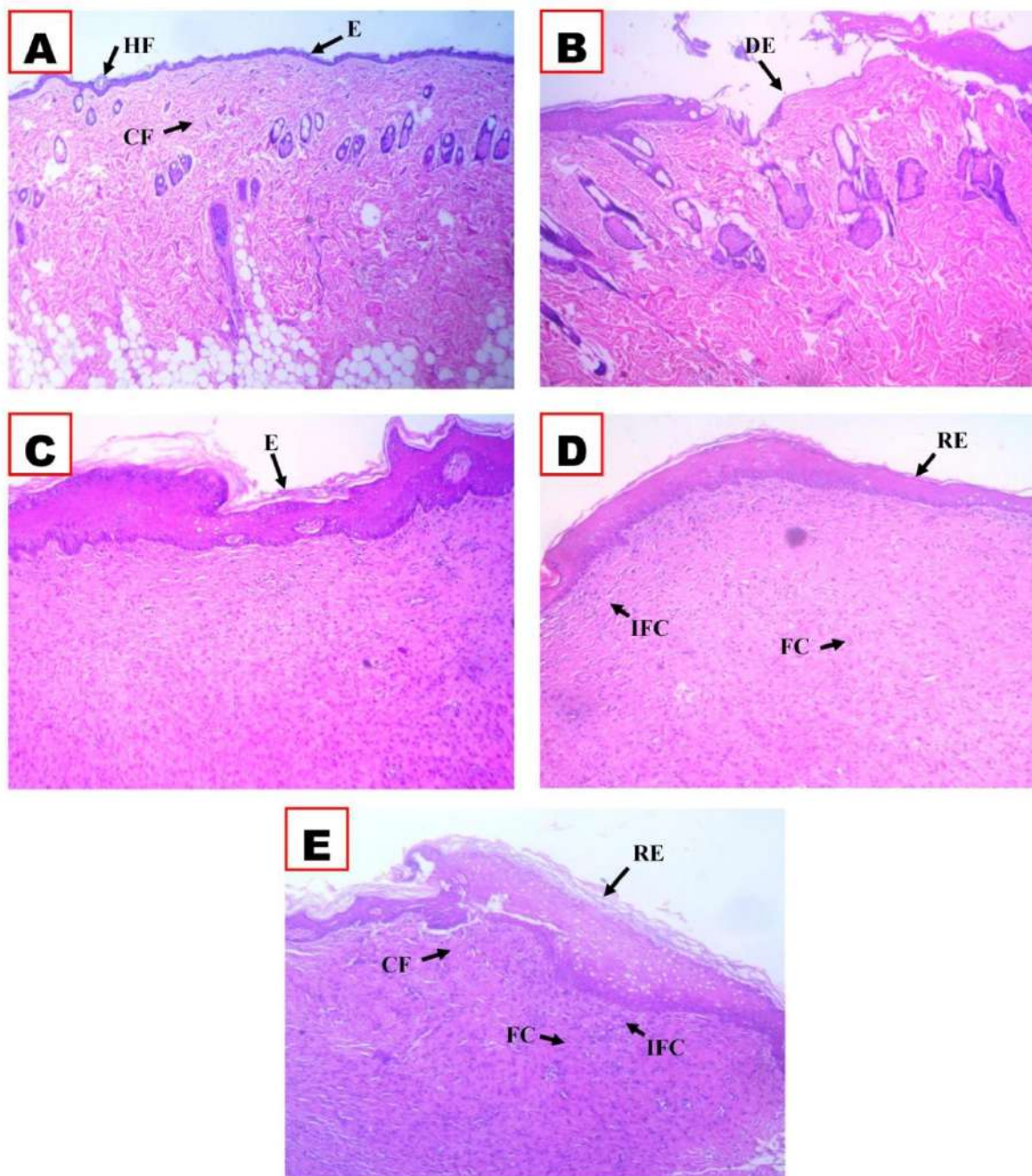


Figure 5.15: Histological section of the skin tissue obtained from the 21st-day excision wound model: (A) Normal control group; (B) Negative control group (untreated); (C)

Group treated with Carbopol plain gel (QS, topical); (D) Group treated with AgNO₃ gel (0.2% w/w, topical); (E) Group treated with AgNP-PF (0.25% w/w, topical)

[Indications of arrow marks: CF: collagen fibres; DE-Damaged epidermis; E-epithelial layer; FC-fibroblast cells; HF: hair follicle; IFC-Inflammatory cells; RE: re-epithelialization).

CHAPTER-6

SUMMARY AND CONCLUSION

6.0 Summary and Conclusion

Indian greeneries are the chief and cheap source of medicinal plants and plant products. For centuries to date, these medicinal plants have been extensively utilized in Ayurveda. Recently, many such plants have been gaining importance due to their unique constituents and their versatile applicability in various developing fields of research and development. Nanotechnology is presently one of the most dynamic disciplines of research in contemporary material science whereby plants and different plant products are finding an imperative use in the synthesis of nanoparticles (NPs). NPs of noble metals like gold, silver, and platinum are well recognized to have significant applications in electronics, magnetism, optoelectronics, and information storage. One such important member of the noble metal NPs is silver NPs (AgNPs).

Currently, a large number of physical, chemical, biological, and hybrid methods are available to synthesize different types of nanoparticles. Physical and chemical methods have been using high radiation and highly concentrated reductants and stabilizing agents that are harmful to the environment and human health. Hence, the biological synthesis of nanoparticles is a single-step bioreduction method and less energy is used to synthesize eco-friendly NPs. Several plants are being currently investigated for their role in the synthesis of nanoparticles. Hence, this research work is mainly focused on a simple process as a green technology using hydroalcoholic extract of *Potentilla fulgens* root for the biosynthesis and characterization of silver nanoparticles. The synthesized AgNPs were investigated for *in vitro* antioxidant, *in vivo* wound healing activity on experimental rats. Further, the antimicrobial activity and the biochemical estimations of the synthesized silver nanoparticles will be carried out in the future.

The following conclusions were obtained from the study:

Phytochemical analysis of the extract

- The qualitative phytochemical analysis of the hydroalcoholic extract of *Potentilla fulgens* roots showed the presence of active classes of phytochemicals which include polyphenolics (tannins, phenolics, and flavonoids), saponin glycoside, steroids, and carbohydrates.

Synthesis and characterization of silver nanoparticle

- The appearance of brown color in root extract treated with silver nitrate is a clear indication for the formation of silver nanoparticles.
- UV visible spectrum analysis of synthesized nanoparticles' absorbance occurs at 400-420 nm. The appearance of this peak, assigned to a surface plasmon, is well-documented in literature for various metal nanoparticles.
- Using dynamic light scattering, the average particle size (before sonication) was found to be 128 nm while the zeta potential was found to be -25.5 mV. A polydispersity index of 0.206 indicates the good mono-dispersity and -ve zeta potential indicates good stability with capping by negatively charged groups of nanoparticles. After sonication, the particle size was found to be 15-20 nm.
- FTIR analysis of synthesized nanoparticles confirmed the presence of flavonoids, phenolics, and terpenoids capped on nanoparticles
- Transmission electron microscopy (TEM) analysis has been used to identify the size, shape, and morphology of nanoparticles, which reveals that the silver

nanoparticles are well dispersed and predominantly spherical in the shape of size ranging from 15-20.

- Energy Dispersive Spectroscopy (EDX) studies revealed the presence of pure silver in the synthesized nanoparticles. The revealing of strong signals by EDX confirmed the presence of silver nanoparticles. EDX of AgNPs revealed the presence of pure silver (Ag 100 %) and was the major constituent element compared to carbon (0.00 %)
- XRD pattern clearly illustrated that the silver nanoparticles formed in this present synthesis are crystalline in nature. A number of Bragg reflections with 2θ values ranging from 26 to 80°, at 26, 32, 38, 47, 66, and 78, the pattern of reflection according to Bragg's equation of silver nanoparticles showing crystalline nature of nanomaterials. These peaks of nanoparticles were matched with JCPDS databases of the standard silver (file No. 04-0783). It confirms that the resultant particles are face-centered cubic (FCC) in shape.

Quantitative evaluation of polyphenolics in the biosynthesized silver nanoparticles

- The data revealed that there is quite a significant amount of polyphenolic components in the synthesized AgNP-PF which is calculated in terms of mg/g of AgNP-PF equivalent to standard tannic acid (for total phenolic and tannin) and quercetin (for total flavonoid)

Antioxidant potential of the silver nanoparticles

- The biosynthesized silver nanoparticles displayed profound *in vitro* antioxidant activity but are not comparable to that of quercetin for scavenging of DPPH radicals.

Formulation and pharmaceutical evaluation of the topical gel (both blank gel and nano gel)

- After the formulation of different concentrations of topical carbopol gel, they were subjected to pharmaceutical evaluation including sensory properties, appearance, grittiness, viscosity, pH, spreadability, and gel strength. From the pharmaceutical evaluation of all the gel formulations, it was apparent that topical gel with 0.3% carbopol 940 was found to be the optimized formulation.
- The biosynthesized silver nanoparticles were loaded into the optimized gel formulation and further evaluated for the same pharmaceutical properties.
- The formulated nanogel was smooth, translucent, clear, homogenous with good spreadability and consistency.

Acute dermal toxicity of biosynthesized AgNPs-PF

- The biosynthesized silver nanoparticles from *Potentilla fulgens* (AgNPs-PF) displayed no dermal toxicity and were found to be safe in experimental rats.

***In vivo* wound healing activity**

- The biosynthesized AgNPs-PF gel (0.2% w/w) showed 96.3 % wound healing which is comparable to standard marketed 0.2% w/w AgNO₃ gel (96.6 % healing).
- The histopathological analysis demonstrates that rats treated topically with reference drug (0.2 % AgNO₃) and AgNP-PF (0.2%), produces a skin with significant healing property, followed by regeneration, re-epithelialization, and improved reformation of collagen fibers, fibroblast cells, and inflammatory cells. Whereas excision tissue of untreated groups showed extreme damage to the epidermis and its epithelial cells with the destructive formation of collagen fibers.

- Hence, it is clear that AgNPs obtained from *Potentilla fulgens* showed significant wound healing activity on experimental rats.

From the above results, it was concluded that *Potentilla fulgens* root extract can act as a source of synthesis for the silver nanoparticles. The biosynthesized silver nanoparticles displayed profound antioxidant and wound healing potential, indicating their relevance in biological applications. These findings add to the existing growing relevance of the biogenic silver nanoparticles for potential application in nanomedicine. **To the best of our knowledge, this is the first scientific report to demonstrate that the biosynthesized silver nanoparticles from the root extract of *Potentilla fulgens* showed significant wound healing activity in rats which may be attributed specifically to their ability to promote cellular re-epithelialization, cell proliferation, collagen deposition and also as potent antioxidants.**

However, it is highly necessary to explore future perspectives in terms of further pharmacological activities.

BIBLIOGRAPHY

Bibliography

- Ahamed M, Khan MM, Siddiqui MK, AlSalhi MS, Alrokayan SA. Green synthesis, characterization and evaluation of biocompatibility of silver nanoparticles. *Physica E: Low-dimensional systems and nanostructures*. 2011 Apr 1; 43(6):1266-71.
- Ahmad N, Sharma S, Alam MK, Singh VN, Shamsi SF, Mehta BR, Fatma A. Rapid synthesis of silver nanoparticles using dried medicinal plant of basil. *Colloids and Surfaces B: Biointerfaces*. 2010 Nov 1; 81(1):81-6.
- Ahmed S, Ahmad M, Swami BL, Ikram S. A review on plants extract mediated synthesis of silver nanoparticles for antimicrobial applications: a green expertise. *Journal of advanced research*. 2016 Jan 1; 7(1):17-28.
- Ahmed S, Saifullah, Ahmad M, Swami BL, Ikram S. Green synthesis of silver nanoparticles using *Azadirachta indica* aqueous leaf extract. *Journal of radiation research and applied sciences*. 2016 Jan 1; 9(1):1-7.
- Aiyalu R, Govindarjan A, Ramasamy A. Formulation and evaluation of topical herbal gel for the treatment of arthritis in animal model. *Brazilian Journal of Pharmaceutical Sciences*. 2016 Jul; 52:493-507.
- Akhtar MS, Panwar J, Yun YS. Biogenic synthesis of metallic nanoparticles by plant extracts. *ACS Sustainable Chemistry & Engineering*. 2013 Jun 3; 1(6):591-602.
- Alam MS, Algahtani MS, Ahmad J, Kohli K, Shafiq-un-Nabi S, Warsi MH, Ahmad MZ. Formulation design and evaluation of aceclofenac nanogel for topical application. *Therapeutic Delivery*. 2020 Dec; 11(12):767-78.

- Ali M, Kim B, Belfield KD, Norman D, Brennan M, Ali GS. Green synthesis and characterization of silver nanoparticles using *Artemisia absinthium* aqueous extract—a comprehensive study. *Materials Science and Engineering: C*. 2016 Jan 1; 58:359-65.
- Alomar TS, AlMasoud N, Awad MA, El-Tohamy MF, Soliman DA. An eco-friendly plant-mediated synthesis of silver nanoparticles: Characterization, pharmaceutical and biomedical applications. *Materials Chemistry and Physics*. 2020 Jul 15; 249:123007.
- Alt V, Bechert T, Steinrück P, Wagener M, Seidel P, Dingeldein E, Domann E, Schnettler R. An in vitro assessment of the antibacterial properties and cytotoxicity of nanoparticulate silver bone cement. *Biomaterials*. 2004 Aug 1; 25(18):4383-91.
- Anisha BS, Biswas R, Chennazhi KP, Jayakumar R. Chitosan–hyaluronic acid/nano silver composite sponges for drug resistant bacteria infected diabetic wounds. *International journal of biological macromolecules*. 2013 Nov 1; 62:310-20.
- Antony E, Sathivelu M, Arunachalam S. Synthesis of silver nanoparticles from the medicinal plant *bauhinia acuminata* and *biophytum sensitivum*—a comparative study of its biological activities with plant extract. *International Journal of Applied Pharmaceutics*. 2017:22-9.
- Antony, J. J., Sivalingam, P., Siva, D., Kamalakkannan, S., Anbarasu, K., & Sukirtha, R. Comparative evaluation of antibacterial activity of silver nanoparticles synthesized using *Rhizophora apiculata* and glucose. *Colloid Surf*. 2011 Jul B, 98: 657

- Atiyeh BS, Costagliola M, Hayek SN, Dibo SA. Effect of silver on burn wound infection control and healing: review of the literature. *burns*. 2007 Mar 1; 33(2):139-48.
- Ayyanar M, Ignacimuthu S. Ethnobotanical survey of medicinal plants commonly used by Kani tribals in Tirunelveli hills of Western Ghats, India. *Journal of ethnopharmacology*. 2011 Apr 12; 134(3):851-64.
- Banerjee P, Satapathy M, Mukhopahayay A, Das P. Leaf extract mediated green synthesis of silver nanoparticles from widely available Indian plants: synthesis, characterization, antimicrobial property and toxicity analysis. *Bioresources and Bioprocessing*. 2014 Dec; 1(1):1-0.
- Bar H, Bhui DK, Sahoo GP, Sarkar P, De SP, Misra A. Green synthesis of silver nanoparticles using latex of *Jatropha curcas*. *Colloids and surfaces A: Physicochemical and engineering aspects*. 2009 May 1; 339(1-3):134-9.
- Begum A, Ramaiah M, Khan I, Veena K. Heavy metal pollution and chemical profile of Cauvery River water. *E-journal of Chemistry*. 2009 Jan 1; 6(1):47-52.
- Behravan M, Panahi AH, Naghizadeh A, Ziaee M, Mahdavi R, Mirzapour A. Facile green synthesis of silver nanoparticles using *Berberis vulgaris* leaf and root aqueous extract and its antibacterial activity. *International journal of biological macromolecules*. 2019 Mar 1; 124:148-54.
- Benelmekki M. An introduction to nanoparticles and nanotechnology. In *Designing hybrid nanoparticles* 2015 Apr 1. Morgan & Claypool Publishers.
- Bhosale RR, Kulkarni AS, Gilda SS, Aloorkar NH, Osmani RA, Harkare BR. Innovative eco-friendly approaches for green synthesis of silver nanoparticles.

- International Journal of Pharmaceutical Sciences and Nanotechnology. 2014 Feb 28; 7(1):2328-37.
- Braca A, De Tommasi N, Di Bari L, Pizza C, Politi M, Morelli I. Antioxidant principles from baubinia t arapotensis. Journal of natural products. 2001 Jul 27; 64(7):892-5.
 - Buchanan, R. Angus (2020, November 18). History of technology. Encyclopedia Britannica. <https://www.britannica.com/technology/history-of-technology>.
 - Chandran SP, Chaudhary M, Pasricha R, Ahmad A, Sastry M. Synthesis of gold nanotriangles and silver nanoparticles using Aloe vera plant extract. Biotechnology progress. 2006; 22(2):577-83.
 - Cheng F, Betts JW, Kelly SM, Hector AL. Green synthesis of highly concentrated aqueous colloidal solutions of large starch-stabilised silver nanoplatelets. Materials Science and Engineering: C. 2015 Jan 1; 46:530-7.
 - Daisy P, Saipriya K. Biochemical analysis of Cassia fistula aqueous extract and phytochemically synthesized gold nanoparticles as hypoglycemic treatment for diabetes mellitus. International journal of nanomedicine. 2012; 7:1189.
 - Das RK, Gogoi N, Bora U. Green synthesis of gold nanoparticles using Nyctanthes arbortristis flower extract. Bioprocess and biosystems engineering. 2011 Jun; 34(5):615-9.
 - Dubey SP, Lahtinen M, Sillanpää M. Green synthesis and characterizations of silver and gold nanoparticles using leaf extract of Rosa rugosa. Colloids and Surfaces A: Physicochemical and Engineering Aspects. 2010 Jul 20; 364(1-3):34-41.

- Ealia SA, Saravanakumar MP. A review on the classification, characterisation, synthesis of nanoparticles and their application. InIOP Conference Series: Materials Science and Engineering 2017 Nov 1 (Vol. 263, No. 3, p. 032019). IOP Publishing..
- Gardea-Torresdey JL, Parsons JG, Gomez E, Peralta-Videa J, Troiani HE, Santiago P, Yacaman MJ. Formation and growth of Au nanoparticles inside live alfalfa plants. Nano letters. 2002 Apr 10; 2(4):397-401.
- Geetha N, Geetha TS, Manonmani P, Thiyagarajan M. Green synthesis of silver nanoparticles using Cymbopogon Citratus (Dc) Stapf. Extract and its antibacterial activity. Aus J Basic Appl Sci. 2014 Mar; 8(3):324-1.
- Gericke M, Pinches A. Biological synthesis of metal nanoparticles. Hydrometallurgy. 2006 Sep 1; 83(1-4):132-40.
- Gnanadesigan M, Anand M, Ravikumar S, Maruthupandy M, Vijayakumar V, Selvam S, Dhineshkumar M, Kumaraguru AK. Biosynthesis of silver nanoparticles by using mangrove plant extract and their potential mosquito larvicidal property. Asian Pacific journal of tropical medicine. 2011 Oct 1; 4(10):799-803.
- Gurunathan S, Lee KJ, Kalishwaralal K, Sheikpranbabu S, Vaidyanathan R, Eom SH. Antiangiogenic properties of silver nanoparticles. Biomaterials. 2009 Oct 1; 30(31):6341-50.
- Harish NM, Prabhu P, Charyulu RN, Gulzar MA, Subrahmanyam EV. Formulation and evaluation of in situ gels containing clotrimazole for oral candidiasis. Indian Journal of Pharmaceutical Sciences. 2009 Jul; 71(4):421.
- Haritha H. *Green Synthesis and Characterization of Silver Nanoparticles using Pterocarpus Marsupium Roxb. and Assessment of its In-Vitro Anti Diabetic*

- Activity* (Doctoral dissertation, Sri Ramakrishna Institute of Paramedical Sciences, Coimbatore).
- Hasan S. A review on nanoparticles: their synthesis and types. *Res. J. Recent Sci.* 2015; 2277:2502.
 - Hashemi SF, Tasharrofi N, Saber MM. Green synthesis of silver nanoparticles using *Teucrium polium* leaf extract and assessment of their antitumor effects against MNK45 human gastric cancer cell line. *Journal of Molecular structure.* 2020 May 15; 1208:127889.
 - He Y, Du Z, Lv H, Jia Q, Tang Z, Zheng X, Zhang K, Zhao F. Green synthesis of silver nanoparticles by *Chrysanthemum morifolium* Ramat. extract and their application in clinical ultrasound gel. *International Journal of Nanomedicine.* 2013; 8:1809.
 - He Y, Wei F, Ma Z, Zhang H, Yang Q, Yao B, Huang Z, Li J, Zeng C, Zhang Q. Green synthesis of silver nanoparticles using seed extract of *Alpinia katsumadai*, and their antioxidant, cytotoxicity, and antibacterial activities. *RSC advances.* 2017; 7(63):39842-51.
 - Hekmati M, Hasanirad S, Khaledi A, Esmaeili D. Green synthesis of silver nanoparticles using extracts of *Allium rotundum* L, *Falcaria vulgaris* Bernh, and *Ferulago angulate* Boiss, and their antimicrobial effects in vitro. *Gene Reports.* 2020 Jun 1; 19:100589.
 - Ingale AG, Chaudhari AN. Biogenic synthesis of nanoparticles and potential applications: an eco-friendly approach. *J Nanomed Nanotechol.* 2013;4(165):1-7.

- Iravani S, Zolfaghari B. Green synthesis of silver nanoparticles using *Pinus eldarica* bark extract. *BioMed research international*. 2013 Oct; 2013..
- Iravani S. Green synthesis of metal nanoparticles using plants. *Green Chemistry*. 2011; 13(10):2638-50.
- Jacob SJ, Finub JS, Narayanan A. Synthesis of silver nanoparticles using *Piper longum* leaf extracts and its cytotoxic activity against Hep-2 cell line. *Colloids and Surfaces B: Biointerfaces*. 2012 Mar 1; 91:212-4.
- Jain D, Daima HK, Kachhwaha S, Kothari SL. Synthesis of plant-mediated silver nanoparticles using papaya fruit extract and evaluation of their anti microbial activities. *Digest journal of nanomaterials and biostructures*. 2009 Sep 1; 4(3):557-63.
- Jayaseelan C, Rahuman AA, Rajakumar G, Kirthi AV, Santhoshkumar T, Marimuthu S, Bagavan A, Kamaraj C, Zahir AA, Elango G. Synthesis of pediculocidal and larvicidal silver nanoparticles by leaf extract from heartleaf moonseed plant, *Tinospora cordifolia* Miers. *Parasitology research*. 2011 Jul; 109(1):185-94.
- Jebril S, Jenana RK, Dridi C. Green synthesis of silver nanoparticles using *Melia azedarach* leaf extract and their antifungal activities: In vitro and in vivo. *Materials Chemistry and Physics*. 2020 Jul 1; 248:122898.
- Jemilugba OT, Parani S, Mavumengwana V, Oluwafemi OS. Green synthesis of silver nanoparticles using *Combretum erythrophyllum* leaves and its antibacterial activities. *Colloid and Interface Science Communications*. 2019 Jul 1; 31:100191.

- Kasthuri J, Veerapandian S, Rajendiran N. Biological synthesis of silver and gold nanoparticles using apiin as reducing agent. *Colloids and Surfaces B: Biointerfaces*. 2009 Jan 1; 68(1):55-60.
- Katta VK, Dubey RS. Green synthesis of silver nanoparticles using *Tagetes erecta* plant and investigation of their structural, optical, chemical and morphological properties. *Materials Today: Proceedings*. 2021 Jan 1; 45:794-8.
- Kaul K, Jaitak V, Kaul VK. Review on pharmaceutical properties and conservation measures of *Potentilla fulgens* Wall. ex Hook.-A medicinal endangered herb of higher Himalaya.
- Kaur LP. Topical gel: a recent approach for novel drug delivery. *Asian journal of biomedical and Pharmaceutical Sciences*. 2013 Feb 1; 3(17):1.
- Kaviya S, Santhanalakshmi J, Viswanathan B, Muthumary J, Srinivasan K. Biosynthesis of silver nanoparticles using *Citrus sinensis* peel extract and its antibacterial activity. *Spectrochimica Acta Part A: Molecular and Biomolecular Spectroscopy*. 2011 Aug 1; 79(3):594-8..
- Kesharwani J, Yoon KY, Hwang J, Rai M. Phytofabrication of silver nanoparticles by leaf extract of *Datura metel*: hypothetical mechanism involved in synthesis. *Journal of Bionanoscience*. 2009 Jun 1; 3(1):39-44.
- Kim JS, Kuk E, Yu KN, Kim JH, Park SJ, Lee HJ, Kim SH, Park YK, Park YH, Hwang CY, Kim YK. Antimicrobial effects of silver nanoparticles. *Nanomedicine: Nanotechnology, biology and medicine*. 2007 Mar 1; 3(1):95-101.

- Krishnaraj C, Jagan EG, Rajasekar S, Selvakumar P, Kalaichelvan PT, Mohan NJ. Synthesis of silver nanoparticles using *Acalypha indica* leaf extracts and its antibacterial activity against water borne pathogens. *Colloids and Surfaces B: Biointerfaces*. 2010 Mar 1; 76(1):50-6.
- Krishnaraj C, Ramachandran R, Mohan K, Kalaichelvan PT. Optimization for rapid synthesis of silver nanoparticles and its effect on phytopathogenic fungi. *Spectrochimica Acta Part A: Molecular and Biomolecular Spectroscopy*. 2012 Jul 1; 93:95-9.
- Kumar AS, Ravi S, Kathiravan V. Green synthesis of silver nanoparticles and their structural and optical properties. *Int J Curr Res*. 2013; 5(10):3238-40.
- Kumar G P, Gupta S, Murugan M P, Bala Singh S. Ethnobotanical studies of Nubra Valley-A cold arid zone of Himalaya. *Ethnobotanical leaflets*. 2009; 2009(6):9.
- Kumar V, Yadav SC, Yadav SK. *Syzygium cumini* leaf and seed extract mediated biosynthesis of silver nanoparticles and their characterization. *Journal of Chemical Technology & Biotechnology*. 2010 Oct; 85(10):1301-9.
- Kumaran A, Karunakaran RJ. In vitro antioxidant activities of methanol extracts of five *Phyllanthus* species from India. *LWT-Food Science and Technology*. 2007 Mar 1; 40(2):344-52.
- Kumarasamyraja D, Jeganathan NS. Green synthesis of silver nanoparticles using aqueous extract of *acalypha indica* and its antimicrobial activity.
- Kundu A, Ghosh A, Singh NK, Singh GK, Seth A, Maurya SK, Hemalatha S, Laloo D. Wound healing activity of the ethanol root extract and polyphenolic rich fraction from *Potentilla fulgens*. *Pharmaceutical biology*. 2016 Nov 1; 54(11):2383-93.

- Laloo D, Kumar M, Prasad SK, Hemalatha S. Quality control standardization of the roots of *Potentilla fulgens* Wall.: A potent medicinal plant of the Western Himalayas and North-eastern India. *Pharmacognosy Journal*. 2013 May 1; 5(3):97-103.
- Laloo D, Prasad SK, Krishnamurthy S, Hemalatha S. Gastroprotective activity of ethanolic root extract of *Potentilla fulgens* Wall. ex Hook. *Journal of ethnopharmacology*. 2013 Mar 27; 146(2):505-14.
- Laloo D, Tahbildar R, Smith K, Ahmed AU, Nath J, Shil D, Das G, Langbang A, Prasad SK, Singh NK. Impact of Quality Control Standardization Parameters and Antioxidant Potential of the Aerial Parts of *Potentilla fulgens* Wall.: A Comprehensive Monographic Study. *Journal of Biologically Active Products from Nature*. 2020 Jul 3; 10(4):338-56.
- Lin D, Xing B. Phytotoxicity of nanoparticles: inhibition of seed germination and root growth. *Environmental pollution*. 2007 Nov 1; 150(2):243-50.
- Liu L, Yang J, Xie J, Luo Z, Jiang J, Yang YY, Liu S. The potent antimicrobial properties of cell penetrating peptide-conjugated silver nanoparticles with excellent selectivity for Gram-positive bacteria over erythrocytes. *Nanoscale*. 2013; 5(9):3834-40.
- Loganathan V, Manimaran S, Jaswanth A, Sulaiman A, Reddy MS, Kumar BS, Rajaseskaran A. The effects of polymers and permeation enhancers on releases of flurbiprofen from gel formulations. *Indian Journal of Pharmaceutical Sciences*. 2001; 63(3):200.

- Logeswari P, Silambarasan S, Abraham J. Synthesis of silver nanoparticles using plants extract and analysis of their antimicrobial property. Journal of Saudi Chemical Society. 2015 May 1; 19(3):311-7.
- Maheshwaran G, Bharathi AN, Selvi MM, Kumar MK, Kumar RM, Sudhahar S. Green synthesis of Silver oxide nanoparticles using Zephyranthes Rosea flower extract and evaluation of biological activities. Journal of Environmental Chemical Engineering. 2020 Oct 1; 8(5):104137.
- Makarov VV, Love AJ, Sinitsyna OV, Makarova SS, Yaminsky IV, Taliansky ME, Kalinina NO. “Green” nanotechnologies: synthesis of metal nanoparticles using plants. Acta Naturae. 2014; 6(1 (20)).
- Makarov VV, Makarova SS, Love AJ, Sinitsyna OV, Dudnik AO, Yaminsky IV, Taliansky ME, Kalinina NO. Biosynthesis of stable iron oxide nanoparticles in aqueous extracts of Hordeum vulgare and Rumex acetosa plants. Langmuir. 2014 May 27; 30(20):5982-8.
- Makkar HP, Blümmel M, Borowy NK, Becker K. Gravimetric determination of tannins and their correlations with chemical and protein precipitation methods. Journal of the Science of Food and Agriculture. 1993; 61(2):161-5.
- Manik UP, Nande A, Raut S, Dhoble SJ. Green synthesis of silver nanoparticles using plant leaf extraction of Artocarpus heterophyllus and Azadirachta indica. Results in Materials. 2020 Jun 1; 6:100086.
- Marambio-Jones C, Hoek EM. A review of the antibacterial effects of silver nanomaterials and potential implications for human health and the environment. Journal of nanoparticle research. 2010 Jun; 12(5):1531-51.

- Mariselvam R, Ranjitsingh AJ, Nanthini AU, Kalirajan K, Padmalatha C, Selvakumar PM. Green synthesis of silver nanoparticles from the extract of the inflorescence of *Cocos nucifera* (Family: Arecaceae) for enhanced antibacterial activity. *Spectrochimica Acta Part A: Molecular and Biomolecular Spectroscopy*. 2014 Aug 14; 129:537-41.
- Masurkar SA, Chaudhari PR, Shidore VB, Kamble SP. Rapid biosynthesis of silver nanoparticles using *Cymbopogon citratus* (lemongrass) and its antimicrobial activity. *Nano-Micro Letters*. 2011 Sep 1; 3(3):189-94.
- Mijndendonckx K, Leys N, Mahillon J, Silver S, Van Houdt R. Antimicrobial silver: uses, toxicity and potential for resistance. *Biometals*. 2013 Aug; 26(4):609-21.
- Mirgorod YA, Borodina VG. Preparation and bactericidal properties of silver nanoparticles in aqueous tea leaf extract. *Inorganic materials*. 2013 Oct; 49(10):980-3.
- Mittal AK, Kaler A, Banerjee UC. Free Radical Scavenging and Antioxidant Activity of Silver Nanoparticles Synthesized from Flower Extract of *Rhododendron dauricum*. *Nano Biomedicine & Engineering*. 2012 Jul 1; 4(3).
- Mittal AK, Tripathy D, Choudhary A, Aili PK, Chatterjee A, Singh IP, Banerjee UC. Bio-synthesis of silver nanoparticles using *Potentilla fulgens* Wall. ex Hook. and its therapeutic evaluation as anticancer and antimicrobial agent. *Materials Science and Engineering: C*. 2015 Aug 1; 53:120-7.

- Moulton MC, Braydich-Stolle LK, Nadagouda MN, Kunzelman S, Hussain SM, Varma RS. Synthesis, characterization and biocompatibility of “green” synthesized silver nanoparticles using tea polyphenols. *Nanoscale*. 2010; 2(5):763-70.
- Murthy S, Gautam MK, Goel S, Purohit V, Sharma H, Goel RK. Evaluation of in vivo wound healing activity of *Bacopa monniera* on different wound model in rats. *BioMed Research International*. 2013 Oct; 2013.
- Nabikhan A, Kandasamy K, Raj A, Alikunhi NM. Synthesis of antimicrobial silver nanoparticles by callus and leaf extracts from saltmarsh plant, *Sesuvium portulacastrum* L. *Colloids and surfaces B: Biointerfaces*. 2010 Sep 1; 79(2):488-93.
- Nakkala JR, Mata R, Gupta AK, Sadras SR. Green synthesis and characterization of silver nanoparticles using *Boerhaavia diffusa* plant extract and their antibacterial activity. *Indus Crop Prod* 2014; 52:562–6.
- Nakkala JR, Mata R, Kumar Gupta A, Rani Sadras S. Biological activities of green silver nanoparticles synthesized with *Acorous calamus* rhizome extract. *Eur J Med Chem* 2014; 85:784–94
- Narayanan KB, Park HH. Antifungal activity of silver nanoparticles synthesized using turnip leaf extract (*Brassica rapa* L.) against wood rotting pathogens. *European journal of plant pathology*. 2014 Oct; 140(2):185-92.
- Nayak SH, Nakhat PD, Yeole PG. Development and evaluation of cosmeceutical hair styling gels of ketoconazole. *Indian journal of pharmaceutical sciences*. 2005; 67(2):231.

- Obaid AY, Al-Thabaiti SA, El-Mossalamy EH, Al-Harbi LM, Khan Z. Extracellular bio-synthesis of silver nanoparticles. *Arabian Journal of Chemistry*. 2017 Feb 1; 10(2):226-31.
- Pala NA, Negi AK, Todaria NP. Traditional uses of medicinal plants of Pauri Garhwal, Uttarakhand. *Nature and Science*. 2010; 8(6):57-61.
- Panda MK, Dhal NK, Kumar M, Mishra PM, Behera RK. Green synthesis of silver nanoparticles and its potential effect on phytopathogens. *Materials Today: Proceedings*. 2021 Jan 1; 35:233-8.
- Panda MK, Panda SK, Singh YD, Jit BP, Behara RK, Dhal NK. Role of nanoparticles and nanomaterials in drug delivery: an overview. *Advances in Pharmaceutical Biotechnology*. 2020 Mar 30:247-65.
- Parashar UK, Saxena PS, Srivastava A. Bioinspired synthesis of silver nanoparticles. *Digest Journal of Nanomaterials & Biostructures (DJNB)*. 2009 Mar 1; 4(1).
- Pfoze NL, Kumar Y, Sheikh N, Myrboh B. Assessment of local dependency on selected wild edible plants and fruits from Senapati district, Manipur, Northeast India. *Ethnobotany Research and Applications*. 2012 Aug 19; 10:357-67.
- Prabhu S, Poulose EK. Silver nanoparticles: mechanism of antimicrobial action, synthesis, medical applications, and toxicity effects. *International nano letters*. 2012 Dec; 2(1):1-0.
- Prasad TN, Elumalai EK. Biofabrication of Ag nanoparticles using *Moringa oleifera* leaf extract and their antimicrobial activity. *Asian Pacific Journal of Tropical Biomedicine*. 2011 Dec 1; 1(6):439-42.

- Qais FA, Shafiq A, Ahmad I, Husain FM, Khan RA, Hassan I. Green synthesis of silver nanoparticles using *Carum copticum*: Assessment of its quorum sensing and biofilm inhibitory potential against gram negative bacterial pathogens. *Microbial pathogenesis*. 2020 Jul 1; 144:104172.
- Queiroz MB, Marcelino NB, Ribeiro MV, Espindola LS, Cunha FR, Silva MV. Development of gel with *Matricaria recutita* L. extract for topic application and evaluation of physical-chemical stability and toxicity. *Lat. Am. J. Pharm.* 2009 Jul 1; 28(4):574-9.
- Raghunandan D, Ravishankar B, Sharanbasava G, Mahesh DB, Harsoor V, Yalagatti MS, Bhagawanraju M, Venkataraman A. Anti-cancer studies of noble metal nanoparticles synthesized using different plant extracts. *Cancer nanotechnology*. 2011 Dec; 2(1):57-65.
- Rai M, Yadav A, Gade A. Silver nanoparticles as a new generation of antimicrobials. *Biotechnology advances*. 2009 Jan 1; 27(1):76-83.
- Raj S, Mali SC, Trivedi R. Green synthesis and characterization of silver nanoparticles using *Enicostemma axillare* (Lam.) leaf extract. *Biochemical and biophysical research communications*. 2018 Sep 18; 503(4):2814-9.
- Rajakumar G, Rahuman AA. Larvicidal activity of synthesized silver nanoparticles using *Eclipta prostrata* leaf extract against filariasis and malaria vectors. *Acta tropica*. 2011 Jun 1; 118(3):196-203.
- Rajasekharreddy P, Rani PU, Sreedhar B. Qualitative assessment of silver and gold nanoparticle synthesis in various plants: a photobiological approach. *Journal of Nanoparticle Research*. 2010 Jun; 12(5):1711-21.

- Rasheed T, Bilal M, Iqbal HM, Li C. Green biosynthesis of silver nanoparticles using leaves extract of *Artemisia vulgaris* and their potential biomedical applications. *Colloids and Surfaces B: Biointerfaces*. 2017 Oct 1; 158:408-15.
- Reichelt KV, Hoffmann-Luecke P, Hartmann B, Weber B, Ley JP, Krammer GE, Swanepoel KM, Engel KH. Phytochemical characterization of South African bush tea (*Athrixia phylicoides* DC.). *South African journal of botany*. 2012 Nov 1; 83:1-8.
- Rout AN, Jena PK, Parida UK, Bindhani BK. Green synthesis of silver nanoparticles using leaves extract of *Centella asiatica* L. For studies against human pathogens. *Int J Pharm Biol Sci*. 2013 Oct; 4(4):661-74.
- Roy B, Swargiary A, Syiem D, Tandon V. *Potentilla fulgens* (Family Rosaceae), a medicinal plant of north-east India: a natural anthelmintic?. *Journal of Parasitic Diseases*. 2010 Oct; 34(2):83-8.
- Sadeghi B, Gholamhoseinpoor F. A study on the stability and green synthesis of silver nanoparticles using *Ziziphora tenuior* (Zt) extract at room temperature. *Spectrochimica Acta Part A: Molecular and Biomolecular Spectroscopy*. 2015 Jan 5; 134:310-5.
- Sahayaraj K, Balasubramanyam G, Chavali M. Green synthesis of silver nanoparticles using dry leaf aqueous extract of *Pongamia glabra* Vent (Fab.), Characterization and phytofungicidal activity. *Environmental Nanotechnology, Monitoring & Management*. 2020 Dec 1; 14: 100349.

- Sankar R, Maheswari R, Karthik S, Shivashangari KS, Ravikumar V. Anticancer activity of *Ficus religiosa* engineered copper oxide nanoparticles. *Materials Science and Engineering: C*. 2014 Nov 1; 44:234-9.
- Sathishkumar M, Sneha K, Won SW, Cho CW, Kim S, Yun YS. Cinnamon *zeylanicum* bark extract and powder mediated green synthesis of nano-crystalline silver particles and its bactericidal activity. *Colloids and Surfaces B: Biointerfaces*. 2009 Oct 15; 73(2):332-8.
- Sathishkumar M, Sneha K, Yun YS. Immobilization of silver nanoparticles synthesized using *Curcuma longa* tuber powder and extract on cotton cloth for bactericidal activity. *Bioresource technology*. 2010 Oct 1; 101(20):7958-65.
- Satyavani K, Gurudeeban S, Ramanathan T, Balasubramanian T. Biomedical potential of silver nanoparticles synthesized from calli cells of *Citrullus colocynthis* (L.) Schrad. *Journal of nanobiotechnology*. 2011 Dec; 9(1):1-8.
- Saxena A, Tripathi RM, Singh RP. Biological synthesis of silver nanoparticles by using onion (*Allium cepa*) extract and their antibacterial activity. *Dig J Nanomater Bios*. 2010 Jun 1; 5(2):427-32.
- Selvakannan PR, Swami A, Srisathiyannarayanan D, Shirude PS, Pasricha R, Mandale AB, Sastry M. Synthesis of aqueous Au core– Ag shell nanoparticles using tyrosine as a pH-dependent reducing agent and assembling phase-transferred silver nanoparticles at the air– water interface. *Langmuir*. 2004 Aug 31; 20(18):7825-36.
- Shankar SS, Ahmad A, Sastry M. Geranium leaf assisted biosynthesis of silver nanoparticles. *Biotechnology progress*. 2003; 19(6):1627-31.

- Shankar T, Karthiga P, Swarnalatha K, Rajkumar K. Green synthesis of silver nanoparticles using Capsicum frutescence and its intensified activity against E. coli. Resource-Efficient Technologies. 2017 Sep 1; 3(3):303-8.
- Si S, Mandal TK. Tryptophan-based peptides to synthesize gold and silver nanoparticles: a mechanistic and kinetic study. Chemistry–A European Journal. 2007 Apr 5; 13(11):3160-8.
- Sondi I, Salopek-Sondi B. Silver nanoparticles as antimicrobial agent: a case study on E. coli as a model for Gram-negative bacteria. Journal of colloid and interface science. 2004 Jul 1; 275(1):177-82.
- Sudha A, Jeyakanthan J, Srinivasan P. Green synthesis of silver nanoparticles using Lippia nodiflora aerial extract and evaluation of their antioxidant, antibacterial and cytotoxic effects. Resource-Efficient Technologies. 2017 Dec 1; 3(4):506-15.
- Sun Q, Cai X, Li J, Zheng M, Chen Z, Yu CP. Green synthesis of silver nanoparticles using tea leaf extract and evaluation of their stability and antibacterial activity. Colloids and surfaces A: Physicochemical and Engineering aspects. 2014 Mar 5; 444:226-31.
- Sun RW, Chen R, Chung NP, Ho CM, Lin CL, Che CM. Silver nanoparticles fabricated in Hepes buffer exhibit cytoprotective activities toward HIV-1 infected cells. Chemical communications. 2005(40):5059-61.
- Suriyakalaa U, Antony JJ, Suganya S, Siva D, Sukirtha R, Kamalakkannan S, Pichiah PT, Achiraman S. Hepatocurative activity of biosynthesized silver nanoparticles fabricated using Andrographis paniculata. Colloids and Surfaces B: Biointerfaces. 2013 Feb 1; 102:189-94.

- Tamilarasi P, Meena P. Green synthesis of silver nanoparticles (Ag NPs) using *Gomphrena globosa* (Globe amaranth) leaf extract and their characterization. *Materials Today: Proceedings*. 2020 Jan 1; 33:2209-16.
- Thombre R, Parekh F, Patil N. Green synthesis of silver nanoparticles using seed extract of *Argyrea nervosa*. *Int J Pharm Biol Sci* 2014; 5(1):114–9.
- Tian J, Wong KK, Ho CM, Lok CN, Yu WY, Che CM, Chiu JF, Tam PK. Topical delivery of silver nanoparticles promotes wound healing. *ChemMedChem: Chemistry Enabling Drug Discovery*. 2007 Jan 15; 2(1):129-36.
- Tripathi D, Modi A, Narayan G, Rai SP. Green and cost effective synthesis of silver nanoparticles from endangered medicinal plant *Withania coagulans* and their potential biomedical properties. *Materials Science and Engineering: C*. 2019 Jul 1; 100:152-64.
- Umoren SA, Obot IB, Gasem ZM. Green synthesis and characterization of silver nanoparticles using red apple (*Malus domestica*) fruit extract at room temperature. *J. Mater. Environ. Sci*. 2014; 5(3):907-14.
- Veerasamy R, Xin TZ, Gunasagaran S, Xiang TF, Yang EF, Jeyakumar N, Dhanaraj SA. Biosynthesis of silver nanoparticles using mangosteen leaf extract and evaluation of their antimicrobial activities. *Journal of saudi chemical society*. 2011 Apr 1; 15(2):113-20.
- Velayutham, K., Rahuman, A.A., Rajakumar, G., Roopan, S.M., Elango, G., Kamaraj, C., Marimuthu, S., Santhoshkumar, T., Iyappan, M. and Siva, C., 2013. Larvicidal activity of green synthesized silver nanoparticles using bark aqueous

- extract of *Ficus racemosa* against *Culex quinquefasciatus* and *Culex gelidus*. *Asian Pacific Journal of Tropical Medicine*, 6(2), pp.95-101.
- Wong KK, Liu X. Silver nanoparticles—the real “silver bullet” in clinical medicine?. *MedChemComm*. 2010; 1(2):125-31.
 - Wright JB. The comparative efficacy of two antimicrobial barrier dressings: in-vitro examination of two controlled release silver dressings. *Wounds*. 1998; 10:179-88.
 - Xu H, Yao L, Sun H, Wu Y. Chemical composition and antitumor activity of different polysaccharides from the roots of *Actinidia eriantha*. *Carbohydrate polymers*. 2009 Sep 5; 78(2):316-22.
 - Zangeneh MM, Joshani Z, Zangeneh A, Miri E. Green synthesis of silver nanoparticles using aqueous extract of *Stachys lavandulifolia* flower, and their cytotoxicity, antioxidant, antibacterial and cutaneous wound-healing properties. *Applied Organometallic Chemistry*. 2019 Sep; 33(9):e5016.
 - Zhang XF, Liu ZG, Shen W, Gurunathan S. Silver nanoparticles: synthesis, characterization, properties, applications, and therapeutic approaches. *International journal of molecular sciences*. 2016 Sep; 17(9):1534.

PUBLISHED ARTICLES

1. **Bharali A**, Deka B, Sarma H, Sarma S, Ahmed A, Bhattacharjee B, Das G, Das B, Upadhyaya M, Phukan M, Gogoi B. Integrating Recommendations to Improve Treatment Outcomes in the Clinical Management of Allergic Conjunctivitis. *Pharmaceutical and Biosciences Journal*. 2021 May 14:22-40.
2. Ahmed A, **Bharali A**, Dutta A, Chetia A, Newar A, Bhattacharjee B, Deka B, Sonowal B, Bingari B, Barman D, Sarmah D. The Role of Pharmacists in Optimizing Molecular Testing with Evolving Biomarkers and Treatment for Non-Small Cell Lung Cancer. *European Journal of Molecular & Clinical Medicine*. 2021 Apr 4;8(3):2240-59.
3. **Bharali A**, Nayak S, Nath TM, Pegu F, Saikia M, Phukan M. FUNCTIONALIZED LIPID-POLYMER HYBRID NANOPARTICLES MEDIATED TARGETED DRUG DELIVERY. *Biomaterials*. 2018; 67(2):86-100.
4. Bhargab BD, Dash B, Newar A, Ahmed A, **Bharali A**, Bordoloi B, Rohman TA, Bingari B, Bhattacharjee B, Sadhukan P, Ikbali AM. Coronavirus disease 2019: A comprehensive review on recent clinical updates and management tools for pharmacists. *Pharmaceutical and Biosciences Journal*. 2021 May 14:01-21.
5. Bhattacharjee B, Deka B, Ahmed N, Sonowal B, Newar A, Ahmed A, Ikbali AM, Rajkhowa A, **Bharali A**, Das G, Bharti R. The Role of Oncology Pharmacists in optimizing patient care in Chronic Immune Thrombocytopenia. *European Journal of Molecular & Clinical Medicine*. 2021 Feb 28;8(3):279-92.
6. Deka B, Bhattacharjee B, Ahmed A, Newar A, Sonowal B, Dey N, Barman D, Ikbali AM, Rajkhowa A, **Bharali A**. Clinical management of allergic rhinitis: A

comprehensive review. Research journal of Pharmacology and Pharmacodynamics. 2021;13(1):9-16.

Accepted articles:

7. Mucormycosis in Covid Patient: Insight into its Pathogenesis, Clinical Manifestation and Management Strategies, 2021, MDPI (**IF: 4.7**)
8. Das S, Das B, Sinha B, **Bharali A** et al. Discovery of therapeutic lead molecules from natural sources: An outstanding contribution to modern medicine In: Biological Sciences: Impacts on Modern Civilization, Current and Future Challenges by Anupam Guha, New Delhi Publishers, New Delhi: 2021, 198-214. (Accepted Book Chapter)
9. Ketamine: More than just NMDA blocker. Ketamine Revisited-New Insights into NMDA Inhibitors (ISBN 978-1-83962-793-4), IntechOpen, 2020

Communicated articles:

10. COVID-19 and Vitamin D: What We Know So Far; Indian Journal of medical Research (**IF: 1.5**)
11. Major challenges and probable scientific solutions towards the large scale production of plant-based metallic nanoparticles: A mini-review; Kournal of Nanoparticle Research, Springer

PEER REVIEW

1. JOURNAL OF PHARMACY PRACTICE (SAGE Publishing)

CO-CURRICULAR ACTIVITIES

1. Presented a scientific poster entitled “**Investigation of adulterants and curcumin content in different marketed brands of turmeric powder**” at two days national seminar on "**Current research in drug discovery and development**"; Dibrugarh University, 13th and 14th november, 2019.
2. Attended "**10th International Conference DISSO India 2021**" organized by SPDS in collaboration with AAPS during 24th, 25th and 26th June, 2021.
3. Successfully completed "**Four days International Advance Training Program**" on "**Recent Advances in Novel Drug Delivery System**" organized by Prisal Foundation (Pharmaceutical Royal International Society), 2020.
4. Presented a scientific poster entitled " Functionalized lipid polymer hybrid nanoparticles mediated targeted drug delivery" at two days national seminar on "PharmaNanotech"; Dibrugarh University.